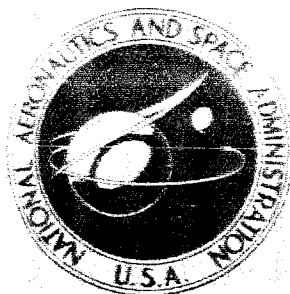


NASA CONTRACTOR  
REPORT



NASA CR-162

NASA CR-162

65 16882  
ACCESSION NUMBER  
113  
PAGES  
DATE OF THIS OR ANY EDITION

THRU  
CODE  
CATEGORY

# INVESTIGATION OF THE FATIGUE PERFORMANCE OF VISCO-ELASTIC PANELS AT ELEVATED TEMPERATURES

by *R. V. Bennett*

Prepared under Contract No. NAS 1-3193 by  
NORTH AMERICAN AVIATION, INC.  
Columbus, Ohio

for

GPO PRICE \$

OTS PRICE(S) \$ 4.00

Hard copy HC

Microfilm MF 5.00

INVESTIGATION OF THE FATIGUE PERFORMANCE OF  
VISCO-ELASTIC PANELS AT ELEVATED TEMPERATURES

By R. V. Bennett

Distribution of this report is provided in the interest of information exchange. Responsibility for the contents resides in the author or organization that prepared it.

Prepared under Contract No. NAS 1-3193 by  
NORTH AMERICAN AVIATION, INC.  
Columbus, Ohio

for

NATIONAL AERONAUTICS AND SPACE ADMINISTRATION

#### ACKNOWLEDGEMENT

The author acknowledges the advice and support of Mr. Phil Edge, Langley Research Center, NASA, during the course of investigation. The investigation was supported by the National Aeronautics and Space Administration under Contract NAS 1-3193.

## ABSTRACT

Experimentally determined data on the fatigue performance of visco-elastic material at elevated temperatures are presented in this report. The test program included sonic fatigue, structural shear fatigue, axial-load static tensile, visco-elastic material static shear, and sonic fatigue panel vibration tests. The test results generally showed the visco-elastic material to have slightly better sonic fatigue properties, slightly lower structural fatigue life, and comparable joint strength as compared to plain aluminum.

INVESTIGATION OF THE FATIGUE PERFORMANCE  
OF VISCO-ELASTIC PANELS AT ELEVATED  
TEMPERATURES

By

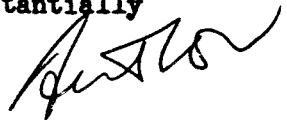
R. V. Bennett\*

SUMMARY

16882

Experimentally determined data on the fatigue performance of visco-elastic panels at elevated temperatures are presented in this report. These data were obtained in the laboratory facilities of the Columbus Division of North American Aviation, Inc., during the period extending from July 1, 1963 to July 31, 1964. The objectives of this program were to evaluate the fatigue characteristics of visco-elastic material and compare them with standard aluminum construction at temperatures up to 300°F and to determine joint characteristics of visco-elastic construction using standard rivets as fasteners at temperatures up to 300°F. The test program included sonic fatigue, structural shear fatigue, axial-load static tensile, visco-elastic material static shear, and sonic fatigue panel vibration tests. The results of this program lead to the following main conclusions:

1. The sonic fatigue life of the visco-elastic material was generally longer than plain aluminum at all realistic temperature-sound pressure level conditions, with the superiority diminishing at 300°F and the higher sound pressure levels.
2. The structural shear fatigue life of round-head riveted visco-elastic shear panels was slightly less than plain aluminum shear panels from ambient temperatures to 300°F; the fatigue life of flush-head riveted visco-elastic panels was slightly less than aluminum panels at ambient temperatures and substantially less at 200°F and 300°F.



\*Columbus Division, North American Aviation, Inc.

3. The static tensile strength of round-head riveted joints in the visco-elastic material was comparable to standard joints in aluminum at temperatures up to 300°F; the static tensile strength of flush-head riveted joints in the visco-elastic material was comparable to standard joints in aluminum at 300°F, but substantially lower at ambient temperatures.

## INTRODUCTION

A program for investigating the fatigue performance of visco-elastic panels at elevated temperatures was conducted by the Columbus Division of North American Aviation, Inc., during the period extending from July 1, 1963 to July 31, 1964. Personnel from the Advanced Environmental Development Group were responsible for technical direction of the project. The program was supported by the National Aeronautics and Space Administration under Contract NAS 1-3193.

This program was initiated to demonstrate the potential usefulness of visco-elastic material for structures subjected to vibratory environments. In structures subjected to acoustically excited vibrations, the responses must be damped to ensure adequate fatigue life. Structural design must provide this damping deliberately and increase it wherever possible. Because of its good damping properties, the visco-elastic laminate would appear to be a potentially useful material for structures subjected to vibratory environments which are either acoustic, pressure, or mechanical in nature. With the type of aircraft being considered, considerable areas of structures are designed by the environment rather than maneuver or gust loads. In such areas the use of damping treatment to reduce stress amplitudes must be considered when optimizing the design for strength and weight. However, there is a reluctance on the part of the structures design engineer to take advantage of this approach. Therefore, this limited experimental program was initiated to provide physical proof of the advantages to be gained.

To establish the suitability of the visco-elastic material in the above application, it was necessary to obtain test data for comparison with conventional materials and to demonstrate the practicability of forming joints. Therefore, the specific objectives of this program were:

1. To evaluate the fatigue characteristics of visco-elastic material and compare them with standard aluminum construction at temperatures up to 300°F.
2. To determine joint characteristics of visco-elastic construction using standard rivets as fasteners at temperatures up to 300°F.

The visco-elastic laminate investigated in this program was a sandwich-type construction consisting of two .020 in. thick aluminum skins bonded to a .020 in. thick elastomer interlayer.

The scope of the experimental tests conducted during this program may be summarized as follows:

1. (54) Sonic fatigue tests in the discrete frequency siren facility
  - A. (2) types of panels - visco-elastic and control
  - B. (3) test temperatures - ambient, 200°F and 300°F
  - C. (3) sound pressure levels - 148, 154 and 160 db
  - D. (1) type of rivet - standard round-head
2. (54) Structural fatigue tests of shear panels
  - A. (2) types of shear panels - V/E and control
  - B. (2) types of rivets - flat-head and round-head
  - C. (3) test temperatures - ambient, 200°F and 300°F
3. (72) Axial-load static tensile tests
  - A. (2) types of specimens - V/E and control
  - B. (2) types of rivets - flat-head and round-head
  - C. (3) test temperatures - ambient, 200°F and 300°F
4. Visco-elastic material static shear tests
  - A. (5) soaking temperatures - ambient, 150°F, 200°F, 250°F and 300°F
  - B. Test temperatures - soaking and ambient
  - C. Specimens cut from (2) sizes of V/E sheets -24 inch x 24 inch (Lot #1) and 36 inch x 48 inch (Lot #2)
5. Sonic fatigue panel vibration tests
  - A. (2) types of panels - V/E and control
  - B. (3) test temperatures - ambient, 200°F and 300°F
  - C. (2) panel suspension systems - hard and soft

This report is composed of the following four main sections:

1. Test Equipment and Procedure
2. Test Data
3. Discussion
4. Conclusions

Each of the first three main sections is divided into the following five sub-sections:

1. Sonic fatigue tests
2. Structural shear fatigue tests
3. Axial-load static tensile tests
4. Visco-elastic material static shear tests
5. Sonic fatigue panel vibration tests

The Test Equipment and Procedure Section describes test hardware, equipment, facilities, and procedures. The Test Data Section summarizes the measurements obtained during the various phases of the test program. The Discussion Section contains observations on data trends and comments on major points of interest and unusual occurrences during the test program. The Conclusions Section has general summarizations of the test results, recommended follow-on work and a statement on the degree of fulfillment of program objectives.

Following the four main sections of this report are the three appendices listed below:

1. Appendix A - Test Specimen Design Philosophy
2. Appendix B - Strain Gage Calibration
3. Appendix C - Painted Circuit Crack Detection System

Appendix A contains a discussion on the philosophy utilized in the design of the sonic fatigue, structural shear fatigue, axial-load static tensile, and static shear test specimens. The technique used for stress calibration of strain gages on the sonic and structural shear fatigue panels is included in Appendix B. Appendix C contains a description of the painted metallic circuit crack detection system developed for remote and automatic detection of initial crack propagation in the sonic fatigue panels.

At the end of the report are the tables with tabulated test data and figures showing test hardware dimensions, instrumentation layouts, equipment set-ups, test facilities, test specimen failures, and plots of test data.

## SYMBOLS

C	damping
E	Young's modulus of elasticity, psi
F	strain gage factor
L	ultimate static shear stress, psi
K	ultimate static tensile strength, lb
P	applied load, lb
R	resistance, ohms
S	Stress, psi
T	test temperature, °F
X	normalized signal displacement
t	time, min.
x	signal displacement
f(X)	probability density
G(f)	power spectral density, (psi <sup>2</sup> )/cps
$\sigma$	signal root mean square displacement
$\omega$	frequency, cps
$\phi$	number of oscillatory cycles
$\beta$	cycle rate, cpm

## SUBSCRIPTS

a	refers to room or ambient temperature
c	critical or calibrated value
o-p	zero to peak value
p	peak value
p-p	peak to peak value
s	refers to soaking temperature
F	refers to failure time or cycles
ave	average value
max	maximum value
rms	root mean square value

## ABBREVIATIONS

Al	Aluminum
F.H.	flush-head rivet
R.H.	round-head rivet
SPL	sound pressure level, decibels (db)

Note: The sound reference pressure =  $.0002 \text{ dynes/cm}^2$   
throughout this report

V/E	visco-elastic
N.F.	no failure

## DEFINITIONS

Control panel - test panel with plain aluminum web, aluminum stiffeners, and aluminum flanges or caps

Visco-elastic panel - test panel with visco-elastic web, plain aluminum stiffeners, and plain aluminum flanges or caps

## TEST EQUIPMENT AND PROCEDURE

### Sonic Fatigue Tests

The sonic fatigue tests were conducted in the Discrete Frequency Siren Test Facility (See Figure 1). For this facility, the air supply from the plant lines is aspirated to 1100 lbs. per minute at two to three psi and delivered to a spherical plenum chamber. The air flows from the chamber to a horn section and is directed through the 12 stator ports of the siren. The sound and air then pass through a progressive wave test section, a muffler, and an exhaust stack. The 12 port siren is operated by a variable speed motor and the frequency range of the device is 50 to 1000 cps. The facility is presently capable of generating sound pressure levels up to 175 db over a frequency range of 200 to 500 cps and 165 db from 50 to 550 cps.

The panel heating fixture was mounted in the discrete frequency siren test section as shown in Figure 2. This fixture consisted of several quartz lamp and reflector arrays strategically mounted on a steel frame to provide even temperature distributions on the inside skins of the test panels. The steel frame was suspended from the top of the siren test section by means of multiple-jointed linkage to isolate it from test section vibrations. The positions of the quartz lamps relative to the test panel are shown in Figure 3.

A sketch of the sonic fatigue test panels is shown in Figure 4. For the program, 27 control and 27 visco-elastic panels were constructed. Two extra control panels were also constructed, one for temperature distribution surveys--the other a spare. The only difference between the two types of panels was the skin or web. The control panels had a solid, .051 inch thick aluminum web, while the visco-elastic panels had a web consisting of two outer aluminum facing sheets, each .020 in. thick, and an .020 in. thick elastomer interlayer. Round-head rivets were used on all panels. Normal construction techniques for built-up riveted aluminum structures were utilized. The design philosophy for the sonic fatigue test panels is discussed in Appendix A.

The mounting fixture used for the sonic fatigue test panels may be seen in Figure 5. In this fixture, the test panel skin was recessed approximately two inches from the side face of the test section. The fixture consisted of a heavy steel outer framework which was rigidly fastened to the side of the test chamber, and a heavy steel inner frame which was hinged to the outer framework. The test panel was mounted rigidly to the inner frame. The inner frame was bolted rigidly to the outer framework during the sonic fatigue tests. These bolts were removed and the inner frame was swung outward for visual inspections and panel changes. For panel vibration tests at room temperature with a soft suspension system, the inner frame was removed entirely from the outer framework and suspended horizontally with bungee cord. For panel vibration tests at room and elevated temperatures with a hard suspension system, the inner frame was rigidly mounted in its normal vertical position in the outer framework.

The sonic fatigue panel and siren test section instrumentation included microphones, thermocouples, strain gages and a non-contacting displacement pickup.

Microphone locations for the sonic fatigue tests are shown in Figure 6. Microphones were used at positions #1 and #2 during the room temperature tests and positions #3 and #4 during the elevated temperature tests to monitor the sound pressure levels in the test section. Before the elevated temperature tests, microphone outputs at positions #3 and #4 were correlated, respectively, with microphone outputs at positions #1 and #2.

Thermocouple locations on the sonic fatigue test panels are shown in Figure 7. Actually, all 30 thermocouples were mounted only on the panel used for temperature distribution surveys. For the regular test panels, only thermocouples #1 to #6 were used to monitor panel temperatures.

Strain gage locations on the sonic fatigue test panels are shown in Figure 8. Position #3 was used only for the first few panels. Both normal and elevated temperature strain gages were used on the panels.

During the elevated temperature sonic fatigue tests, a non-contacting displacement probe, developed in the NAA-Columbus Dynamics Lab, was mounted in line with the center of the panel as shown in Figure 5. The main functions of this probe were to measure static buckling of the panel due to thermal stresses and to monitor the dynamic displacement of the panel center bay for siren tuning purposes after all panel strain gages had failed.

Various means were used during the sonic fatigue tests to prevent strain gage and thermocouple leads from breaking loose due to panel vibrations. A thin strip of silicone rubber compound was finally used to keep all leads tied securely to the panels. In addition, the ends of the thermocouple leads were inserted through #80 holes in the panel web and coated on both sides with a conductive paint solution. The two #80 holes for each pair of leads were spaced approximately 1/8 in. apart. Peening the thermocouple leads in the holes was insufficient in itself, since panel vibrations worked the leads loose and caused erratic thermocouple output signals. Also, the use of an epoxy resin was unsuccessful in keeping leads tied down, since the epoxy became brittle and cracked, breaking the leads in the process. Various types of tape were also unsuccessful, since they lost their adhesive properties at the elevated temperatures.

The power to the heating units in the siren test section was supplied and regulated by a power regulator and controller. This unit is capable of providing three controlled temperature zones by proportioning heater power through ignitrons controlled by a closed-loop thermocouple feedback circuit. Actually, only two temperature control zones were used on the sonic fatigue panels (See Figure 3). Settings for the power controller were determined during the panel temperature distribution surveys. These surveys were obtained for each combination of test temperature and air flow velocity in the test section prior to conduction of the sonic fatigue tests at these prescribed conditions. Lamps and reflectors were rearranged until the prescribed mean panel temperature, within  $\pm 5\%$ , was obtained at all 30 thermocouple positions with each air flow velocity. Since the tests were conducted under steady state conditions, no programming of the power controller was necessary.

The control console and associated equipment for the discrete frequency siren facility are shown in Figure 9. The console is instrumented to monitor plant air supply pressure and temperature, differential pressures, frequency and wave form of acoustic excitation, sound pressure level at six microphone positions, RMS voltage output of panel strain gages, siren bearing temperatures and siren vibration levels. The console contains rough and fine tuning dials for siren speed control. Associated equipment includes the manually operated valve which is used to regulate air flow through the 6 inch plant supply line to the siren aspirator.

The step-by-step procedure followed during the sonic fatigue tests is listed below:

1. Strain gages were applied to the panel according to normal techniques. Strain gage and thermocouple leads were secured as described previously.

2. The panel was fastened securely to the mounting frame on the side of the siren test section with (32) 5/16 inch bolts. Instrumentation leads were connected to the recording equipment.
3. Microphones were calibrated. Before the elevated temperature tests, microphones at #3 and #4 positions were correlated with the microphones at the #1 and #2 positions. The latter two microphones were then removed before the heat was turned on.
4. Power was gradually applied to the lamp arrays prior to the elevated temperature tests. The panel was brought up to the prescribed temperature, slowly, before the test started to minimize thermal stresses, to facilitate balancing strain gages, and to obtain uniform data during the test runs.
5. Strain gage calibrations were applied to the oscillograph and X-Y plotter (See Appendix B). The frequency coordinate of the X-Y plotter was also calibrated.
6. The siren was swept from 70 to 500 cps with the prescribed test sound pressure level and mean panel temperature. During these frequency surveys, the outputs from all panel strain gages were recorded on the oscillograph and X-Y plotter.
7. The frequency at which the maximum output of Gage #1 occurred on the X-Y plotter was selected as the initial setting for the siren speed control. At this time the test began.
8. The siren speed control was adjusted to maintain peak output from Gage #1 on the X-Y plotter as required. The sound pressure level was maintained in the test section by manual adjustment of the valve on the plant air supply line.
9. At frequent intervals, the siren and heating fixture were shut down for visual panel inspections.
10. The test runs were continued until 10 hours were accumulated or until the panel failed, whichever came first. Failure was defined as the initial formation of a visible crack in the center bay skin area of the panel.

When Gage #1 failed before test completion, the other strain gages were used to adjust the siren to the maximum panel response frequency. When all gages failed before test completion, the displacement probe described previously was used.

A log was made of all changes in panel response frequencies to facilitate computation of cycles to failure for each panel.

An automatic crack detection system was introduced into the sonic fatigue program during the 300°F tests to supplement and eventually replace the visual inspection method. The crack detection system is described in Appendix C.

Some panel strain gage data were recorded on magnetic tape for probability density and power spectral density analyses. These strain gage data were obtained from sonic fatigue panel #23 (control panel tested at 154 db and 300°F).

Three visco-elastic panels and three control panels were tested at each combination of three temperatures (room, 200°F and 300°F) and three sound pressure levels (148, 154 and 160 db).

Frequency correlation between the microphones, strain gages, and displacement probe was checked frequently during the tests.

### Structural Shear Fatigue Tests

The structural shear fatigue tests were conducted in the NAA-Columbus Dynamics Laboratory. Figures 10 and 11 show the general arrangement of equipment and test panels.

A sketch of the structural fatigue test panels is shown in Figure 12. For the program 9 control panels with round-head rivets, 36 visco-elastic panels with round-head rivets, and 9 visco-elastic panels with flush-head rivets were constructed. Two extra control panels with round-head rivets were also constructed, one for temperature distribution surveys--the other a spare. Three control panels with R.H. rivets, nine V/E panels with R.H. rivets, and three control panels with F.H. rivets were tested at each of three mean temperatures (room, 200°F and 300°F). Excepting the rivets, the only difference between the panels was the skin or web. The control panels had a solid, .051 inch thick aluminum web, while the visco-elastic panels had a web consisting of two outer aluminum facing sheets, each .020 inch thick, and an .020 inch thick elastomer interlayer. For the visco-elastic panels with flush-head rivets, the visco-elastic web was dimpled into countersunk rivet holes in the aluminum back-up structure before riveting. Otherwise, normal construction techniques for built-up riveted aluminum structures were utilized. The design philosophy for the structural fatigue test panels is discussed in Appendix A.

The structural fatigue panel mounting system, consisting of a vertical steel column and panel end attachments, may be seen in Figure 10. The panel end attachment fittings tied the caps and shear web to the vertical column in a manner which provided symmetrical load paths.

The structural fatigue panel heating fixture is shown in Figure 10. This mobile fixture consisted of several quartz lamp and reflector arrays strategically mounted on a steel frame to provide even temperature distributions on one side of the panel web. The positions of the quartz lamps relative to the test panel are shown in Figure 13.

The loading system utilized for the structural fatigue tests is shown in Figures 10 and 11. This system consisted of the control console, hydraulic circuit, hydraulic actuator, and hydraulic pumping unit.

The actuator applied a load simultaneously to two panels mounted in vertical alignment on the upright steel column. Thus, the two panels were loaded against each other, and no reactions occurred at the base of the column. Steel end fittings were used to attach the panel webs to the actuator. The panels were loaded in one direction only--toward each other.

The hydraulic circuit consisted of the hydraulic lines, a pressure relief valve, a metering valve, a servo valve, and a pressure meter. The pressure relief valve limited the maximum fluid pressure in the lines. The metering valve limited the rate of fluid flow to the actuator. The servo valve regulated the cycling rate of fluid flow to the actuator.

The control console regulated or programmed the action of the servo valve. The console contained dials for setting the time for the "on" and "off" portion of the load cycle. It was possible to regulate the load cycle rate, load application rate, and maximum applied load to the panels by proper adjustment of the console dials, the metering valve, and the loading valve on the pumping unit. The console also contained a load cycle counter and a switching unit which permitted application of direct static loads to the panels.

The power to the structural fatigue panel heating fixture was supplied and regulated by the same type of unit used for the sonic fatigue tests. Again, only two temperature control zones were used for the structural fatigue test set-up--one for each panel (See Figure 13). Settings for the power controller were determined during the panel temperature distribution surveys. These surveys were obtained for each test temperature prior to the actual tests. Lamps and reflectors were rearranged until the prescribed mean panel temperature, within  $\pm 5\%$ , was obtained at all 27 thermocouple positions. Since the tests were conducted under steady state conditions, no programming of the power controller was necessary.

The structural fatigue panel instrumentation included strain gages and thermocouples. Thermocouple locations are shown in Figure 14. Actually, all 27 thermocouples were mounted only on the panel used for temperature distribution surveys. For the regular test panels, only thermocouples #1 and #4 were used to monitor panel temperatures.

Strain gage locations on the structural fatigue test panels are shown in Figure 15. After the first two panels were tested, gages were mounted only at positions #2, #3, #6 and #8. Both normal and elevated temperature strain gages were used on the panels.

The step-by-step procedure followed during the structural fatigue tests is listed below:

1. Strain gages were applied to the panels according to normal techniques. Strain gage and thermocouple leads were secured as described for the sonic fatigue tests, except that tape was substituted for the silicone rubber.
2. The end fittings were fastened to the panels, and the panels were mounted securely to the vertical column.
3. The heating fixture was moved into position and the hydraulic actuator was connected between the free ends of the pair of panels. A calibrated load link was inserted into the actuator linkage and connected to the strain indicator. Panel instrumentation leads were connected to the recording equipment.
4. Power was gradually applied to the lamp arrays prior to the elevated temperature tests. The panels were brought up to the prescribed temperature, slowly, before the test started to minimize thermal stresses, to facilitate balancing strain gages, and to obtain uniform data during the tests.
5. Strain gage calibrations were applied to the oscillograph as described in Appendix B.
6. The control console was set so that manual static loads could be applied to the panels.
7. The hydraulic pressure was increased in 50 psi increments until the panels were loaded to 4 times the critical buckling load. Outputs from the load link were recorded on the strain indicator and converted to lb. readings for correlation with the pressure readings. Outputs from the panel strain gages were recorded on the oscillograph. The critical buckling load for the panels was established as that load at which the panel stiffener gages registered initial strain readings. The maximum pressure applied during the regular tests was that corresponding to 4 times the critical buckling load value.

8. The load link was removed from the actuator linkage.
9. The metering valve, load valve and console controls were adjusted to apply the established peak load to the panels at a smooth cycling rate of approximately 20 times per minute. Panel strain gage outputs were recorded on the oscillograph for approximately 10 load cycles at the beginning of each test.
10. At frequent intervals visual inspections were made while the test was running.
11. The test runs were continued until 50,000 load cycles were accumulated or until the panel failed, whichever came first. Failure was defined as the initial formation of a visible crack in the panel web.

The maximum applied panel load was specified as 3 times the critical buckling load in the contract for this program. However, the first two panels tested with this applied load did not fail within the specified 50,000 cycle limit. Therefore, since the peak load value was established arbitrarily anyway, this value was changed to 4 times the critical buckling load to ensure panel failures within the 50,000 cycle limit.

The critical buckling load was established only for the first two control panels and the first two visco-elastic panels. Thereafter, maximum panel loads for each type of panel were maintained approximately constant. A slight deviation in maximum applied load for the same type of panel did actually occur, since the peak load was always set up on the pressure meter at the 25 psi mark nearest the corresponding desired peak load. Since the meter calibration differed slightly from run to run, so did the apparent peak load values.

#### Axial-Load Static Tensile Tests

The axial-load static tensile tests were conducted in the NAA-Columbus Metals Laboratory. A general view of the test set-up is shown in Figure 16.

A sketch of the axial-load static tensile specimen is shown in Figure 17. For the program 18 specimens with .040 inch thick aluminum splice plates and round-head rivets, 36 specimens with .060 inch thick visco-elastic splice plates and round-head rivets, and 18 specimens with .060 inch thick visco-elastic splice plates and flush-head rivets were constructed. An equal number of each of the above groups was tested at each of three

temperatures (room, 200°F and 300°F). Riveting techniques for these specimens were the same as for the structural fatigue panels. The design philosophy for these test specimens is discussed in Appendix A.

The axial-load static tensile tests were conducted using a 60,000 lb. hydraulic test machine. The specimens were loaded through pins secured in adjustable clevis-type grips attached to self aligning loading rods. Elevated temperatures were obtained by exposing the specimen and loading train in an electrical resistance air circulating furnace. The specimens were brought to temperature and soaked for 1/2 hour to insure temperature equilibrium prior to testing. Specimen temperature was continuously monitored using a strip chart recorder and a chromel-alumel thermocouple attached to the specimen. All specimens were tested to failure in obtaining ultimate tensile strengths.

### Static Shear Tests

The visco-elastic material static shear tests were conducted in the NAA-Columbus Non-Metallics Laboratory. A sketch of the static shear test specimens is shown in Figure 18. The test specimens were obtained from two different lots of visco-elastic material. The first lot specimens were cut from a 24 inch x 24 inch visco-elastic sheet. This size sheet was used to construct the sonic fatigue test panels. The second lot specimens were obtained from a 36 inch x 48 inch visco-elastic sheet. The structural fatigue test panels were cut from this size sheet. The design philosophy for these test specimens is discussed in Appendix A.

The visco-elastic material static shear specimens were tested at five different temperatures: room, 150°F, 200°F, 250°F, and 300°F. Each specimen was soaked at the test temperature for 30 minutes prior to testing. Three specimens were tested at each of the five temperatures and from each of the two lots. Additional specimens from each of the two lots were also tested at room temperature after being soaked for 30 minutes at selected temperatures.

The ultimate static shear strength was determined for each specimen by pulling the ends of the specimen until failure occurred and recording the maximum applied load. Loads were applied on a test machine operating at a jaw speed of 0.075 inch/minute.

## Sonic Fatigue Panel Vibration Tests

The sonic fatigue panel vibration tests were conducted in the NAA-Columbus Dynamics Laboratory. The vibration tests were conducted on one visco-elastic panel and one control panel. A hard and a soft suspension system was used with each panel.

Figure 19 shows the sonic fatigue panel vibration test set-up with the soft suspension system. The panel mounting fixture was the inner frame used to fasten the panels to the side of the siren test section. The inner frame was removed from the test section and suspended horizontally with bungee cord for the soft suspension vibration tests. Excitation was provided with two 25 lb. electromagnetic shakers attached vertically to the panel mounting fixture. Resonant frequencies, node lines, and damping coefficients were determined for the fundamental vibration modes. Accelerometers and standard read-out equipment were used to measure the dynamic response of the panels. Salt was used to establish node lines. Damping coefficients were determined from the decay rates of accelerometer outputs recorded on an oscillograph. The vibration tests with the soft suspension system were conducted at room temperature only.

Figure 20 shows the sonic fatigue panel vibration test set-up with the hard suspension system. For these tests the panels were mounted in their normal position on the side of the siren test section. Excitation was again provided with two 25 lb. electromagnetic shakers attached horizontally to the panel mounting fixture. Resonant frequencies, node lines, and damping coefficients were determined for the fundamental vibration modes at three mean panel temperatures (room, 200°F and 300°F). A non-contacting dynamic displacement pickup and standard read-out equipment were used to measure the dynamic response of the panels. A strobe light was used to establish node lines. Damping coefficients were determined from the decay rates of the displacement pickup outputs recorded on an oscillograph. Panel heat was supplied by the quartz lamp arrays used for the sonic fatigue tests.

### TEST DATA

#### Sonic Fatigue Tests

The sonic fatigue test data are tabulated in Table 1 and plotted in Figure 21. Table 1 contains test frequencies, time to failure, and cycles to failure for each panel. Figure 21 is a plot of sound pressure level vs. average cycles to failure for each type of panel at room temperature, 200°F and 300°F.

At 160 db the average number of cycles to failure for the control panels was  $0.440 \times 10^6$  at room temperature,  $0.145 \times 10^6$  at 200°F, and  $.060 \times 10^6$  at 300°F. For the visco-elastic panels at the same sound pressure level, the average number of cycles to failure was  $0.617 \times 10^6$  at ambient temperature,  $0.233 \times 10^6$  at 200°F, and  $0.065 \times 10^6$  at 300°F.

At 154 db the average number of cycles to failure for the control panels was  $.866 \times 10^6$  at room temperature,  $.993 \times 10^6$  at 200°F, and  $1.306 \times 10^6$  at 300°F. For the visco-elastic panels at the same sound pressure level, the average number of cycles to failure was  $1.93 \times 10^6$  at room temperature,  $1.212 \times 10^6$  at 200°F, and  $.92 \times 10^6$  at 300°F.

At 148 db the average number of cycles to failure for the control panels was  $4.26 \times 10^6$  at room temperature and  $4.52 \times 10^6$  at 300°F. At 200°F and 154 db one control panel failed after  $4.49 \times 10^6$  cycles, while the other two did not fail within the 10 hour test limit. At 148 db no visco-elastic panels failed at any of the three test temperatures.

The sonic fatigue panel stress levels are tabulated in Table 2. These stress data are maximum peak-to-peak levels obtained on the oscillograph during siren frequency surveys prior to each test.

Power spectral density and probability density analyses of selected strain gage data are shown in Figures 22 to 25. Figure 26 is a probability density analysis of a pure sine wave. Figure 27 is a record of selected strain gage oscilloscope displays. Figures 28 to 45 show plots of strain gage output vs. siren frequency. These plots were obtained during the siren frequency surveys.

### Structural Shear Fatigue Tests

The data from the structural shear fatigue tests are tabulated in Table 3 and plotted in Figure 46. Table 3 lists the web material, type of rivet, test temperature, cycle rate, peak load and cycles to failure for each panel. Figure 46 is a plot of temperature vs. average cycles to failure for each type of panel.

The average number of cycles to failure for the control panels with round-head rivets was 28,543 at room temperature, 26,387 at 200°F, and 14,977 at 300°F. For the visco-elastic panels with round-head rivets, the average number of cycles to failure was 30,632 at room temperature, 23,070 at 200°F, and 15,775 at 300°F. The average number of cycles to failure for the visco-elastic panels with flush-head rivets was 29,300 at room temperature, 16,347 at 200°F, and 8,490 at 300°F.

Tables 4 and 5 contain static and dynamic stress data, respectively, for each structural fatigue test panel. The static stress levels were obtained from oscillograph records during the load calibration runs prior to the actual tests. The dynamic stress levels were obtained while the tests were in progress.

### Axial-Load Static Tensile Tests

The data from the axial-load static tensile tests are tabulated in Table 6 and plotted in Figure 47. For the purpose of brevity, the axial-load static tensile specimens will be categorized as follows:

<u>Type</u>	<u>Splice Plate</u> <u>Material</u>	<u>Rivet</u>
I	Visco-elastic	Round-Head
II	Aluminum	Round-Head
III	Visco-elastic	Flush-Head

The average ultimate static tensile strength for the Type I specimens was 2040 lb. at room temperature, 1944 lb. at 200°F, and 1642 lb. at 300°F. The average ultimate static tensile strength for the Type II specimens was 2110 lb. at room temperature, 1897 lb. at 200°F, and 1592 lb. at 300°F. For the Type III specimens, the average ultimate static tensile strength was 1775 lb. at room temperature, 1806 lb. at 200°F and 1590 lb. at 300°F.

### Static Shear Tests

The data from the static shear tests are tabulated in Table 7 and plotted in Figure 48. The average ultimate static shear strength for the Lot #1 specimens tested at the soaking temperature was 782 psi at room temperature, 632 psi at 150°F, 486 psi at 200°F, 495 psi at 250°F, and 331 psi at 300°F. For the Lot #2 specimens tested at the soaking temperature, the average ultimate static shear strength was 484 psi at room temperature, 339 psi at 150°F, 169 psi at 200°F, 212 psi at 250°F, and 165 psi at 300°F. The average ultimate static shear strength for the Lot #1 specimens tested at room temperature was 399 psi for a soaking temperature of 250°F and 395 psi for a soaking temperature of 300°F. For the Lot #2 specimens tested at room temperature, the average ultimate static shear strength was 351 psi for a soaking temperature of 250°F and 285 psi for a soaking temperature of 300°F.

## Sonic Fatigue Panel Vibration Tests

The data from the sonic fatigue panel vibration tests are tabulated in Table 8. This table contains resonant frequencies and damping coefficients for the first four vibration modes of a control panel and a visco-elastic panel. The vibration tests were conducted with a soft suspension system at room temperature only, and with a hard suspension system at room temperature, 200°F and 300°F.

For the control panel the resonant frequency of the first vibration mode, which was the fundamental mode of the center bay section, was 142 cps at room temperature with the soft suspension system. With the hard suspension system the resonant frequency of this mode was 170 cps at room temperature, 177 cps at 200°F and 177 cps at 300°F.

For the visco-elastic panel the resonant frequency of the first vibration mode was 152 cps at room temperature with the soft suspension system. With the hard suspension system the resonant frequency of this mode was 170 cps at room temperature, 173 cps at 200°F, and 177 cps at 300°F.

The damping coefficient for the first vibration mode of the control panel was .0103 at room temperature with the soft suspension system. For the same mode of the visco-elastic panel, the damping coefficient was .0143 with the same suspension system and temperature.

Node lines for all four vibration modes of both panels at room temperature with both suspension systems are shown in Figures 49 to 52. The modal patterns did not change significantly at 200°F and 300°F with the hard suspension system.

## DISCUSSION

### Sonic Fatigue Tests

The sonic fatigue test results are difficult to analyze precisely, because the data scatter tends to detract from the accuracy of an average time or cycles to failure obtained from only three test panels. The amount of scatter indicates that more than three panels should be tested at each SPL-temperature condition to obtain more accurate fatigue data.

The 160 db sound pressure level was slightly too high for the higher temperature tests, because the panels failed so quickly at these conditions that it was difficult to obtain accurate data and stabilize test conditions.

The 148 db sound pressure level was too low for the 10 hour test limit restriction. At this sound pressure level two control panels at 200°F and all visco-elastic panels at all three test temperatures did not fail within the 10 hour limit. This, of course, reduced the amount of available data for comparing fatigue characteristics of the two types of panels.

The sonic fatigue data obtained from this test program, however, do indicate some trends. With one exception, the average cycles to failure for the visco-elastic panels are greater than the control panels at each temperature-sound pressure level test condition. The one exception occurred at 154 db and 300°F. As expected, at each sound pressure level the average cycles to failure for both visco-elastic and control panels decreased as the temperature increased, with the exception of the control panels at 154 db. At each temperature the average cycles to failure for both visco-elastic and control panels decreased as the sound pressure level increased. The superiority in fatigue life of the visco-elastic panels diminished as the temperature increased.

The most common type of sonic fatigue panel failure is shown in Figure 53. These failures were characterized by cracks propagating from the rivets in the panel center bay sections and running along the rivet lines. During the room temperature tests, most cracks appeared along the stiffener rivet lines for both types of panels. At 200°F and 300°F most cracks appeared along the flange rivet lines for both types of panels. Figure 54 shows a sonic fatigue visco-elastic panel failure characterized by complete skin separation, which occurred on all visco-elastic panels tested at 300°F and 154 and 160 db. These panels cracked along the flange rivet lines in the outer bay sections. Destructive post-test examinations disclosed complete skin separation on all sections of the webs. Better bonding techniques would undoubtedly enhance the sonic fatigue properties of the visco-elastic material, especially at the higher temperature-sound pressure level conditions. Figure 55 shows an uncommon sonic fatigue panel failure characterized by loss of a web section. This explosive-type failure occurred on one control panel only at 160 db and 200°F.

The sonic fatigue panel stress data showed that the control panels responded at much higher stress levels than visco-elastic panels at the same sound pressure levels. Otherwise, stress correlation was not good. This condition existed at all sound pressure levels and temperatures for both types of panels. Even apparently identical panels produced substantially different peak stress levels at the same temperature and sound pressure level. Therefore, it was impossible to test all panels in a group at the same peak stress level, since the prescribed sound pressure level had to be maintained. It was also impossible to maintain a complete log of actual panel stress levels during the test runs, since the strain gages generally failed before completion of the tests.

Four sonic fatigue panels (#5, #6, #8 and #48) were mounted in the siren test section with the stiffeners in a horizontal position instead of the normal vertical position. No noticeable effect was evident on either the fatigue or stress data.

The ordinate axes of the strain gage output vs. siren frequency plots in Figures 28 to 45 are scaled with only approximate values of the zero-to-peak stress levels. The stress scales are only approximate because the X-Y plotter was calibrated on the basis of an expected sinusoidal output or a 1.414 peak to rms ratio from the panel strain gages. Actual strain gage wave forms were sinusoidal within experimental accuracy at room temperature, "near-sinusoidal" at 200°F, and somewhat complex at 300°F.

The complex nature of the panel response modes at 300°F was detected by oscilloscope observations, a deviation in the frequencies at which the maximum dynamic amplitude and stress level peaked, probability density analyses, and power spectral density analyses. Records of oscilloscope displays (Figure 27), probability density analyses (Figures 24 and 25), and power spectral density analyses (Figures 22 and 23) show the presence of higher frequency modes in the panel response. Probability density analyses define the likelihood of a given amplitude occurrence. For comparison, Figure 26 is a probability density analysis of a pure sine wave. During the siren frequency sweeps, the dynamic amplitude monitored by the non-contacting displacement probe sometimes peaked at a frequency 8 to 10 cps lower than the stress. This factor was taken into account when using the displacement pickup to tune the siren. There were no obvious explanations for the presence of higher frequency modes with the predominant fundamental mode in panels responding to discrete frequency excitation.

During the sonic fatigue tests, fluctuations or variations of the panel fundamental resonant frequency were observed frequently for both the visco-elastic panels and the plain aluminum or control panels. The net result of these fluctuations was that the panels were responding at low amplitude and stress levels during a significant portion of the elapsed test time. This response at a less than maximum stress level could have had a detrimental effect on the correlation of the cycles or time-to-failure for the series of test panels.

The fluctuations of the panel fundamental resonant frequency were especially prevalent during the elevated temperature tests on both types of panels and during tests on the visco-elastic panels at all temperatures. These fluctuations were caused by:

1. The damping characteristics of the visco-elastic material
2. Loss of panel stiffness
3. Non-linear nature of the panel response
4. Small variations in the panel temperature distribution
5. Thermal expansion of the panel mounting fixture

Damping action of the visco-elastic webs was observed during some test runs at steady-state conditions. These panels damped themselves out and then built up to a maximum response amplitude again without any change in siren speed. On these occasions the response amplitude could also be restored by a slight adjustment of the siren speed in either direction.

Loss of stiffness was evident on both control and visco-elastic panels during the sonic fatigue test program. This phenomenon was characterized by a gradual drop in the resonant frequency of the fundamental panel response mode during some test runs at steady-state conditions, including room temperature tests. On the control panels this reduction in stiffness was caused by the working action of the web around the rivets. In addition to this reason, loss of stiffness on the visco-elastic panels was definitely caused by a reduction in bonding strength, especially at the higher temperatures and sound pressure levels.

The non-linear nature of the panel response caused both visco-elastic and control panels to exhibit sharp drop-offs from the peak stress level when the siren speed was increased slightly over the panel resonant frequency. This sudden drop-off made the tuning process for these panels extremely tedious, because the inertia of the siren rotor would not allow immediate speed adjustments.

Although temperature variations on the panel webs were held within  $\pm 5\%$  of the mean test temperature, the variations which did occur within these limits were enough to cause small fluctuations in the fundamental resonant frequency of the panel center bay section. These small frequency variations necessitated continual minor tuning adjustments throughout the test runs.

The thermal expansion of the panel mounting fixture caused fluctuations of the panel resonant frequencies by changing the degree of restraint on the panel edges. As the massive steel fixture slowly heated up during progressive test runs throughout the day, the gradual thermal expansion of the fixture resulted in a slow increase in the degree of restraint on the panel edges, with a resultant increase in the resonant frequency of the panel center bay section.

Since there are no practical means of eliminating all the causes of the frequency fluctuations, better comparative sonic fatigue data could be obtained for visco-elastic and plain aluminum material by using random or broad-band excitation instead of discrete or narrow-band excitation. Random excitation would negate the undesirable characteristics of fluctuating resonant frequencies, since the panels would always respond at maximum amplitude even though the resonant frequency shifted substantially throughout the test.

### Structural Shear Fatigue Tests

The results of the structural shear fatigue tests show that the fatigue life of round-head riveted and flush-head riveted visco-elastic panels and round-head riveted control panels decreased as the temperature increased to 300°F. The control panels displayed a sharp drop-off in fatigue life at 300°F. The round-head riveted visco-elastic and control panels had a comparable fatigue life at all three test temperatures. The fatigue life of the flush-head riveted visco-elastic panels was comparable to the other two types of panels at room temperature, but significantly less at 200°F and 300°F.

In comparing the fatigue life of visco-elastic and control panels, two factors must be considered. The effective shear area of the visco-elastic panels was only 80% of the control panels and the applied load to the visco-elastic panels was only 67% of the control panels. Although it is difficult to extrapolate accurately the visco-elastic panel structural fatigue data from this program to provide correlation of fatigue life for visco-elastic and control panels with equal shear areas and applied loads, such an extrapolation would undoubtedly show the structural fatigue life of round-head riveted visco-elastic panels to be slightly less than the control panels at all three test temperatures and the fatigue life of flush-head riveted visco-elastic panels to be slightly less than the control panels at room temperature and significantly less at 200°F and 300°F.

The webs of the visco-elastic and control panels were not designed with the same shear area because one of the objectives of this test program was to determine how much reduction in structural fatigue life would result if visco-elastic material were substituted for plain aluminum material without accepting a weight penalty due to the presence of the elastomer interlayer. Actually, a more comprehensive program would consist in testing one set of visco-elastic and control panels with equal web shear areas and another set with equal web densities.

The difference in applied loads to the visco-elastic and control panels was a result of the stipulation that the peak load of all panels be the same multiple value ( $4x$ ) of the critical buckling load for each type of panel. Since the critical buckling load of the visco-elastic panels was only 67% of the control panels, the peak applied loads differed by the same amount. Although the unequal applied loads produced approximately the same maximum deflections and stresses in the visco-elastic and control panels, a better comparative measure of fatigue life would have been provided with equal loads. Again, a more comprehensive program would consist in testing sets of visco-elastic and control panels with several different peak loads.

Good correlation was obtained between static and dynamic stress levels for all panel webs. The maximum stress levels for visco-elastic and control panel webs were approximately the same at all test conditions. No difficulties were encountered with structural fatigue panel instrumentation throughout the test program.

The structural fatigue data scatter indicated that more than three panels should be tested to obtain a good average fatigue life. In this program three flush-head riveted visco-elastic panels, three round-head riveted control panels, and twelve round-head riveted visco-elastic panels were tested at each of three temperatures.

The most common mode of structural fatigue panel failure is shown in Figure 56. These failures were characterized by cracks propagating from cap or stiffener rivets in the bay corners. An exception to the above mode of failure is shown in Figure 57. This exception occurred on all three control panels tested at 300°F and was characterized by shearing of cap rivets.

## Axial-Load Static Tensile Tests

The results of the axial-load static tensile tests may be summarized as follows:

1. At room temperature, the ultimate static tensile strength of the specimens with aluminum splice plates and round-head rivets was slightly greater than the specimens with visco-elastic splice plates and round-head rivets and approximately 20% greater than the specimens with visco-elastic splice plates and flush-head rivets.
2. At 200°F, the ultimate static tensile strength of the specimens with visco-elastic splice plates and round-head rivets was slightly greater than the specimens with aluminum splice plates and round-head rivets and approximately 8% greater than the specimens with visco-elastic splice plates and flush-head rivets.
3. At 300°F, the ultimate static tensile strength of the specimens with visco-elastic splice plates and round-head rivets was slightly greater than both the specimens with aluminum splice plates and round-head rivets and the specimens with visco-elastic splice plates and flush-head rivets.
4. The ultimate static tensile strength of both the specimens with visco-elastic splice plates and round-head rivets and the specimens with aluminum splice plates and round-head rivets decreased as the test temperature increased.
5. The ultimate static tensile strength of the specimens with visco-elastic splice plates and flush-head rivets increased very slightly from room temperature to 200°F, and then decreased from 200°F to 300°F.

Figure 58 shows typical axial-load static tensile specimen failures. The specimens in each group were very consistent in the ultimate static tensile strength and mode of failure. At room temperature, failure of specimens with visco-elastic splice plates and round-head rivets was produced by a combination of tearing of the visco-elastic material and shearing of rivets. At 200°F and 300°F, failure of specimens with visco-elastic splice plates and round-head rivets was produced by shearing of rivets. At all three test temperatures, failure of specimens with visco-elastic splice plates and flush-head rivets was produced by tearing of the visco-elastic material at the rivets. At all three test

temperatures, failure of specimens with plain aluminum splice plates and round-head rivets was produced by shearing of rivets. The ultimate static tensile strength of all specimens in each group was within  $\pm 10\%$  of the average value. Discounting the tests at room temperature with the specimens with visco-elastic splice plates and flush-head rivets, the ultimate static tensile strength of all specimens in each group was within  $\pm 4.5\%$  of the average value.

### Static Shear Tests

The results of the visco-elastic material static shear tests conducted at the soaking temperature show that the static shear strength of the visco-elastic material decreases as the temperature increases from room temperature to 300°F and that the static shear strength of the specimens cut from the 24 inch x 24 inch lot size sheets (Lot #1) is substantially greater than the 36 inch x 48 inch lot size sheets (Lot #2) through the entire test temperature range. Therefore, since the 24 inch x 24 inch sheets were used as webs for the sonic fatigue panels and the structural fatigue panel webs were cut from the 36 inch x 48 inch sheets, it may be surmised that the structural fatigue panel webs had a lower bonding efficiency.

The results of the visco-elastic material static shear tests conducted at room temperature after soaking at prescribed temperatures are inconclusive because of an insufficient number of specimens.

### Sonic Fatigue Panel Vibration Tests

The results of the sonic fatigue panel vibration tests may be summarized as follows:

1. The resonant frequency of the fundamental vibration mode of the center bay section was approximately the same for both the control and visco-elastic panels. Therefore, since the densities of the two panels were approximately the same, so also were the bending stiffnesses.
2. The damping coefficient for the fundamental center bay mode of the visco-elastic panel was approximately 40% greater than the same mode of the control panel with the soft suspension system.

3. The flexibility of the panel mounting fixture reduced the damping of both panels with the hard suspension system.
4. The modal patterns for the control panel were approximately the same with both the hard and soft suspension systems; the shapes of the higher modes of the visco-elastic panel changed somewhat with the two suspension systems.
5. Changing to the hard suspension system increased the resonant frequency of the lower modes for both panels; heating the panels produced the same results.
6. The fundamental vibration mode of the center bay section of both panels was at a lower resonant frequency than any other mode.

### CONCLUSIONS

Results of this program for investigating the fatigue performance of visco-elastic panels at elevated temperatures lead to the following conclusions:

1. Scatter and insufficient quantity of sonic fatigue data gathered in this program prohibit firm, unqualified recommendations for aircraft design purposes; however, the trend of the data showed longer sonic fatigue life for the visco-elastic material at all realistic temperature-sound pressure level conditions, with the superiority diminishing at 300°F and the higher sound pressure levels.
2. Better bonding techniques would enhance the sonic fatigue properties of the visco-elastic material, especially at the higher temperature-sound pressure level conditions.
3. Fluctuating resonant frequencies caused by the damping characteristics of the visco-elastic material, the non-linear nature of the panel response, small variations in the panel temperature distribution, and thermal expansion of the panel mounting fixture adversely affected the correlation of the sonic fatigue data obtained with discrete excitation; better comparative sonic fatigue data for visco-elastic material and plain aluminum could be obtained by conducting the sonic fatigue tests in the random siren facility instead of the discrete siren facility.

4. Better comparative sonic fatigue data for visco-elastic material and plain aluminum could also be obtained by testing more than three panels at each temperature-sound pressure level condition and by testing each panel to failure.
5. Although direct correlation of visco-elastic and plain aluminum structural fatigue data is difficult due to differences in applied loads and shear areas, extrapolation of the visco-elastic data would show that the structural fatigue life of round-head riveted visco-elastic panels was slightly less than the control panels from room temperature to 300°F and the fatigue life of flush-head riveted panels was slightly less than the control panels at room temperature and significantly less at 200°F and 300°F.
6. Better comparative structural fatigue data for visco-elastic material and plain aluminum could be obtained by testing sets of visco-elastic and control panels with both equal web shear areas and equal web densities, with several different applied peak loads, and with more than three panels per set.
7. The static tensile strength of round-head riveted joints in the visco-elastic material was comparable to standard joints in aluminum at temperatures up to 300°F; the static tensile strength of flush-head riveted joints in the visco-elastic material was comparable to standard joints in aluminum at 300°F, but significantly lower at room temperature.
8. The static shear strength of the visco-elastic material decreased significantly as the temperature increased from 70 to 300°F and also varied with sheet size.
9. The crack detection system consisting of a painted metallic strip interwoven along the rivets and connected to a battery and alarm bell was a reliable method for determining the time of initial crack formation and eliminated the necessity of visual inspections during the test runs.

The overall test results show that the objectives of this program were accomplished satisfactorily, since substantial knowledge has been gained about the relative sonic and structural fatigue properties of visco-elastic material at ambient and elevated temperatures.

## APPENDIX A

### TEST SPECIMEN DESIGN PHILOSOPHY

#### Sonic Fatigue Panels

The sonic fatigue test panels were designed so that the fatigue strength of the web structure would be the major factor during the test program. The webs were designed to fail within the 10 hour test limit under the prescribed testing conditions (sound pressure level and thermal environment), while the stiffeners and supporting flanges were designed not to fail under the same conditions. Three visco-elastic panels, identical to the panels designed for this program except for very minor changes, were successfully tested previously in a company-sponsored program. Therefore, there was reasonable assurance that, with the panel design for this program, the sonic fatigue properties of two types of web material (visco-elastic sheets and plain aluminum sheets) could be compared under three thermal environments at three sound pressure levels without having failures in other panel components interfering with the test results.

The overall size of the sonic fatigue panels was 24 x 24 inch. The panel flanges were fastened to the support fixture in a manner which allowed only normal forces to be transmitted to the panel. The panels consisted of three bays, with the center bay having a 10 inch width. A thickness of .051 inch was selected for the plain aluminum webs of the control panels so that these webs would have the same density as the .060 inch thick visco-elastic webs. All parts of the sonic fatigue panels were fabricated from flat sheet stock.

#### Structural Shear Fatigue Panels

The structural shear fatigue test panels were designed so that the fatigue strength of the web structure also would be the major factor during the test program. In other words, the webs were designed to fail within the 50,000 load cycle limit under the prescribed loading conditions. On the other hand, the stiffeners, caps, and end attachments were designed not to fail under the same conditions. In this manner, the structural shear fatigue properties of two types of web material (visco-elastic sheets and plain aluminum sheets) and two types of web fasteners (round-head rivets and flush-head rivets) could be compared under three temperature environments without having failures in other panel components interfering with the test results.

The above criteria, together with the overall panel size and the available visco-elastic panel thickness, dictated the sizes for the caps, stiffeners and end attachment fittings. An overall panel size of 37.5 inch x 12 inch was selected to conform approximately with the proposed size and to permit cutting three webs from each visco-elastic sheet on order. The panels consisted of three bays, each 10.5 inch wide, with 3 inches on each end to make an adequate shear attachment. The caps and shear web on each panel were connected to reaction or load application fittings (end attachment fittings) in a manner which provided symmetrical load paths.

A thickness of .051 inch was selected for the plain aluminum webs of the control panels so that these webs would have the same density as the .060 inch thick visco-elastic webs. The webs from the two types of panels were not designed with the same shear area because one of the objectives of this test program was to determine how much reduction in structural fatigue life would result if visco-elastic material were substituted for plain aluminum material without accepting a weight penalty due to the presence of the elastomer interlayer. The plain aluminum web thickness of .051 inch and the high aspect ratio of the panel resulted in a very high calculated buckling shear load. Since the maximum applied load was four times the critical buckling load, the caps, stiffeners, and end attachment fittings were designed of heavy structure to reduce stresses and prevent fatigue failures in these parts during the tests.

#### Axial-Load Static Tensile Specimens

The axial-load static tensile specimens were designed to compare riveted joint characteristics of visco-elastic and conventional aluminum sheets at three different temperatures. The test specimens consisted of two loading plates joined together with a splice plate. Reinforcement plates were spot-welded to the ends of the loading plates to prevent the loading pins from shearing through the loading plates before a failure occurred in the joint section. The loading plates were constructed of .063 inch thick aluminum sheet stock for all (72) specimens. The splice plates were constructed of either .040 inch thick aluminum sheet stock or .060 inch thick visco-elastic sheet stock. Since the visco-elastic sheets were constructed with .020 inch thick aluminum skins and an .020 inch thick elastomer interlayer, the visco-elastic and solid aluminum splice plates had the same axial stiffness. The rivets which joined the splice plates and loading plates together were either round-head or flush-head. Therefore, the axial-load static tensile tests produced comparative ultimate tensile strength data on two types of material at three different temperatures.

## Static Shear Specimens

The visco-elastic material static shear test program was set up to determine the variation of the static shear strength with temperature and lot size. It was desirous to learn whether heat deteriorated the quality of bonding between the aluminum skins and elastomer interlayer and whether the bonding on 36 inch x 48 inch lot size sheets was poorer quality than the 24 inch x 24 inch lot size sheets as indicated by the non-destructive inspection process and fabrication difficulties encountered by the manufacturer.

The specimens were prepared as shown in Figure 18 so that the static shear strength of the bond layer could be determined independent of the aluminum skins. The specimens were 9-1/2 inch long and 1 inch wide, and the effective shear area was 1 square inch. The 1 inch over-lap was prepared by machine-milling a 1/8 inch cut through each facing side. A razor blade was used to cut through the silicone interlayer and sever any possible linkage that might contribute to an increase in lap-shear strength. To determine the effect of lot size on the static shear strength, the first lot specimens were cut from a 24 inch x 24 inch visco-elastic sheet, while the second lot specimens were obtained from 36 inch x 48 inch visco-elastic sheet. The 24 inch x 24 inch size sheet was used to construct the sonic fatigue test panels, while the structural fatigue panels were cut from the larger size sheet.

## APPENDIX B

### STRAIN GAGE CALIBRATION TECHNIQUE

This section describes the technique used to convert oscillograph records of sonic and structural shear fatigue panel strain gage outputs to peak-to-peak or zero-to-peak stress values. For both sonic and structural fatigue test panels, the strain gage bridge consisted of one active arm on the panel and three dummy resistors. The calibration was accomplished by balancing the bridge, switching a calibrated resistor across one arm of the bridge, and recording the resulting displacement on the oscillograph. For a one active arm bridge, the zero-to-peak stress value of this displacement is calculated as follows:

$$S_{o-p} = \frac{E R}{F(R + R_c)}$$

where  $S_{o-p}$  = zero-to-peak stress value of oscillograph displacement, psi

$E$  = Young's modulus of elasticity for panel material  
( $10 \times 10^6$  psi for aluminum)

$R$  = resistance of each bridge arm, ohms

$R_c$  = resistance of calibrated resistor, ohms

$F$  = gage factor for strain gage

To obtain actual test stress levels, peak-to-peak or zero-to-peak amplitudes on the oscillograph traces were compared directly with the calibrated displacements.

## APPENDIX C

### PAINTED CIRCUIT CRACK DETECTION SYSTEM

An automatic crack detection system was introduced into the sonic fatigue program during the 300°F tests to supplement and eventually replace the visual inspection method. This system was used on the three control panels tested at 300°F and 154 db, the three visco-elastic panels tested at 300°F and 148 db, the three control panels tested at 300°F and 160 db, and the three visco-elastic panels tested at 300°F and 154 db. By using this system, exact failure times were obtained and the necessity of shutting down the siren and heating system for visual inspections on both sides of the panels was eliminated. As a result, more accurate fatigue data were obtained and the overall test time was reduced.

The crack detection system consisted of a painted metallic strip interwoven along the center bay rivet lines and connected to a battery and alarm bell. The system was capable of detecting short, hair-line cracks propagating from center bay rivets (See Figure 59). Subsequent inspection of the panels showed that the cracks did extend through the paint and into the metal. It had been previously feared that the paint might become too brittle and crack before the metal skin cracked, especially at the higher sound pressure levels and temperatures. Applying the paint in as thin a layer as possible helped prevent premature paint cracks.

TABLE 1

## SONIC FATIGUE TEST RESULTS

Panel No.	Type Panel	SPL db	T °F	θ cps	$t_F$ min.	$\dot{\epsilon}_F \times 10^{-6}$
3	Control	148	Room	166-172	540	5.46
4	Control	148	Room	166-168	465	4.65
29	Control	148	Room	162-166	270	2.66
Ave.					<u>408</u>	<u>4.26</u>
5	Control	154	Room	173-177	100	1.05
6	Control	154	Room	182-186	70	.774
7	Control	154	Room	172	75	.773
Ave.					<u>82</u>	<u>.866</u>
8	Control	160	Room	188	41	.463
9	Control	160	Room	175-177	41	.433
10	Control	160	Room	172-173	42	.435
Ave.					<u>41.7</u>	<u>.440</u>
30	V/E	148	Room	131-136	600(N.F.)	4.78
31	V/E	148	Room	127-131	600(N.F.)	4.65
32	V/E	148	Room	133-135	600(N.F.)	4.69
Ave.					<u>600</u>	<u>4.71</u>
33	V/E	154	Room	116-128	150	1.09
34	V/E	154	Room	116-128	300	2.24
35	V/E	154	Room	117-133	300	2.45
Ave.					<u>250</u>	<u>1.93</u>
36	V/E	160	Room	127-131	66	.510
37	V/E	160	Room	120-124	111	.813
38	V/E	160	Room	122-144	66	.527
Ave.					<u>81</u>	<u>.617</u>
11	Control	148	200	190-209	630(N.F.)	7.55
12	Control	148	200	208-212	840(N.F.)	10.60
13	Control	148	200	208	360	4.49
Ave.					<u>610</u>	<u>7.55</u>
14	Control	154	200	174-198	157	1.70
15	Control	154	200	174	65	.678
16	Control	154	200	208	48	.600
Ave.					<u>90</u>	<u>.993</u>

TABLE 1 (Cont'd)

## SONIC FATIGUE TEST RESULTS (Cont'd)

Panel No.	Type Panel	SPL db	T °F	θ cps	t <sub>F</sub> min.	Φ F x 10 <sup>-6</sup>
17	Control	160	200	206	16	.198
18	Control	160	200	204	6	.073
19	Control	160	200	195-197	14	.165
Ave.					<u>12</u>	<u>.145</u>
39	V/E	148	200	158-164	630(N.F.)	6.05
40	V/E	148	200	160-163	600(N.F.)	5.80
41	V/E	148	200	151-158	720(N.F.)	6.65
Ave.					<u>650</u>	<u>6.18</u>
42	V/E	154	200	146-165	120	1.119
43	V/E	154	200	150-152	212	1.92
44	V/E	154	200	166	60	.598
Ave.					<u>131</u>	<u>1.212</u>
45	V/E	160	200	166	16	.159
46	V/E	160	200	173-186	21	.227
47	V/E	160	200	168-170	31	.314
Ave.					<u>23</u>	<u>.233</u>
20	Control	148	300	169-209	390	4.49
21	Control	148	300	145-213	390	4.09
22	Control	148	300	181-207	480	4.97
Ave.					<u>420</u>	<u>4.52</u>
23	Control	154	300	114-128	266	2.21
24	Control	154	300	123-124	77	.572
25	Control	154	300	124-132	148	1.135
Ave.					<u>164</u>	<u>1.306</u>
26	Control	160	300	198-208	35*	.423*
27	Control	160	300	164	4	.039
28	Control	160	300	168	8	.080
Ave.					<u>6</u>	<u>.060</u>

\* Test results invalid due to loss of power to heating unit at unknown time.

TABLE 1 (Cont'd)

## SONIC FATIGUE TEST RESULTS (Cont'd)

Panel No.	Type Panel	SPL db	T °F	$\theta$ cps	$t_F$ min.	$\phi_F$ $\times 10^{-6}$
48	V/E	148	300	143-162	600(N.F.)	5.51
49	V/E	148	300	187-199	630(N.F.)	7.49
50	V/E	148	300	149-168	600(N.F.)	5.73
Ave.					610	6.24
51	V/E	154	300	125-127	165**	1.25**
52	V/E	154	300	122-132	57**	.511**
53	V/E	154	300	141-150	118**	1.01**
Ave.					113	.92
54	V/E	160	300	166	7 **	.070**
55	V/E	160	300	186-166	6 **	.063**
56	V/E	160	300	176	6 **	.063
Ave.					6.3	.065

\* Test results invalid due to loss of power to heating unit at unknown time.

\*\* Post test examination disclosed complete skin separation on web.

TABLE 2

## SONIC FATIGUE PANEL STRESS

Panel No.	Type Panel	T °F	SPL db	S <sub>p-p</sub> max, psi (Dynamic)*		
				Gage #1	#2	#4
3	Control	Room	148	7,090	-	11,900
4	Control	Room	148	12,030	11,830	14,330
29	Control	Room	148	14,630	16,170	22,130
Ave.				11,250	14,000	16,120
5	Control	Room	154	22,300	19,620	28,100
6	Control	Room	154	29,000	23,070	37,870
7	Control	Room	154	30,300	22,350	39,200
Ave.				27,200	21,680	35,060
8	Control	Room	160	36,030	21,270	-
9	Control	Room	160	32,050	18,225	36,850
10	Control	Room	160	27,100	16,300	33,000
Ave.				31,725	18,600	34,925
30	V/E	Room	148	4,425	7,855	11,065
31	V/E	Room	148	4,230	7,775	14,500
32	V/E	Room	148	5,730	10,600	15,750
Ave.				4,795	8,745	13,770
33	V/E	Room	154	14,575	15,500	32,350
34	V/E	Room	154	14,300	17,075	33,650
35	V/E	Room	154	13,200	16,650	-
Ave.				14,025	16,410	33,000
36	V/E	Room	160	14,900	15,525	-
37	V/E	Room	160	15,350	19,900	-
38	V/E	Room	160	16,850	14,785	-
Ave.				15,700	16,735	-
11	Control	200	148	16,345	12,015	15,735
12	Control	200	148	13,030	10,520	15,590
13	Control	200	148	15,550	11,135	16,265
Ave.				14,975	11,225	15,865
14	Control	200	154	30,400	16,965	20,500
15	Control	200	154	18,915	19,650	30,250
16	Control	200	154	29,700	16,250	28,900
Ave.				26,340	17,620	26,550

TABLE 2 (Cont'd)

## SONIC FATIGUE PANEL STRESS (Cont'd)

Panel No.	Type Panel	T °F	SPL db	S <sub>p-p</sub> max, psi (Dynamic)*		
				Gage #1	#2	#4
17	Control	200	160	21,535	15,085	18,600
18	Control	200	160	-	-	-
19	Control	200	160	28,650	-	20,550
Ave.				25,095	15,085	19,575
39	V/E	200	148	7,180	6,025	13,520
40	V/E	200	148	6,640	4,725	7,560
41	V/E	200	148	6,415	-	10,205
Ave.				6,745	5,375	10,430
42	V/E	200	154	13,165	14,265	14,835
43	V/E	200	154	6,780	7,270	13,700
44	V/E	200	154	11,365	9,260	15,615
Ave.				10,435	10,265	14,715
45	V/E	200	160	16,685	8,245	9,745
46	V/E	200	160	17,100	-	-
47	V/E	200	160	16,900	7,210	13,450
Ave.				16,895	7,730	11,600
20	Control	300	148	7,680	7,745	-
21	Control	300	148	19,465	10,300	14,515
22	Control	300	148	16,850	9,305	15,615
Ave.				14,665	9,115	15,065
23	Control	300	154	20,515	19,485	18,100
24	Control	300	154	17,265	17,025	21,500
25	Control	300	154	21,400	18,350	-
Ave.				19,725	18,285	19,800
26	Control	300	160	17,115	13,780	38,365
27	Control	300	160	23,835	20,000	22,535
28	Control	300	160	24,165	21,565	22,935
Ave.				21,705	18,450	27,945

TABLE 2 (Cont'd)

## SONIC FATIGUE PANEL STRESS (Cont'd)

Panel No.	Type Panel	T °F	SPL db	S <sub>p-p</sub> max, psi (Dynamic)*		
				Gage #1	#2	#4
48	V/E	300	148	5,645	5,670	8,800
49	V/E	300	148	1,815	9,650	6,375
50	V/E	300	148	6,025	4,885	5,110
Ave.				4,495	6,735	6,760
51	V/E	300	154	12,215	11,755	13,785
52	V/E	300	154	11,265	11,600	13,810
53	V/E	300	154	10,500	12,715	12,600
Ave.				11,325	12,025	13,400
54	V/E	300	160	6,450	14,615	12,700
55	V/E	300	160	19,465	16,365	9,175
56	V/E	300	160	18,500	8,150	12,900
				14,805	13,045	11,590

\* Obtained on oscillograph during frequency surveys prior to tests. Stress values represent maximum peak-to-peak levels on trace. No frequency correlation is available.

TABLE 3

## STRUCTURAL FATIGUE TEST RESULTS

Panel No.	Type Panel	Type Rivets	T °F	$\delta$ cpm	P <sub>p</sub> * lbs.	$\phi$ F
1	V/E	R.H.	Room	21.4-22.8	3,924	24,070
2	V/E	R.H.	Room	21.4-22.8	3,924	31,383
3	V/E	R.H.	Room	21.4	3,900	35,202
4	V/E	R.H.	Room	21.4	3,900	29,360
5	V/E	R.H.	Room	21.2-21.9	3,890	26,280
6	V/E	R.H.	Room	21.2-21.9	3,890	38,875
7	V/E	R.H.	Room	21.4-22.4	3,920	38,135
8	V/E	R.H.	Room	21.4-22.4	3,920	35,326
9	V/E	R.H.	Room	21.8	3,900	32,050
10	V/E	R.H.	Room	21.8	3,900	20,070
11	V/E	R.H.	Room	22.1-22.8	3,920	23,700
12	V/E	R.H.	Room	22.1-22.8	3,920	33,128
Ave.						30,632
13	V/E	R.H.	200	20.1-20.3	3,960	24,185
14	V/E	R.H.	200	20.1-20.3	3,960	24,185
15	V/E	R.H.	200	19.3-20.4	4,020	24,600
16	V/E	R.H.	200	20.3-20.7	4,000	24,250
17	V/E	R.H.	200	19.3-20.4	4,020	22,900
18	V/E	R.H.	200	20.3-20.7	4,000	24,300
19	V/E	R.H.	200	20.3-20.4	4,000	22,160
20	V/E	R.H.	200	20.3-20.4	4,000	22,180
21	V/E	R.H.	200	20.1-20.8	3,970	18,975
22	V/E	R.H.	200	20.1-20.8	3,970	30,350
23	V/E	R.H.	200	18.3-23.3	3,990	19,500
24	V/E	R.H.	200	18.3-23.3	3,990	19,250
Ave.						23,070
25	V/E	R.H.	300	22.8-23.1	3,905	20,725
26	V/E	R.H.	300	22.8-23.1	3,905	17,600
27	V/E	R.H.	300	22.6-23.8	3,990	11,630
28	V/E	R.H.	300	22.6-23.8	3,990	11,420
29	V/E	R.H.	300	22.3-23.3	3,950	19,300
30	V/E	R.H.	300	22.5-22.6	3,940	8,740
31	V/E	R.H.	300	22.5-22.6	3,940	14,400
32	V/E	R.H.	300	22.3-23.3	3,950	14,230
33	V/E	R.H.	300	21.2-22.2	3,950	16,370
34	V/E	R.H.	300	21.2-22.2	3,950	15,840
35	V/E	R.H.	300	20.7-21.1	3,950	16,475
36	V/E	R.H.	300	20.7-21.1	3,950	22,550
Ave.						15,775

TABLE 3 (Cont'd)

## STRUCTURAL FATIGUE TEST RESULTS (Cont'd)

Panel No.	Type Panel	Type Rivets	T. $\sigma_F$	$\delta$ cpm	P <sub>p</sub> * lbs.	$\phi_F$
37	V/E	F.H.	Room	22.8-23.8	3,900	36,660
38	V/E	F.H.	Room	22.8-23.8	3,900	32,640
39	V/E	F.H.	Room	22.0-22.8	3,900	18,600
Ave.						29,300
40	V/E	F.H.	200	23.2	3,990	11,610
41	V/E	F.H.	200	23.2	3,990	20,310
42	V/E	F.H.	200	23.2	3,960	17,120
Ave.						16,347
43	V/E	F.H.	300	18.3	3,965	7,080
44	V/E	F.H.	300	18.3	3,965	6,215
45	V/E	F.H.	300	19.3-19.5	4,000	11,460
Ave.						8,490
46	Control	R.H.	Room	17.3-20.0	5,830	25,276**
47	Control	R.H.	Room	17.3-20.0	5,830	25,276**
48	Control	R.H.	Room	18.2-22.2	5,866	29,050
55	Control	R.H.	Room	18.2-22.2	5,866	28,036
Ave.						28,543
49	Control	R.H.	200	24.2-25.1	5,800	30,455
50	Control	R.H.	200	24.2-25.1	5,800	23,280
51	Control	R.H.	200	19.8-23.8	5,840	25,425
Ave.						26,387
52	Control	R.H.	300	18.0-20.9	5,890	19,192
53	Control	R.H.	300	21.2	5,910	11,800
54	Control	R.H.	300	18.0-19.2	5,890	13,940
Ave.						14,977

\* Load applied in one direction only. Peak load equal to approximately 4 times critical buckling load for all panels.

\*\* Data not included in average. Panels were previously tested to 50,000 cycle limit without failure with peak load equal to 3 times critical buckling load.

TABLE 4

## STRUCTURAL FATIGUE PANEL STATIC STRESS LEVELS

Panel No.	Type Panel	Type Rivets	T °F	P <sub>p</sub> ** lbs.	S <sub>o-p</sub> max, psi (Static)* Gage #2	#3	#6
1	V/E	R.H.	Room	3,924	7,440	6,540	21,800
2	V/E	R.H.	Room	3,924	5,640	6,840	21,200
3	V/E	R.H.	Room	3,900	6,070	6,990	20,700
4	V/E	R.H.	Room	3,900	4,980	6,670	20,300
5	V/E	R.H.	Room	3,890	-	6,680	20,800
6	V/E	R.H.	Room	3,890	6,730	6,250	21,800
7	V/E	R.H.	Room	3,920	6,440	6,670	21,500
8	V/E	R.H.	Room	3,920	5,620	5,640	21,600
9	V/E	R.H.	Room	3,900	6,110	6,300	21,150
10	V/E	R.H.	Room	3,900	4,920	6,750	20,500
11	V/E	R.H.	Room	3,920	6,650	4,580	20,400
12	V/E	R.H.	Room	3,920	6,920	7,460	20,700
Ave.					6,140	6,450	21,040
13	V/E	R.H.	200	3,960	4,650	4,470	18,600
14	V/E	R.H.	200	3,960	4,310	4,410	17,200
15	V/E	R.H.	200	4,020	-	4,500	-
16	V/E	R.H.	200	4,000	3,480	4,880	16,150
17	V/E	R.H.	200	4,020	3,810	5,440	-
18	V/E	R.H.	200	4,000	3,000	3,625	16,950
19	V/E	R.H.	200	4,000	3,090	3,140	15,750
20	V/E	R.H.	200	4,000	5,990	5,060	15,900
21	V/E	R.H.	200	3,970	5,130	6,400	19,050
22	V/E	R.H.	200	3,970	4,940	5,470	17,850
23	V/E	R.H.	200	3,990	4,640	5,430	20,200
24	V/E	R.H.	200	3,990	6,300	6,050	19,200
Ave.					4,485	4,905	17,685
25	V/E	R.H.	300	3,905	3,690	4,170	18,150
26	V/E	R.H.	300	3,905	5,390	4,450	18,300
27	V/E	R.H.	300	3,990	1,320	2,635	16,450
28	V/E	R.H.	300	3,990	3,340	3,425	17,950
29	V/E	R.H.	300	3,950	2,560	2,450	15,100
30	V/E	R.H.	300	3,940	3,370	1,870	16,650
31	V/E	R.H.	300	3,940	3,700	3,250	16,250
32	V/E	R.H.	300	3,950	3,470	2,840	16,700
33	V/E	R.H.	300	3,950	1,650	2,825	14,800
34	V/E	R.H.	300	3,950	1,630	1,620	22,000
35	V/E	R.H.	300	3,970	3,680	1,530	16,350
36	V/E	R.H.	300	3,970	2,555	3,290	15,960
Ave.					3,030	2,865	17,055

TABLE 4 (Cont'd)

## STRUCTURAL FATIGUE PANEL STATIC STRESS LEVELS (Cont'd)

Panel No.	Type Panel	Type Rivets	T °F	Pp ** lbs.	So-p max, psi (Static)*		
					Gage #2	#3	#6
37	V/E	F.H.	Room	3,900	6,050	5,850	21,300
38	V/E	F.H.	Room	3,900	6,600	6,220	20,800
39	V/E	F.H.	Room	3,900	-	-	-
Ave.					<u>6,325</u>	<u>6,035</u>	<u>21,050</u>
40	V/E	F.H.	200	3,990	3,985	2,980	15,300
41	V/E	F.H.	200	3,990	3,260	2,870	18,000
42	V/E	F.H.	200	3,960	4,320	5,550	20,500
Ave.					<u>3,855</u>	<u>3,800</u>	<u>18,265</u>
43	V/E	F.H.	300	3,965	1,555	1,885	12,050
44	V/E	F.H.	300	3,965	3,625	3,590	15,250
45	V/E	F.H.	300	4,000	2,600	1,780	13,900
Ave.					<u>2,595</u>	<u>2,420</u>	<u>13,735</u>
46	Control	R.H.	Room	5,830	4,300	5,260	20,800
47	Control	R.H.	Room	5,830	10,000	7,420	23,000
48	Control	R.H.	Room	5,866	5,720	6,930	25,150
55	Control	R.H.	Room	5,866	-	4,030	20,600
Ave.					<u>6,675</u>	<u>5,910</u>	<u>22,390</u>
49	Control	R.H.	200	5,800	4,750	3,960	9,950
50	Control	R.H.	200	5,800	3,780	4,030	20,400
51	Control	R.H.	200	5,840	6,140	6,580	26,200
Ave.					<u>4,890</u>	<u>4,855</u>	<u>18,850</u>
52	Control	R.H.	300	5,890	2,900	3,005	19,250
53	Control	R.H.	300	5,910	4,530	4,430	-
54	Control	R.H.	300	5,890	3,780	2,760	22,200
Ave.					<u>3,737</u>	<u>3,398</u>	<u>20,725</u>

\* Static stress values obtained from oscillograph records prior to tests.

\*\* Load applied in one direction only. Peak load equal to approximately 4 times critical buckling load for all panels.

TABLE 5

## STRUCTURAL FATIGUE PANEL DYNAMIC STRESS LEVELS

Panel No.	Type Panel	Type Rivets	T °F	P <sub>p</sub> ** lbs.	S <sub>o-p</sub> max, psi (Dynamic)*		
					Gage #2	#3	#6
1	V/E	R.H.	Room	3,924	8,140	6,860	20,600
2	V/E	R.H.	Room	3,924	6,700	7,400	21,500
3	V/E	R.H.	Room	3,900	7,010	8,380	20,200
4	V/E	R.H.	Room	3,900	5,650	7,030	20,800
5	V/E	R.H.	Room	3,890	-	7,180	19,700
6	V/E	R.H.	Room	3,890	7,800	6,980	20,100
7	V/E	R.H.	Room	3,920	7,310	7,400	20,700
8	V/E	R.H.	Room	3,920	6,530	6,500	21,100
9	V/E	R.H.	Room	3,900	7,210	6,810	21,700
10	V/E	R.H.	Room	3,900	5,650	8,100	21,600
11	V/E	R.H.	Room	3,920	7,400	5,550	20,700
12	V/E	R.H.	Room	3,920	7,850	8,710	20,700
Ave.					7,025	7,240	20,785
13	V/E	R.H.	200	3,960	6,630	5,750	20,600
14	V/E	R.H.	200	3,960	5,610	5,600	19,350
15	V/E	R.H.	200	4,020	-	5,800	-
16	V/E	R.H.	200	4,000	4,250	5,970	19,150
17	V/E	R.H.	200	4,020	4,470	5,070	-
18	V/E	R.H.	200	4,000	4,590	5,700	19,700
19	V/E	R.H.	200	4,000	4,760	5,290	19,200
20	V/E	R.H.	200	4,000	7,290	7,045	18,500
21	V/E	R.H.	200	3,970	6,180	8,420	20,800
22	V/E	R.H.	200	3,970	6,450	6,920	19,200
23	V/E	R.H.	200	3,990	5,110	6,330	21,800
24	V/E	R.H.	200	3,990	7,400	7,220	19,700
Ave.					5,705	6,260	19,800
25	V/E	R.H.	300	3,905	5,150	5,440	20,400
26	V/E	R.H.	300	3,905	6,350	4,790	20,200
27	V/E	R.H.	300	3,990	2,830	4,050	18,230
28	V/E	R.H.	300	3,990	5,170	5,120	20,100
29	V/E	R.H.	300	3,950	3,080	3,240	14,950
30	V/E	R.H.	300	3,940	5,060	3,610	18,100
31	V/E	R.H.	300	3,940	4,720	3,880	18,650
32	V/E	R.H.	300	3,950	5,120	3,490	17,100
33	V/E	R.H.	300	3,950	2,760	3,770	16,400
34	V/E	R.H.	300	3,950	3,010	1,780	14,000
35	V/E	R.H.	300	3,970	1,160	3,040	17,900
36	V/E	R.H.	300	3,970	3,440	3,290	17,700
Ave.					3,990	3,790	17,810

TABLE 5 (Cont'd)

## STRUCTURAL FATIGUE PANEL DYNAMIC STRESS LEVELS (Cont'd)

Panel No.	Type Panel	Type Rivets	T °F	P <sub>p</sub> ** lbs.	S <sub>o-p</sub> max, psi (Dynamic)*		
					Gage #2	#3	#6
37	V/E	F.H.	Room	3,900	7,050	6,650	20,500
38	V/E	F.H.	Room	3,900	7,780	6,740	20,800
39	V/E	F.H.	Room	3,900	-	-	-
Ave.					<u>7,415</u>	<u>6,695</u>	<u>20,650</u>
40	V/E	F.H.	200	3,990	4,850	4,620	19,400
41	V/E	F.H.	200	3,990	4,640	4,035	20,250
42	V/E	F.H.	200	3,960	5,300	6,750	22,200
Ave.					<u>4,930</u>	<u>5,135</u>	<u>20,615</u>
43	V/E	F.H.	300	3,965	3,340	3,625	13,650
44	V/E	F.H.	300	3,965	5,370	5,580	19,350
45	V/E	F.H.	300	4,000	3,850	2,940	16,600
Ave.					<u>4,185</u>	<u>4,050</u>	<u>16,535</u>
46	Control	R.H.	Room	5,830	4,260	5,200	20,200
47	Control	R.H.	Room	5,830	8,450	7,120	22,200
48	Control	R.H.	Room	5,866	7,360	7,175	25,200
55	Control	R.H.	Room	5,866	5,660	4,730	21,050
Ave.					<u>6,435</u>	<u>6,055</u>	<u>22,165</u>
49	Control	R.H.	200	5,800	6,330	5,760	14,350
50	Control	R.H.	200	5,800	4,950	4,800	22,700
51	Control	R.H.	200	5,840	7,140	8,300	25,600
Ave.					<u>6,140</u>	<u>6,285</u>	<u>20,885</u>
52	Control	R.H.	300	5,890	942	3,280	19,700
53	Control	R.H.	300	5,910	3,870	4,370	-
54	Control	R.H.	300	5,890	4,370	3,160	21,500
Ave.					<u>3,061</u>	<u>3,603</u>	<u>20,600</u>

\* Dynamic stress values obtained from oscillograph records during tests.

\*\* Load applied in one direction only. Peak load equal to approximately 4 times critical buckling load for all panels.

TABLE 6

## AXIAL-LOAD STATIC TENSILE TEST RESULTS

Specimen No.	Splice Plate Material	Type Rivet	T °F	K lb.
1	V/E	R.H.	Room	2050
2	V/E	R.H.	Room	1950
3	V/E	R.H.	Room	2050
4	V/E	R.H.	Room	2050
5	V/E	R.H.	Room	2100
6	V/E	R.H.	Room	2100
7	V/E	R.H.	Room	2075
8	V/E	R.H.	Room	2050
9	V/E	R.H.	Room	2000
10	V/E	R.H.	Room	1950
11	V/E	R.H.	Room	2050
12	V/E	R.H.	Room	2050
Ave.				<u>2040</u>
13	V/E	R.H.	200	1955
14	V/E	R.H.	200	1910
15	V/E	R.H.	200	1920
16	V/E	R.H.	200	1945
17	V/E	R.H.	200	1950
18	V/E	R.H.	200	1950
19	V/E	R.H.	200	1990
20	V/E	R.H.	200	1930
21	V/E	R.H.	200	1935
22	V/E	R.H.	200	1960
23	V/E	R.H.	200	1950
24	V/E	R.H.	200	1930
Ave.				<u>1944</u>

TABLE 6 (Cont'd)

## AXIAL-LOAD STATIC TENSILE TEST RESULTS (Cont'd)

Specimen No.	Splice Plate Material	Type Rivet	T °F	K lb.
25	V/E	R.H.	300	1655
26	V/E	R.H.	300	1675
27	V/E	R.H.	300	1585
28	V/E	R.H.	300	1650
29	V/E	R.H.	300	1610
30	V/E	R.H.	300	1630
31	V/E	R.H.	300	1660
32	V/E	R.H.	300	1660
33	V/E	R.H.	300	1665
34	V/E	R.H.	300	1645
35	V/E	R.H.	300	1650
36	V/E	R.H.	300	1615
Ave.				<u>1642</u>
37	V/E	F.H.	Room	1700
38	V/E	F.H.	Room	1600
39	V/E	F.H.	Room	1900
40	V/E	F.H.	Room	1750
41	V/E	F.H.	Room	1850
42	V/E	F.H.	Room	1850
Ave.				<u>1775</u>
43	V/E	F.H.	200	1860
44	V/E	F.H.	200	1870
45	V/E	F.H.	200	1790
46	V/E	F.H.	200	1760
47	V/E	F.H.	200	1830
48	V/E	F.H.	200	1730
Ave.				<u>1806</u>
49	V/E	F.H.	300	1630
50	V/E	F.H.	300	1555
51	V/E	F.H.	300	1580
52	V/E	F.H.	300	1630
53	V/E	F.H.	300	1575
54	V/E	F.H.	300	1575
Ave.				<u>1590</u>

TABLE 6 (Cont'd)

## AXIAL-LOAD STATIC TENSILE TEST RESULTS (Cont'd)

Specimen No.	Splice Plate <u>Material</u>	Type Rivet	T °F	K lb.
55	A1	R.H.	Room	2110
56	A1	R.H.	Room	2050
57	A1	R.H.	Room	2100
58	A1	R.H.	Room	2180
59	A1	R.H.	Room	2120
60	A1	R.H.	Room	2110
Ave.				<u>2110</u>
61	A1	R.H.	200	1910
62	A1	R.H.	200	1890
63	A1	R.H.	200	1955
64	A1	R.H.	200	1855
65	A1	R.H.	200	1870
66	A1	R.H.	200	1875
Ave.				<u>1897</u>
67	A1	R.H.	300	1630
68	A1	R.H.	300	1580
69	A1	R.H.	300	1610
70	A1	R.H.	300	1585
71	A1	R.H.	300	1580
72	A1	R.H.	300	1570
Ave.				<u>1592</u>

TABLE 7

## VISCO-ELASTIC MATERIAL STATIC SHEAR TEST RESULTS

$T_{CF}$	Specimen No.	L, psi			
		Lot #1		Lot #2	
		Tested at $T_s$	Tested at $T_a$	Tested at $T_s$	Tested at $T_a$
Room	1	788		502	
	2	800		505	
	3	758		446	
	Ave.	782		484	
150	1	687		326	
	2	623		351	
	3	585		339	
	Ave.	632		339	
200	1	539		141	
	2	468		132	
	3	452		234	
	Ave.	486		169	
250	1	497	352	214	396
	2	447	445	193	307
	3	540		228	
	Ave.	495	399	212	351
300	1	385	408	181	285
	2	308	381	137	
	3	300		178	
	Ave.	331	395	165	285

Notes:

1. Lot #1 Specimens were obtained from a 24 x 24 inch sheet. This size sheet was used for the sonic fatigue test panels.
2. Lot #2 Specimens were obtained from a 36 x 48 inch sheet. This size sheet was used for the beam-bending test panels.
3. Soaking time was 30 min.

TABLE 8

## SONIC FATIGUE PANEL VIBRATION TEST RESULTS

## I. Soft Suspension System - Room Temperature

<u>Panel #28</u> (Control)			<u>Panel #56</u> (Visco-elastic)		
Mode	$\theta$	$C/C_c$	Mode	$\theta$	$C/C_c$
1	142	.0103	1	152	.0143
2	198	.0030	2	201	.0106
3	250	.0069	3	250	.0128
4	352	.0036	4	351	.0024

## II. Hard Suspension System - Room Temperature

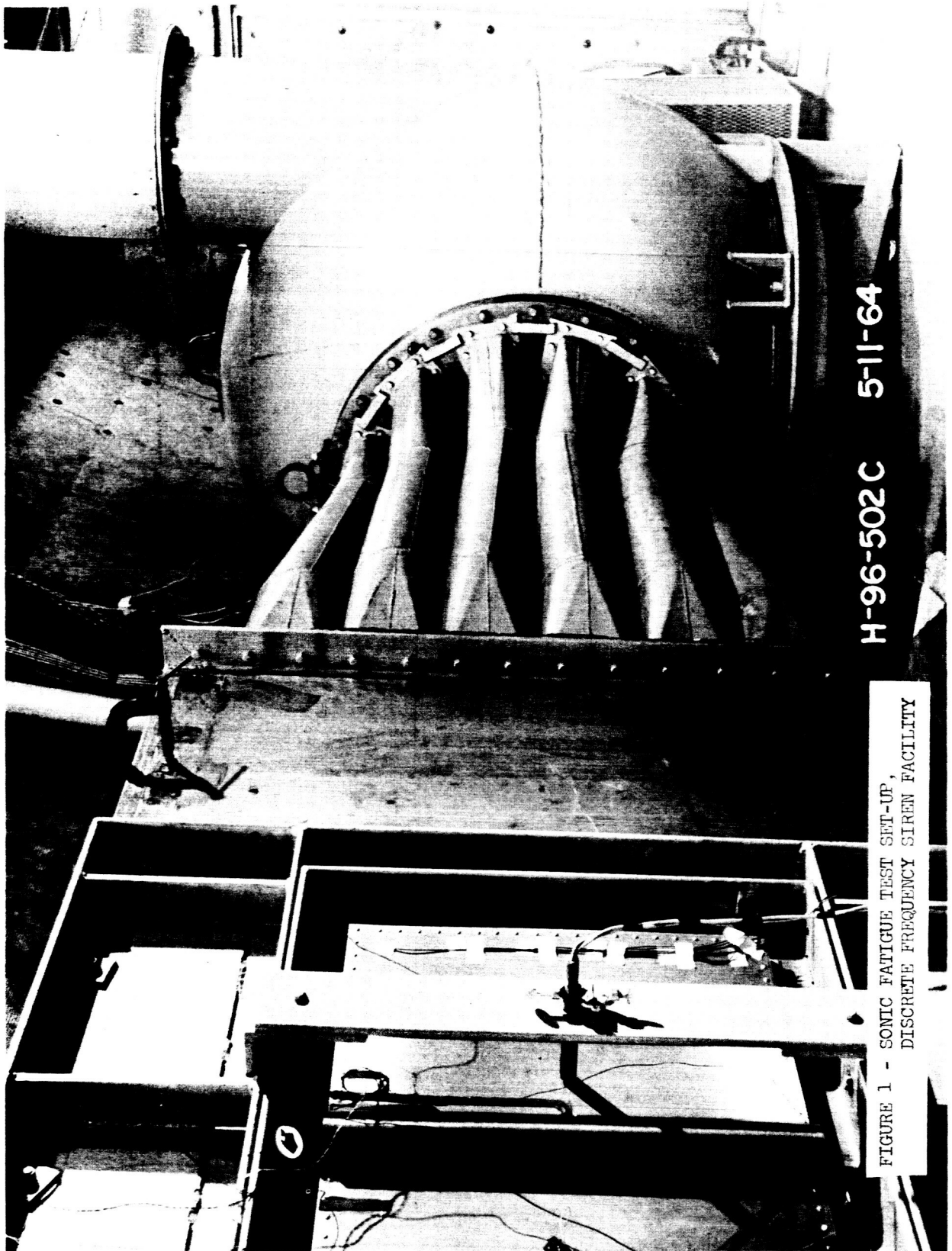
<u>Panel #28</u> (Control)			<u>Panel #56</u> (Visco-elastic)		
Mode	$\theta$	$C/C_c$	Mode	$\theta$	$C/C_c$
1	170	.0051	1	170	.0048
2	208	.0040	2	233	.0075
3	255	.0054	3	258	.0122
4	370	.0142	4	360	.0114

## III. Hard Suspension System - 200°F

<u>Panel #28</u> (Control)			<u>Panel #56</u> (Visco-elastic)		
Mode	$\theta$	$C/C_c$	Mode	$\theta$	$C/C_c$
1	177	.0035	1	173	.0065
2	231	.0043	2	229	.0080
3	293	.0040	3	279	.0082
4	361	.0064	4	338	.0142

## IV. Hard Suspension System - 300°F

<u>Panel #28</u> (Control)			<u>Panel #56</u> (Visco-elastic)		
Mode	$\theta$	$C/C_c$	Mode	$\theta$	$C/C_c$
1	177	.0094	1	178	.0066
2	229	.0059	2	230	.0054
3	279	.0054	3	279	.0082
4	361	.0035	4	339	.0075



H-96-502 C 5-11-64

FIGURE 1 - SONIC FATIGUE TEST SET-UP,  
DISCRETE FREQUENCY SIREN FACILITY

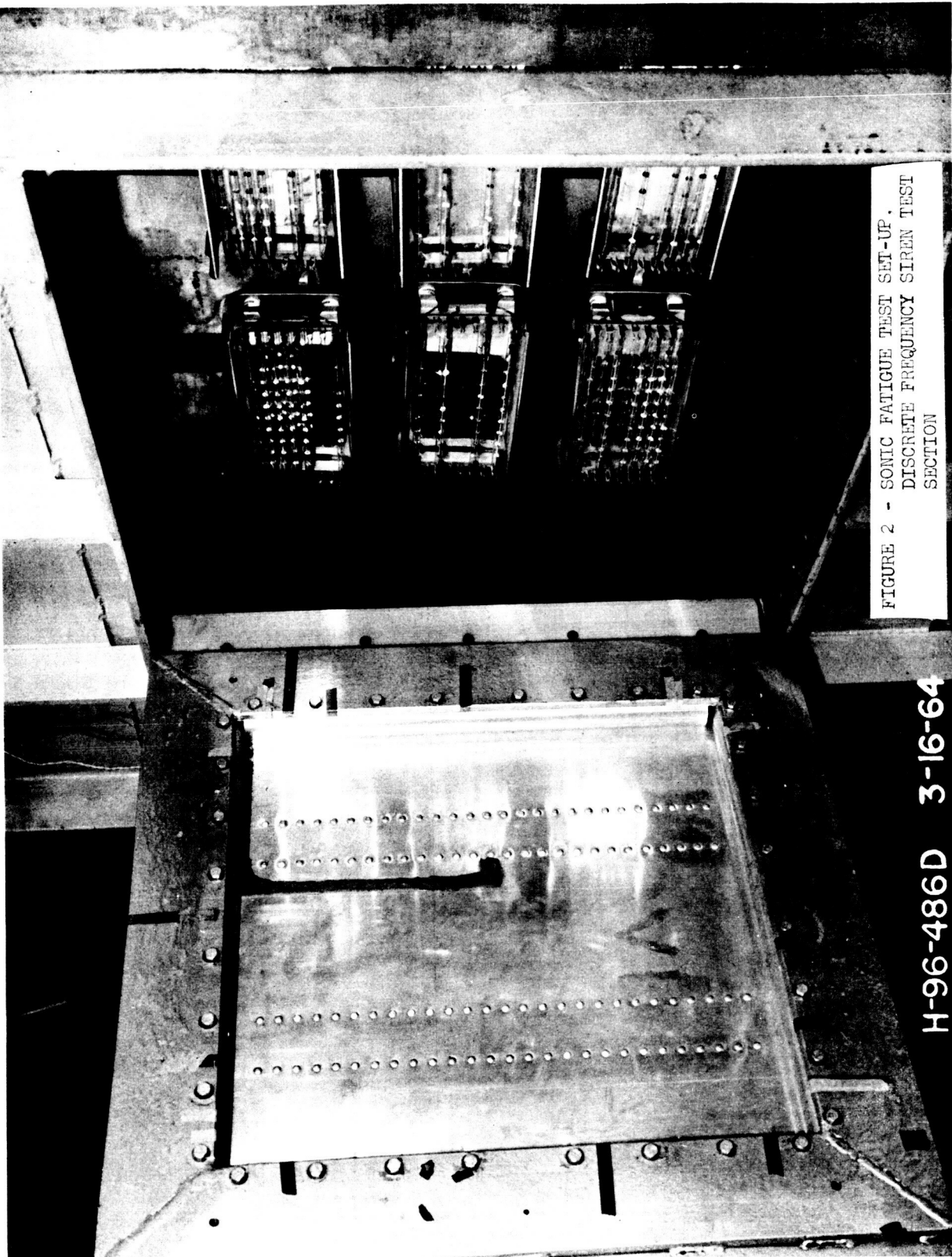


FIGURE 2 - SONIC FATIGUE TEST SET-UP.  
DISCRETE FREQUENCY SIREN TEST  
SECTION

H-96-486D 3-16-64

[illegible]

53

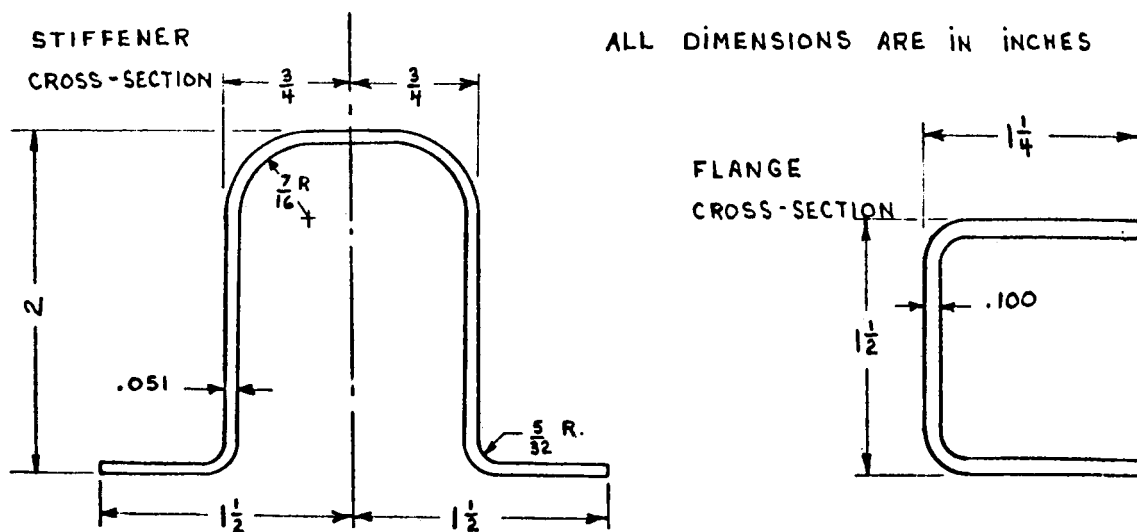
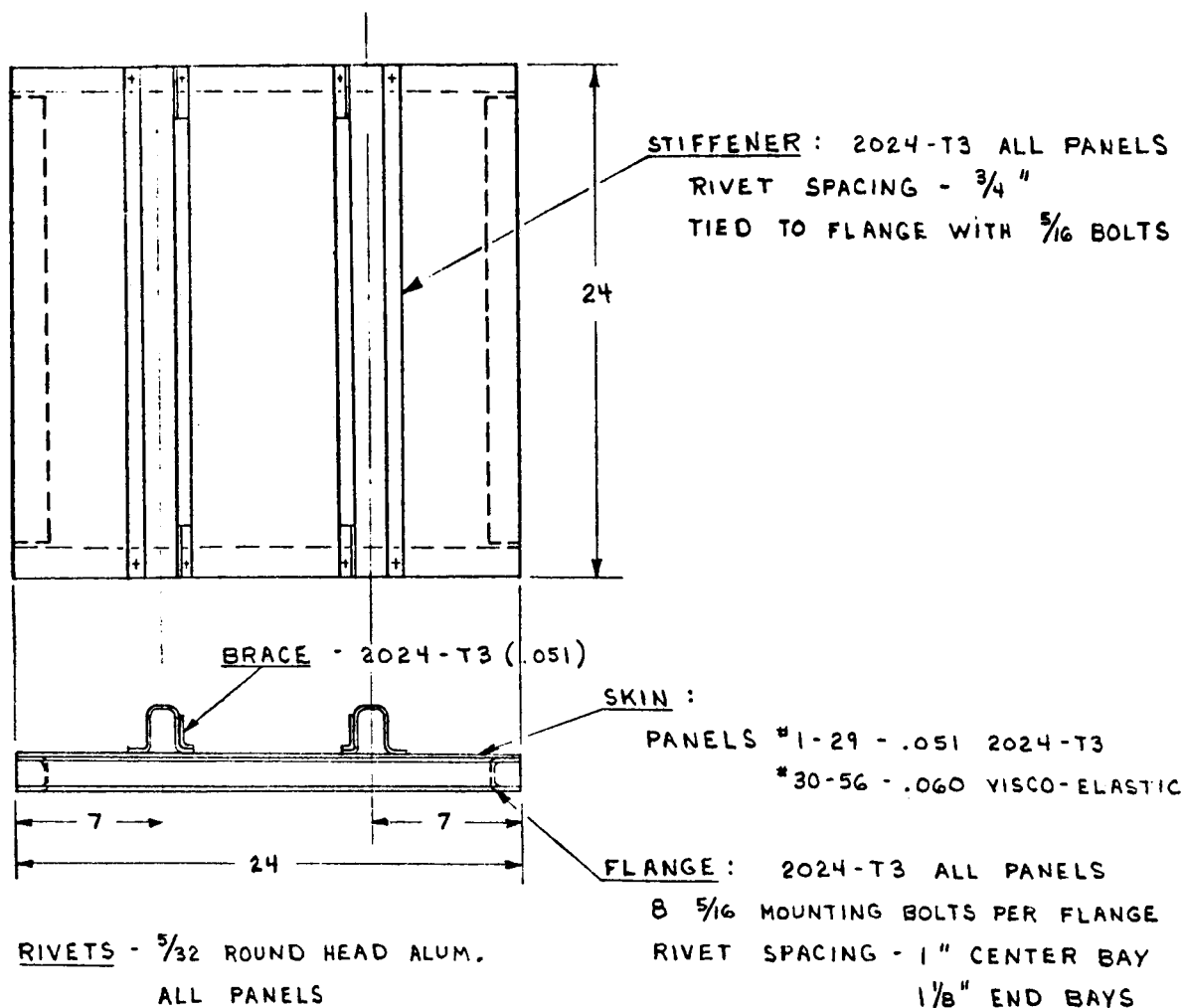


FIGURE 4 - SONIC FATIGUE TEST PANEL

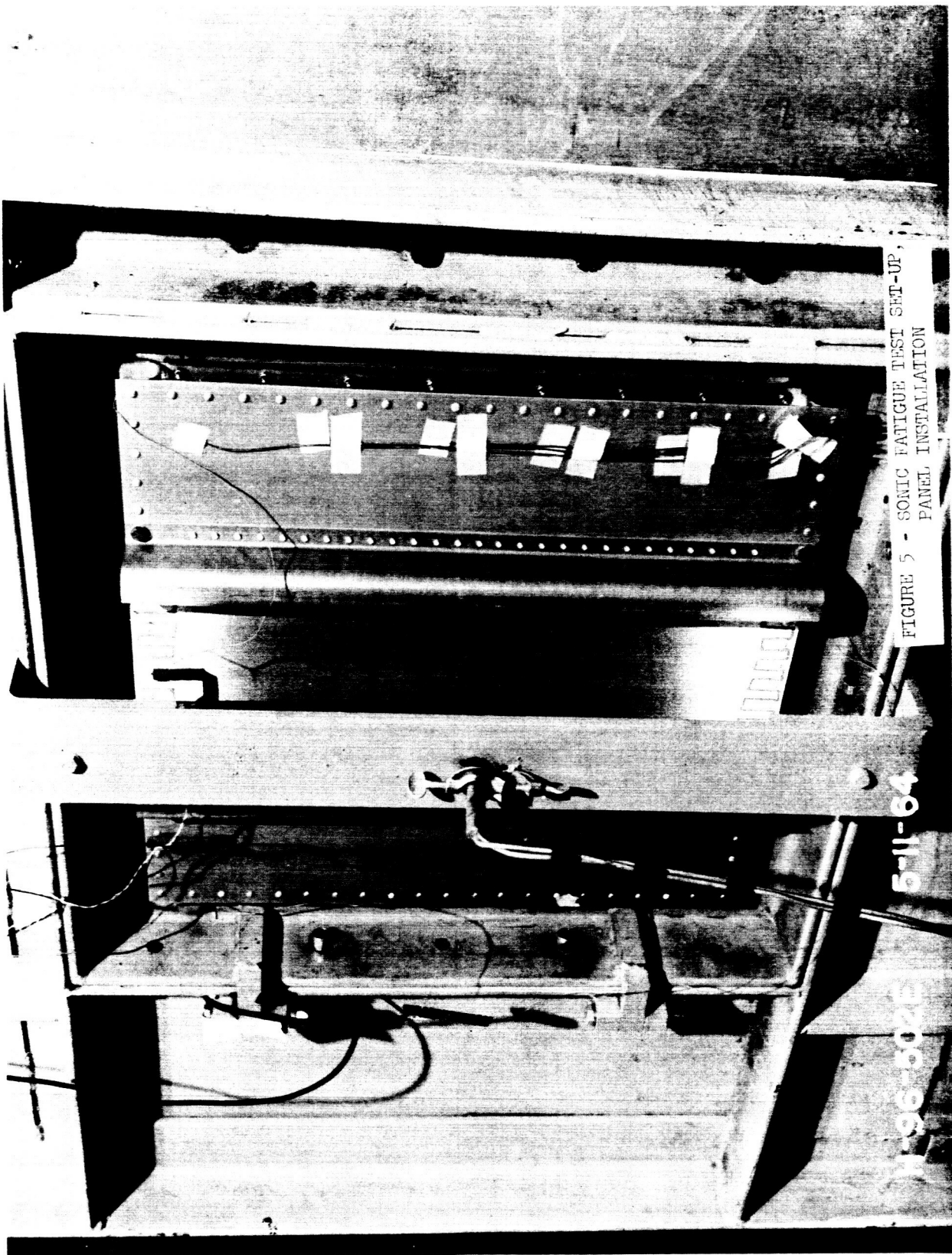


FIGURE 5 - SONIC FATIGUE TEST SET-UP,  
PANEL INSTALLATION

5-11-64

W-96-802E

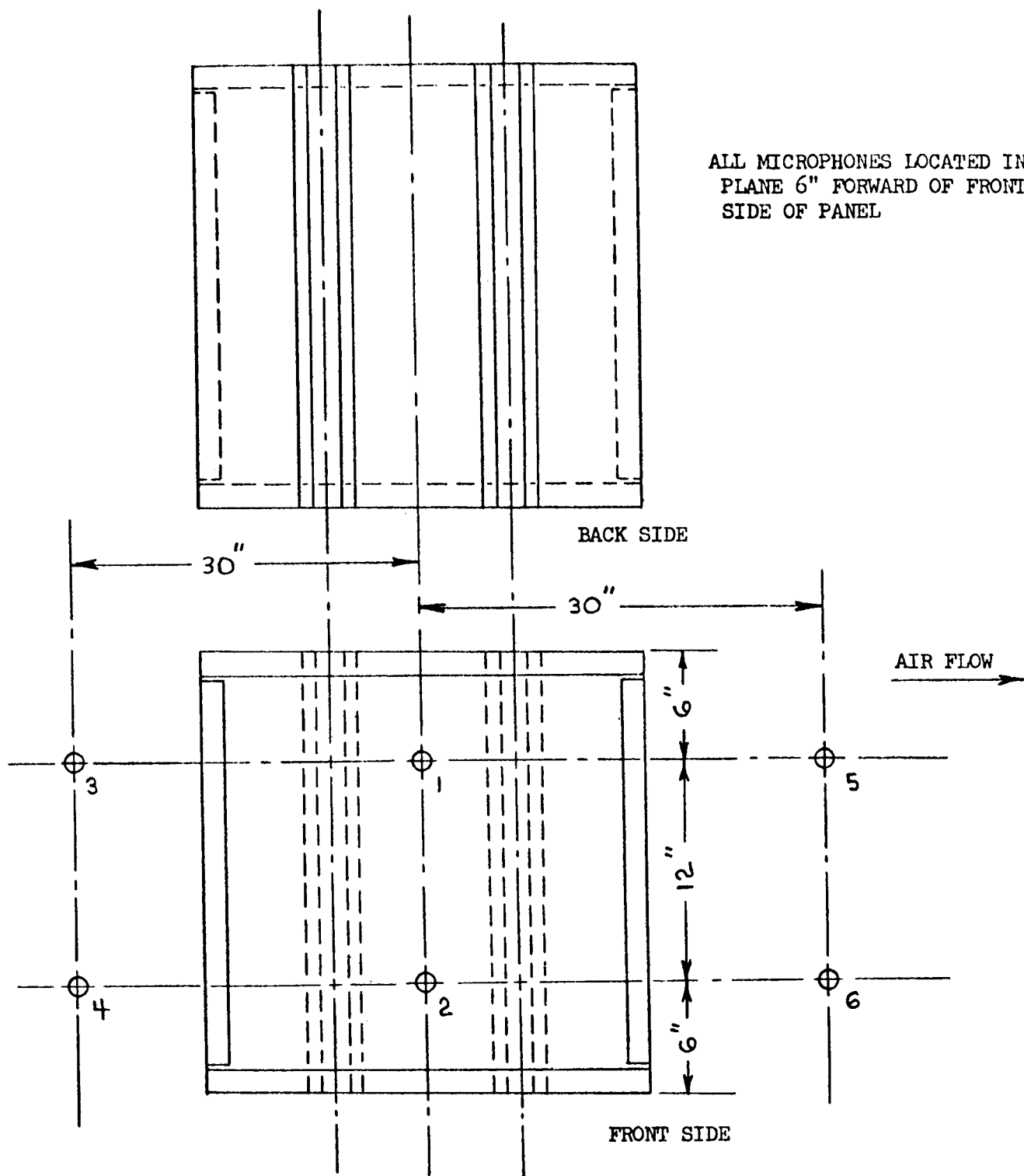
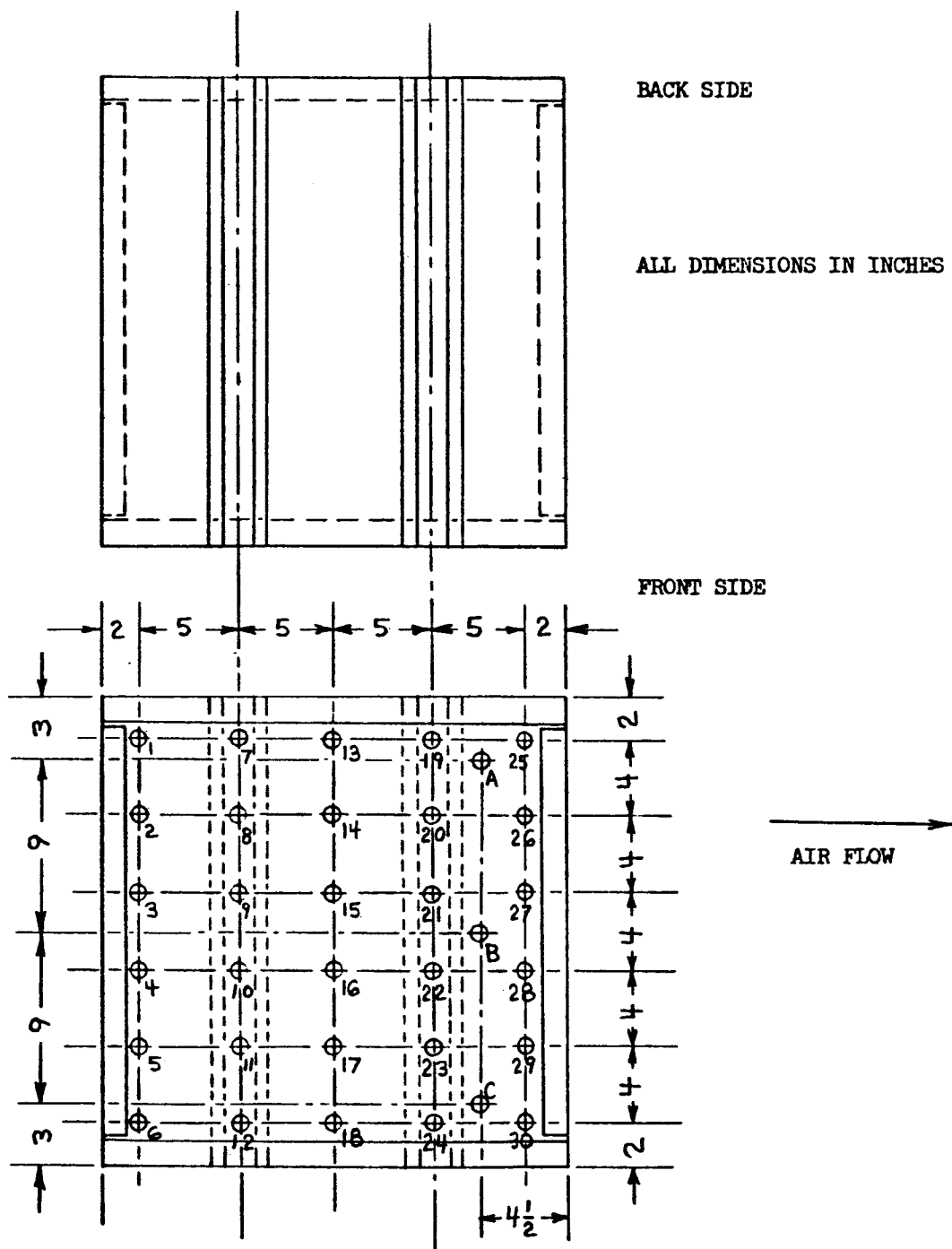


FIGURE 6 - MICROPHONE LOCATIONS FOR SONIC  
FATIGUE TESTS



CONTROL THERMOCOUPLES LOCATED AT POINTS A, B, & C  
THERMOCOUPLES AT POINTS 1 TO 6 MONITORED DURING TESTS

FIGURE 7 - THERMOCOUPLE LOCATIONS FOR SONIC FATIGUE TESTS AND PANEL TEMPERATURE DISTRIBUTION SURVEYS

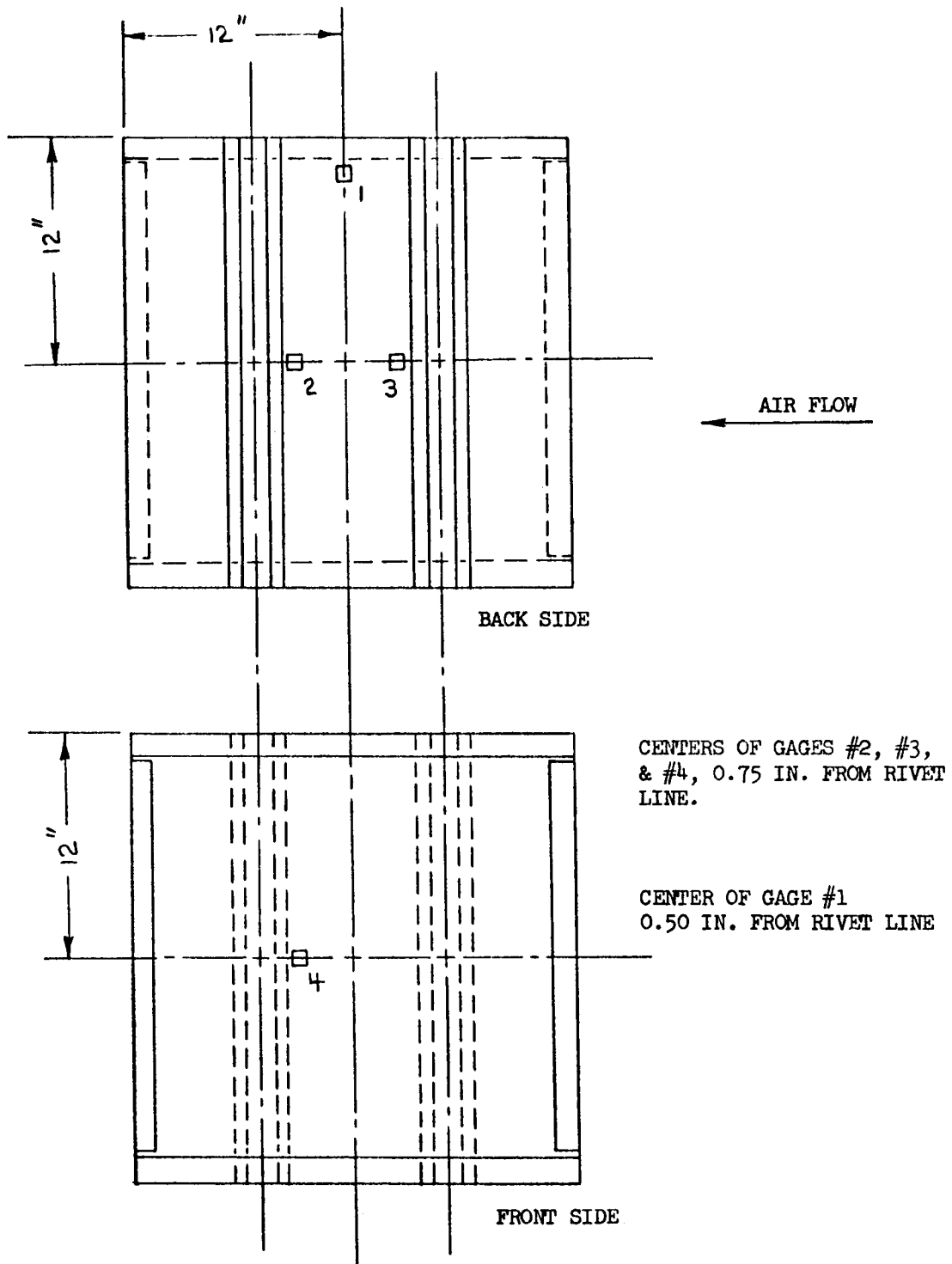


FIGURE 8 - STRAIN GAGE LOCATIONS FOR SONIC FATIGUE TESTS

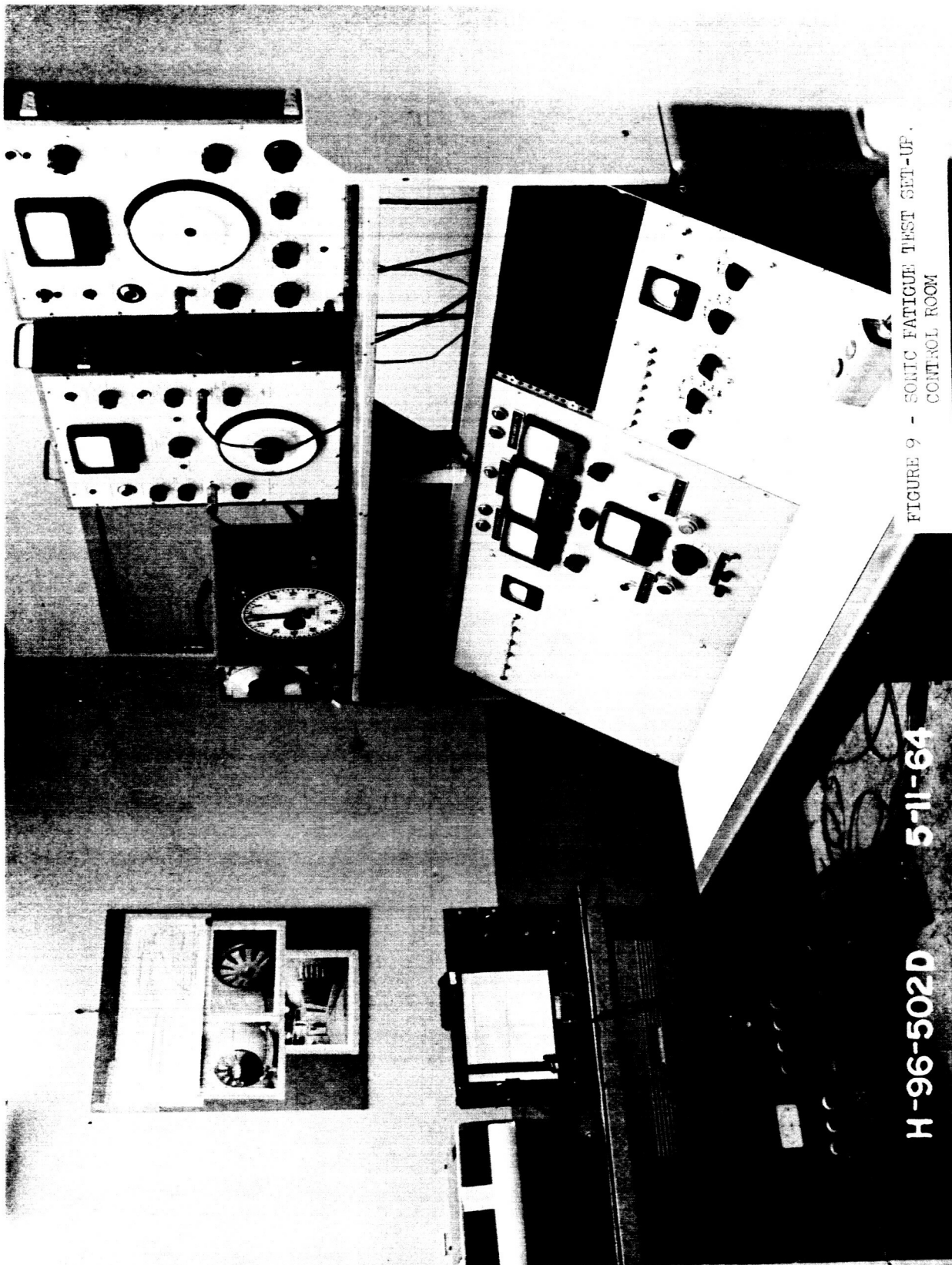
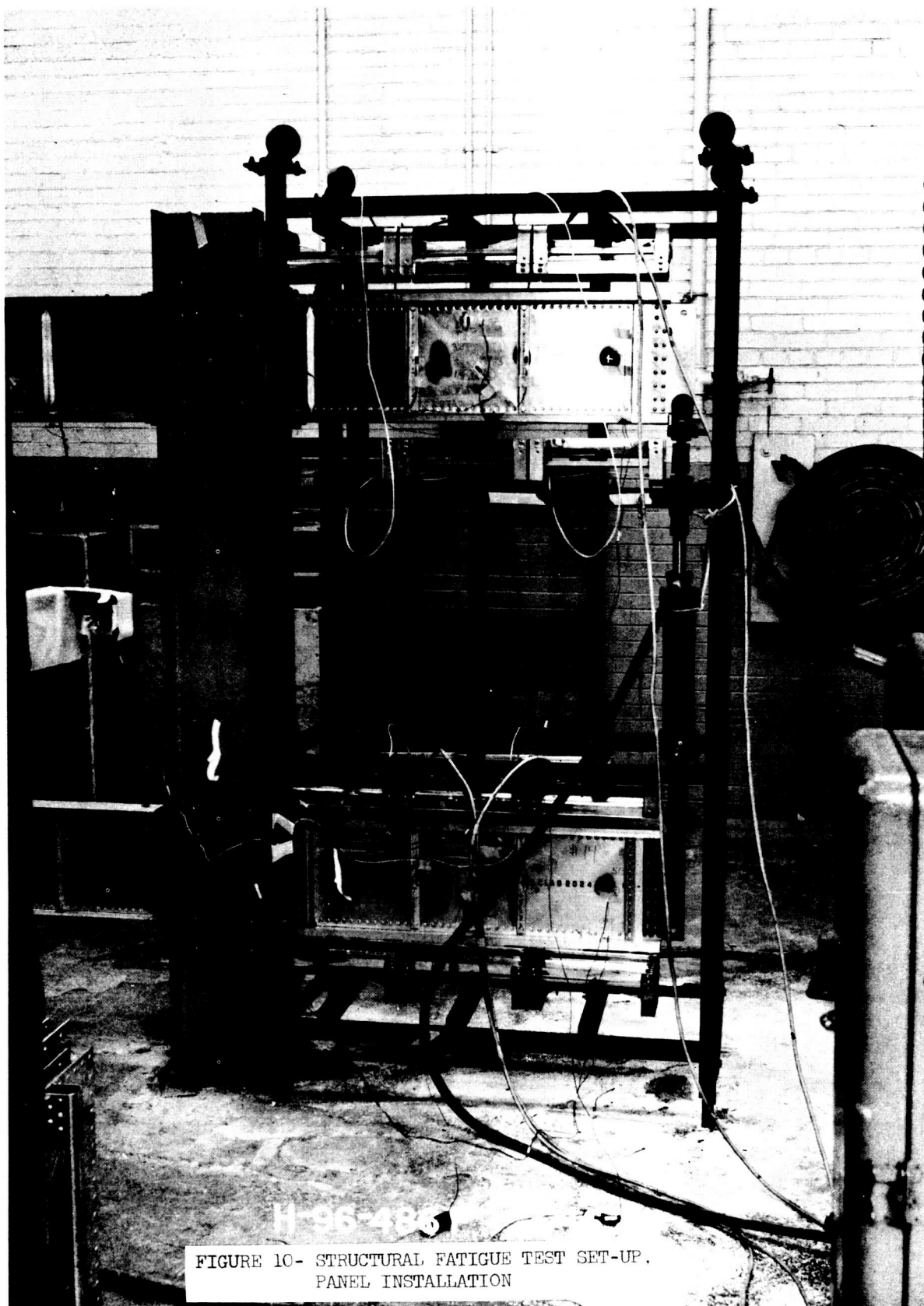


FIGURE 9 - SONIC FATIGUE TEST SET-UP.  
CONTROL ROOM

5-11-64

H-96-502D



H-96-486  
FIGURE 10- STRUCTURAL FATIGUE TEST SET-UP.  
PANEL INSTALLATION

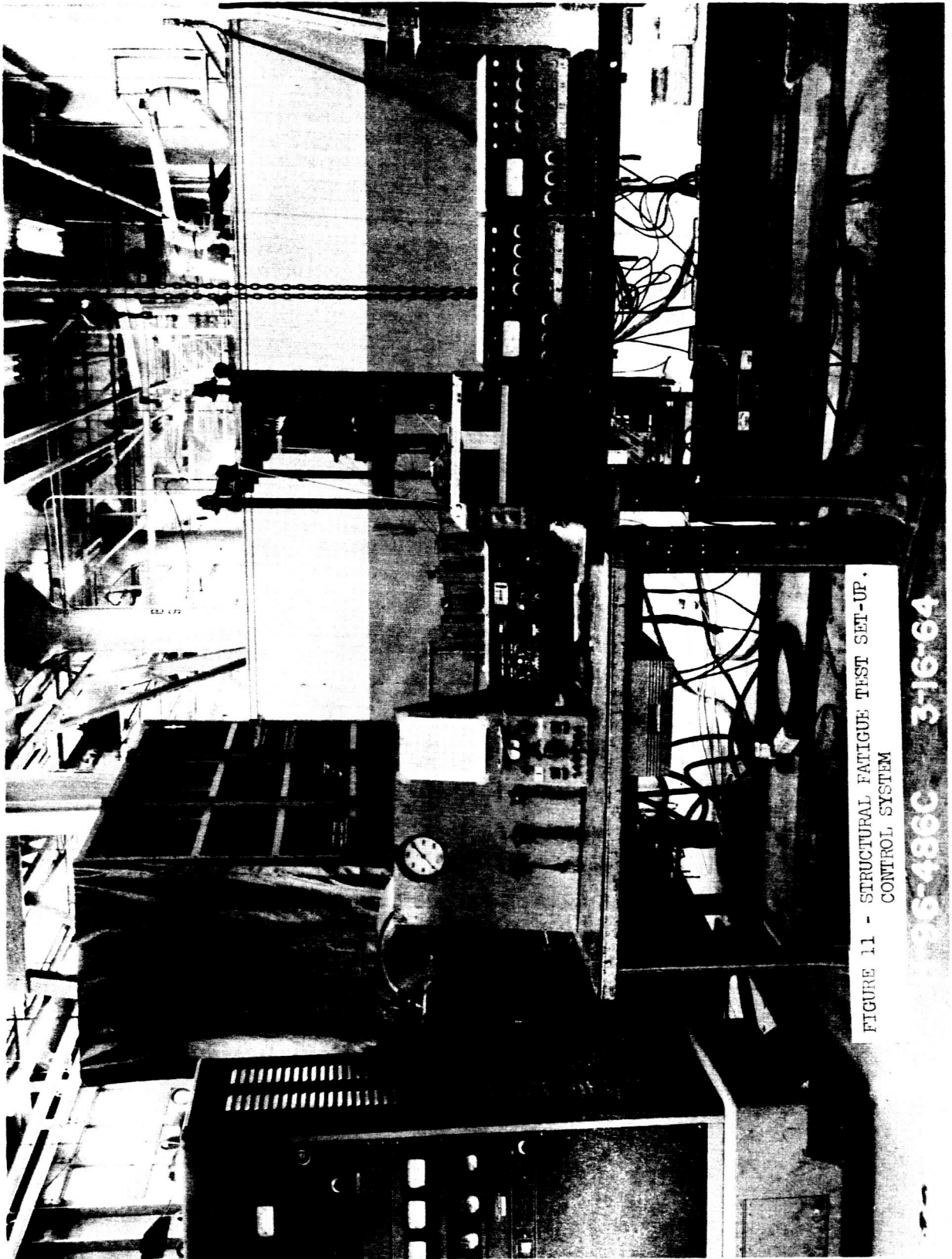


FIGURE 11 - STRUCTURAL FATIGUE TEST SET-UP,  
CONTROL SYSTEM

3-16-64 3-16-64

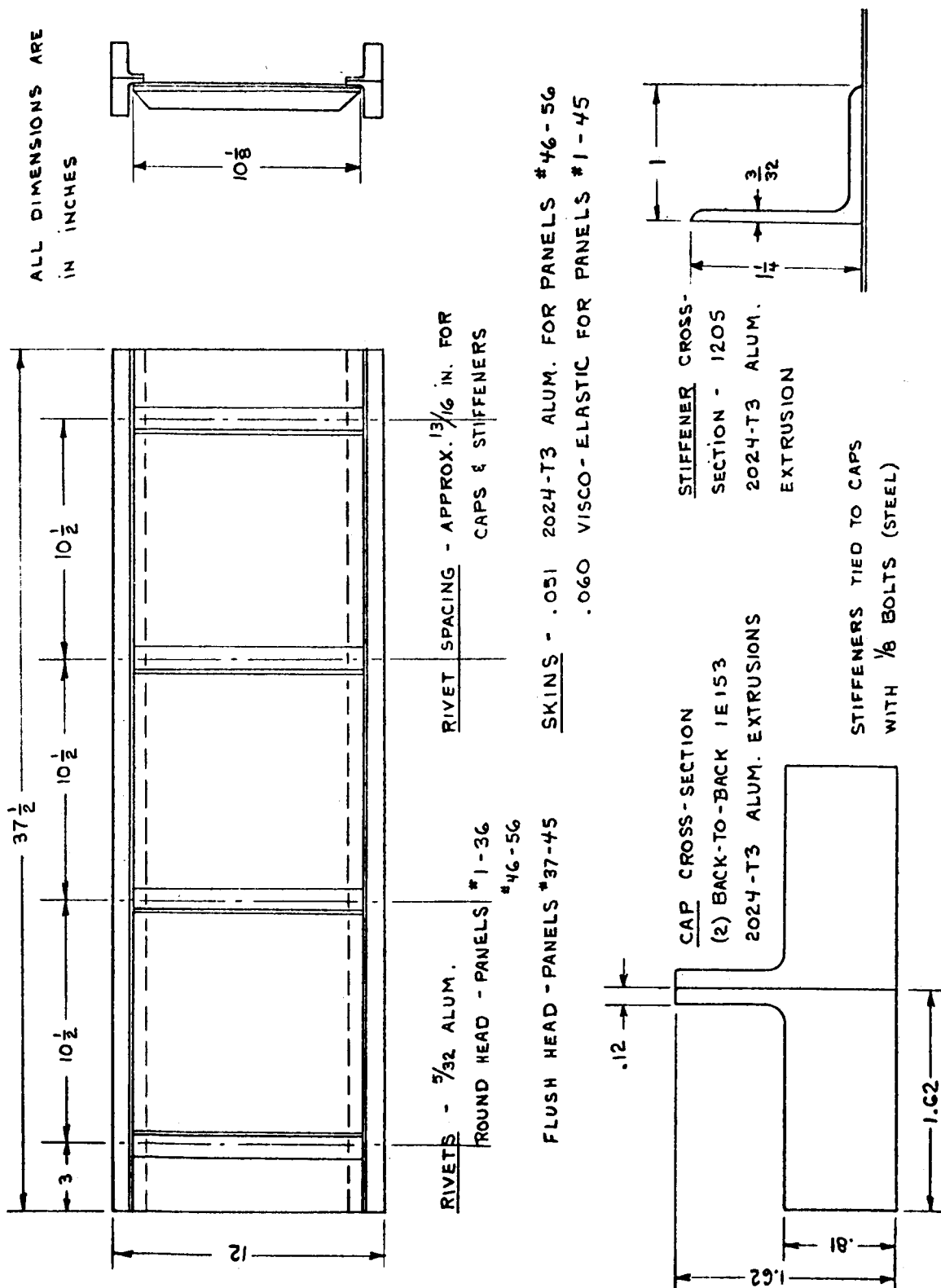


FIGURE 12 - STRUCTURAL FATIGUE TEST PANEL



CONTROL THERMOCOUPLE  
LOCATED AT POINT A

THERMOCOUPLES #1 & #4 MONITORED  
DURING TESTS

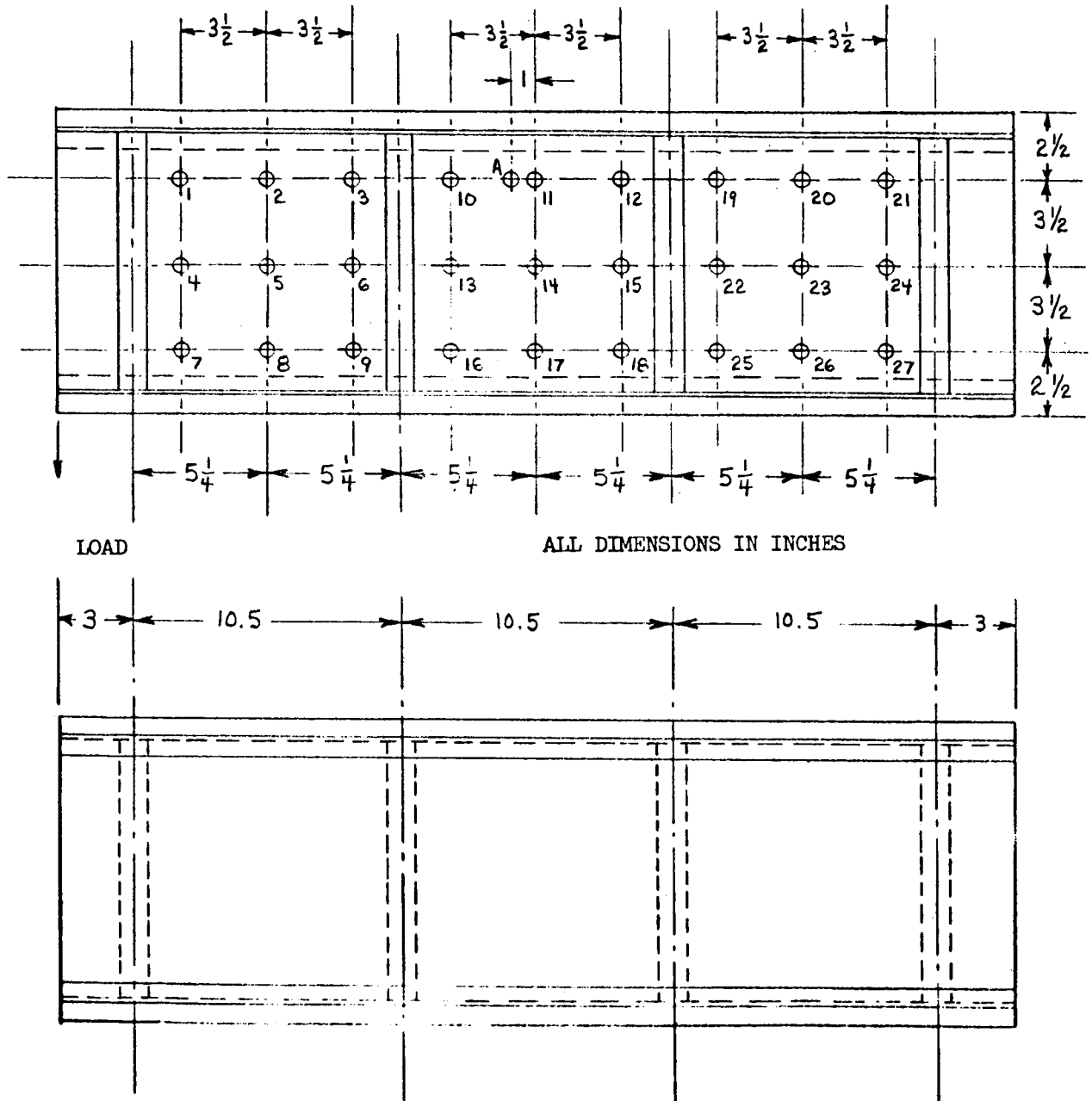


FIGURE 14 - THERMOCOUPLE LOCATIONS FOR STRUCTURAL FATIGUE TESTS AND PANEL TEMPERATURE DISTRIBUTION SURVEYS

CENTERS OF GAGES #5, #6 & #7 0.87 IN. FROM BAY CENTER.  
CENTERS OF GAGES #8, & #9 0.50 IN. FROM RIVET LINES.

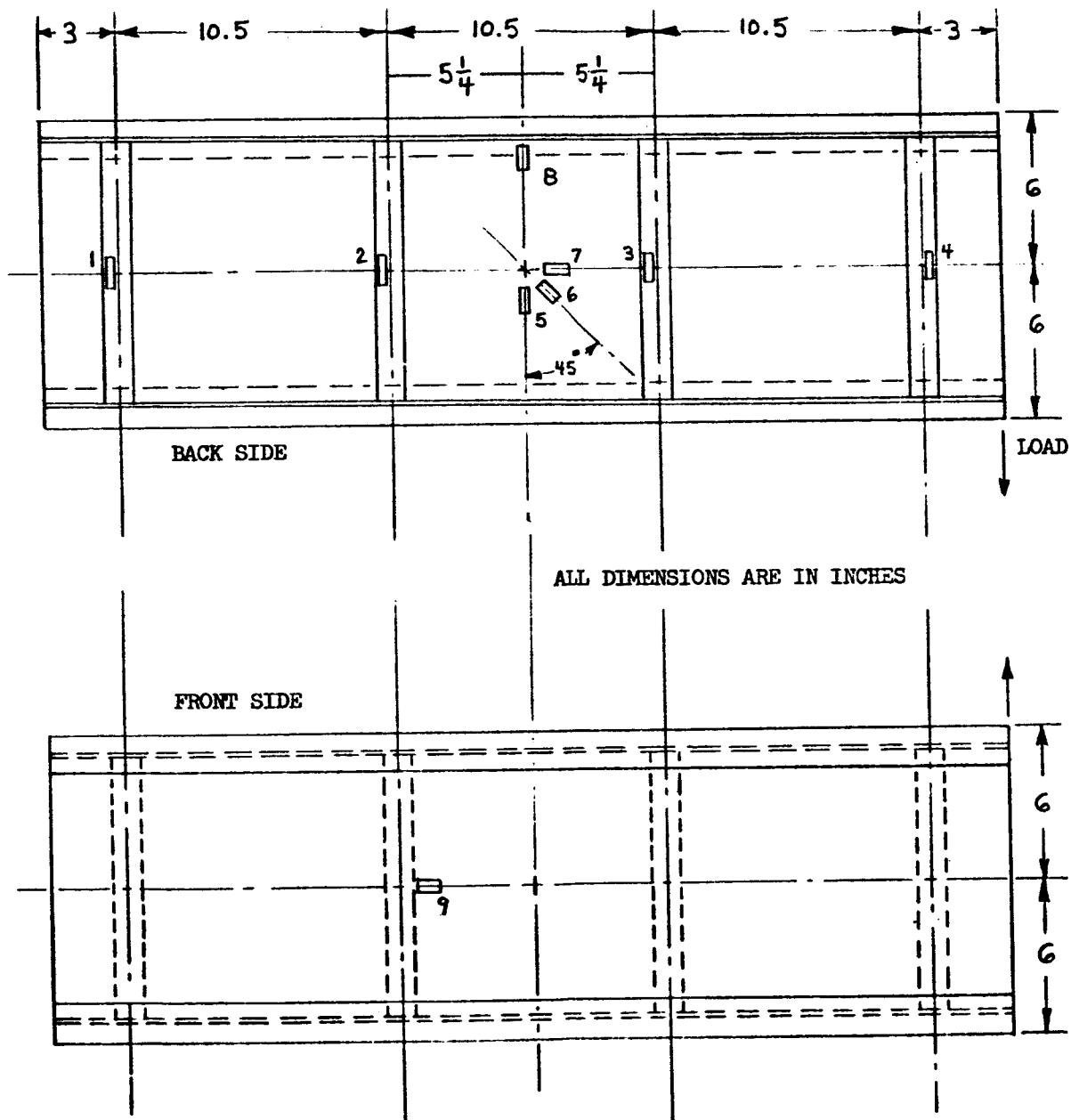
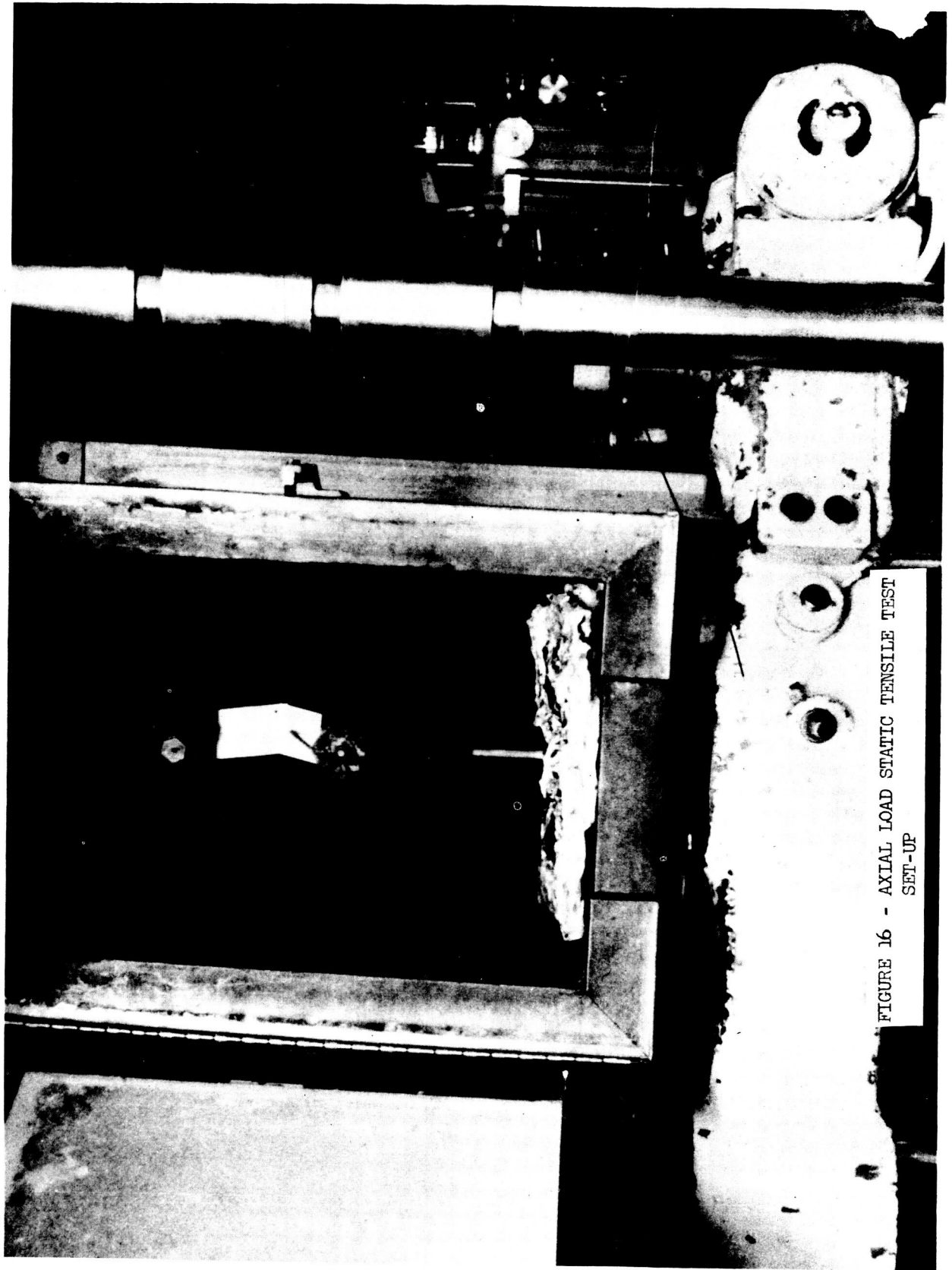


FIGURE 15 - STRAIN GAGE LOCATIONS FOR STRUCTURAL FATIGUE TESTS





**ALUM. REINFORCEMENT & LOADING PLATES USED FOR ALL SPECIMENS**

VISCO-ELASTIC MATERIAL (DYNA-DAMP) HAS:

- .020 IN. THICK 2024-T3 ALUM. ALLOY SKINS
- .020 IN. THICK ELASTOMER INTERLAYER

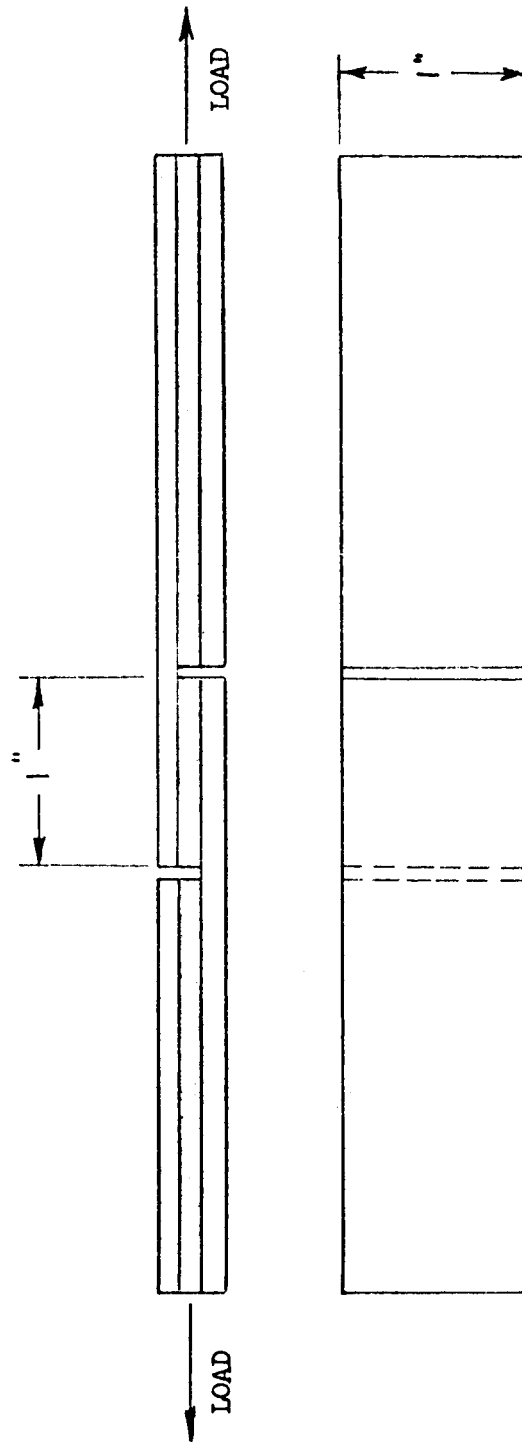


FIGURE 18 - VISCO-ELASTIC MATERIAL STATIC SHEAR SPECIMEN

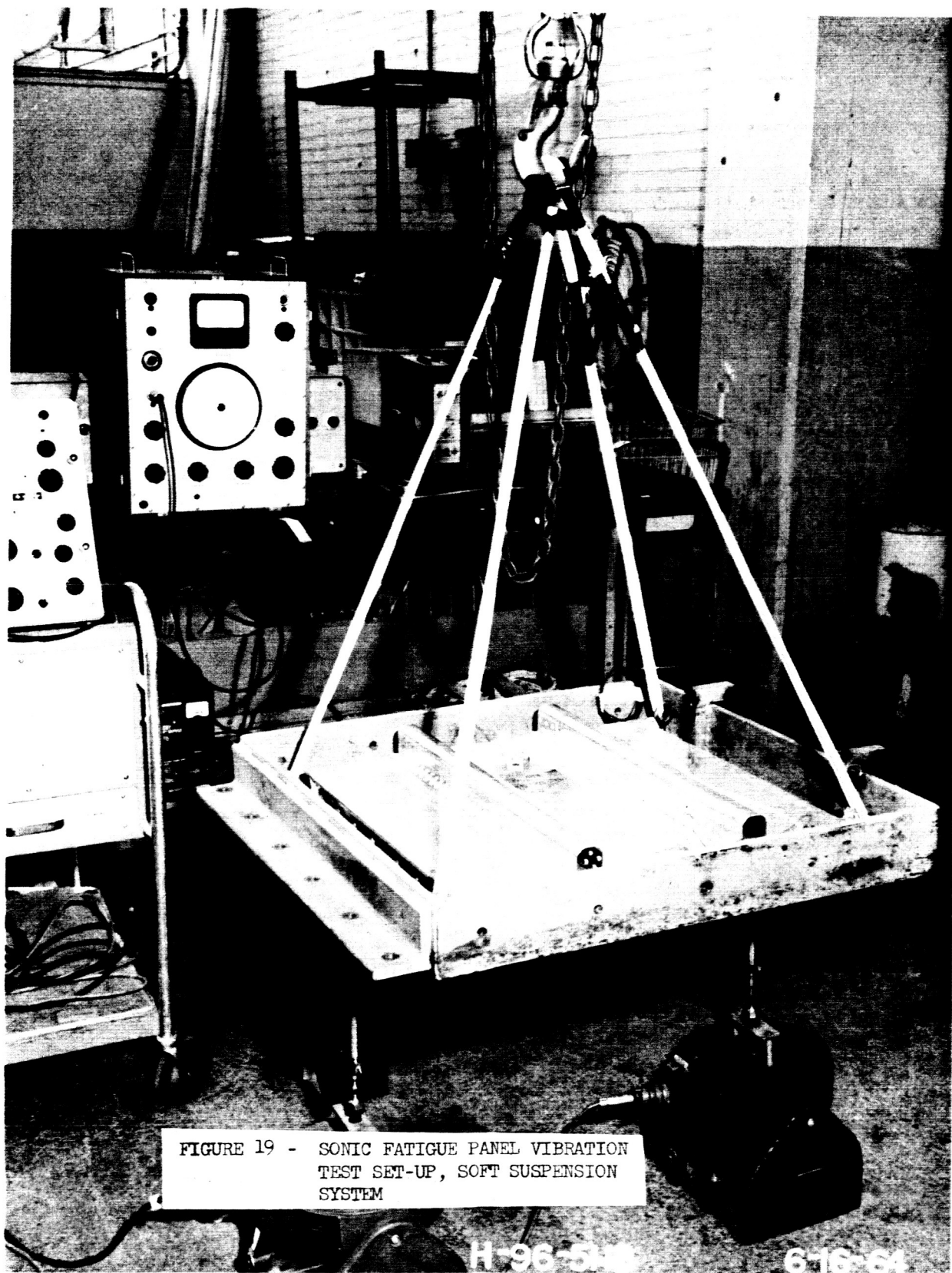


FIGURE 19 - SONIC FATIGUE PANEL VIBRATION  
TEST SET-UP, SOFT SUSPENSION  
SYSTEM

H-96-5-10

6-16-64

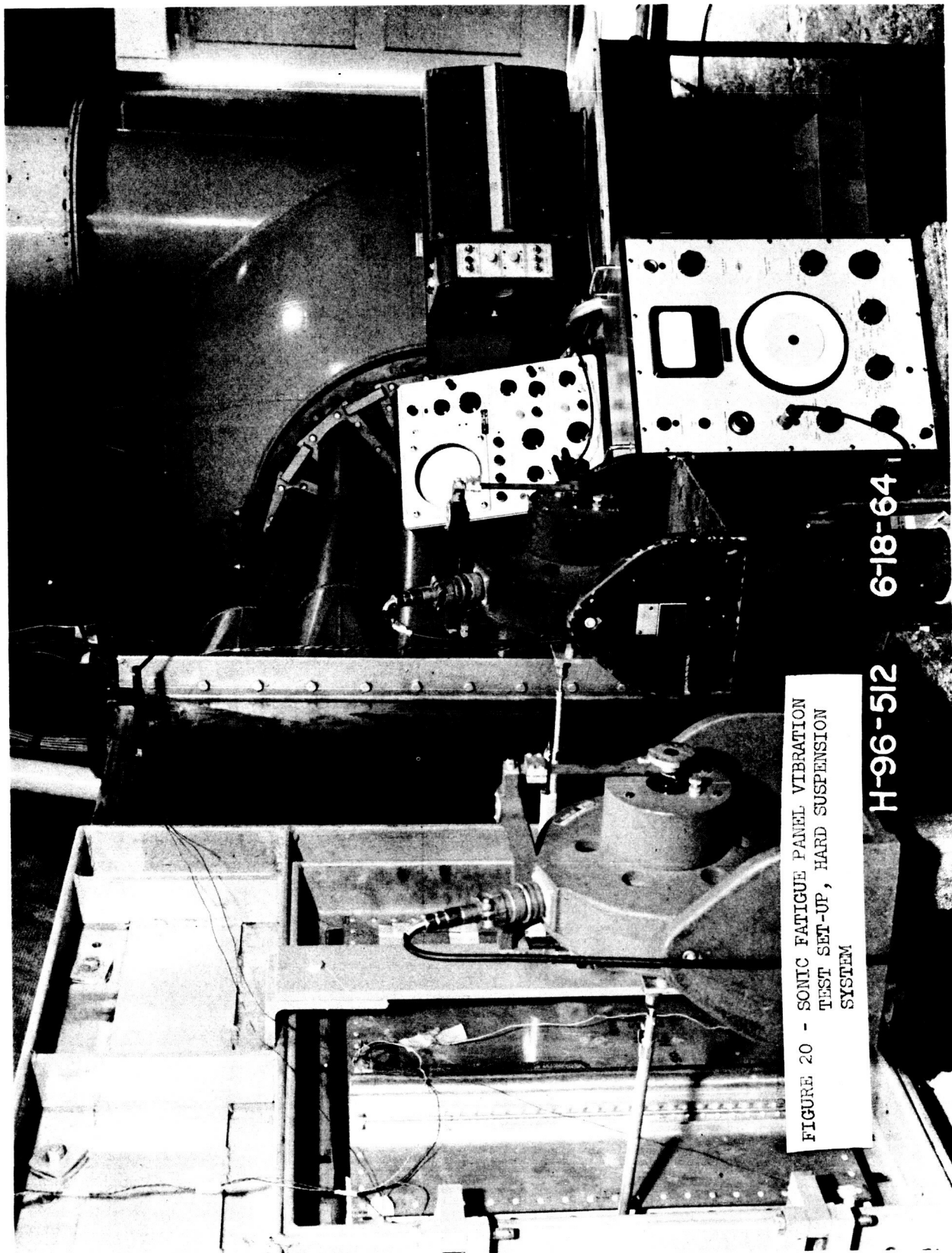
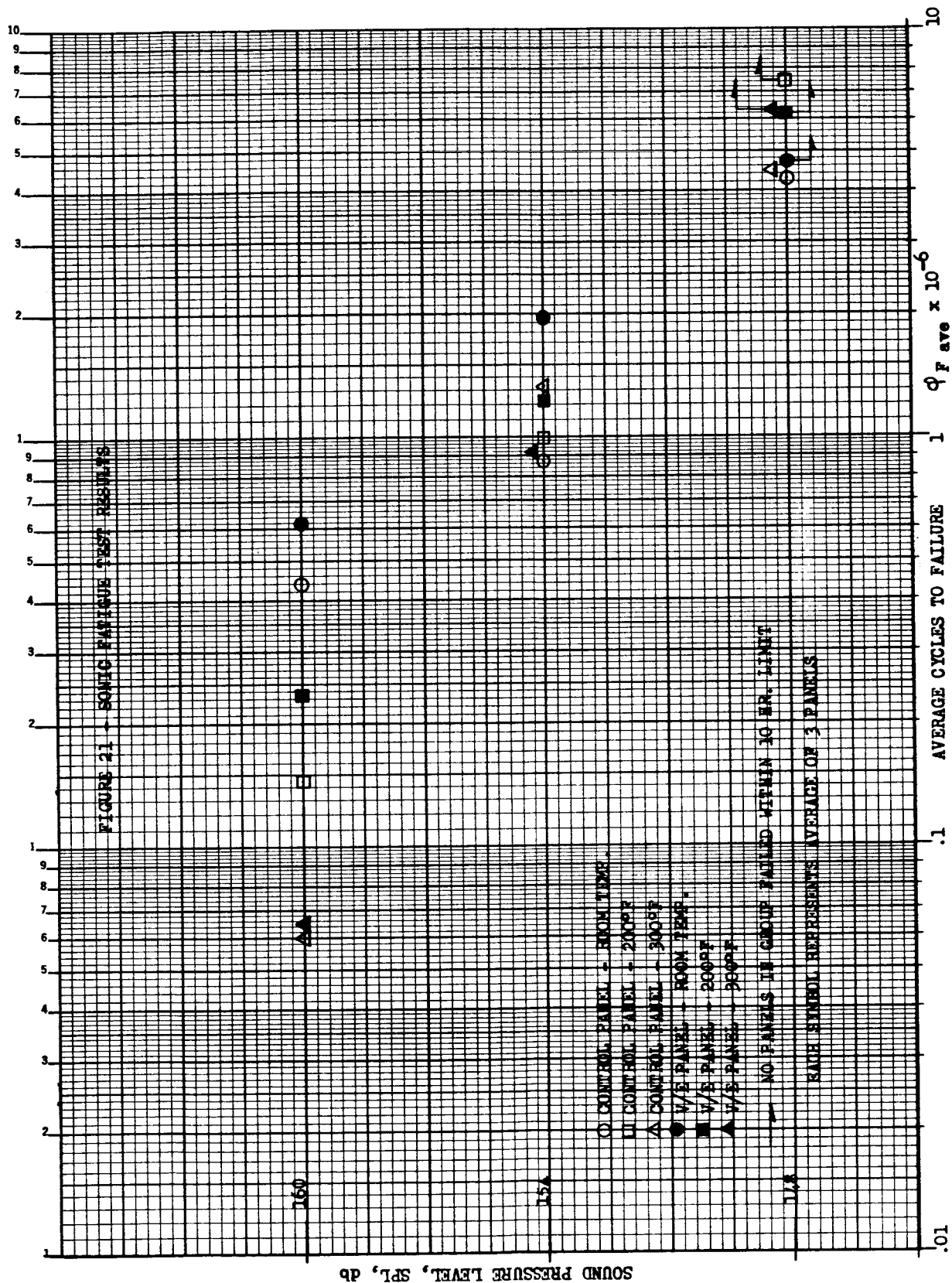


FIGURE 20 - SONIC FATIGUE PANEL VIBRATION  
TEST SET-UP, HARD SUSPENSION  
SYSTEM

6-18-64

H-96-512



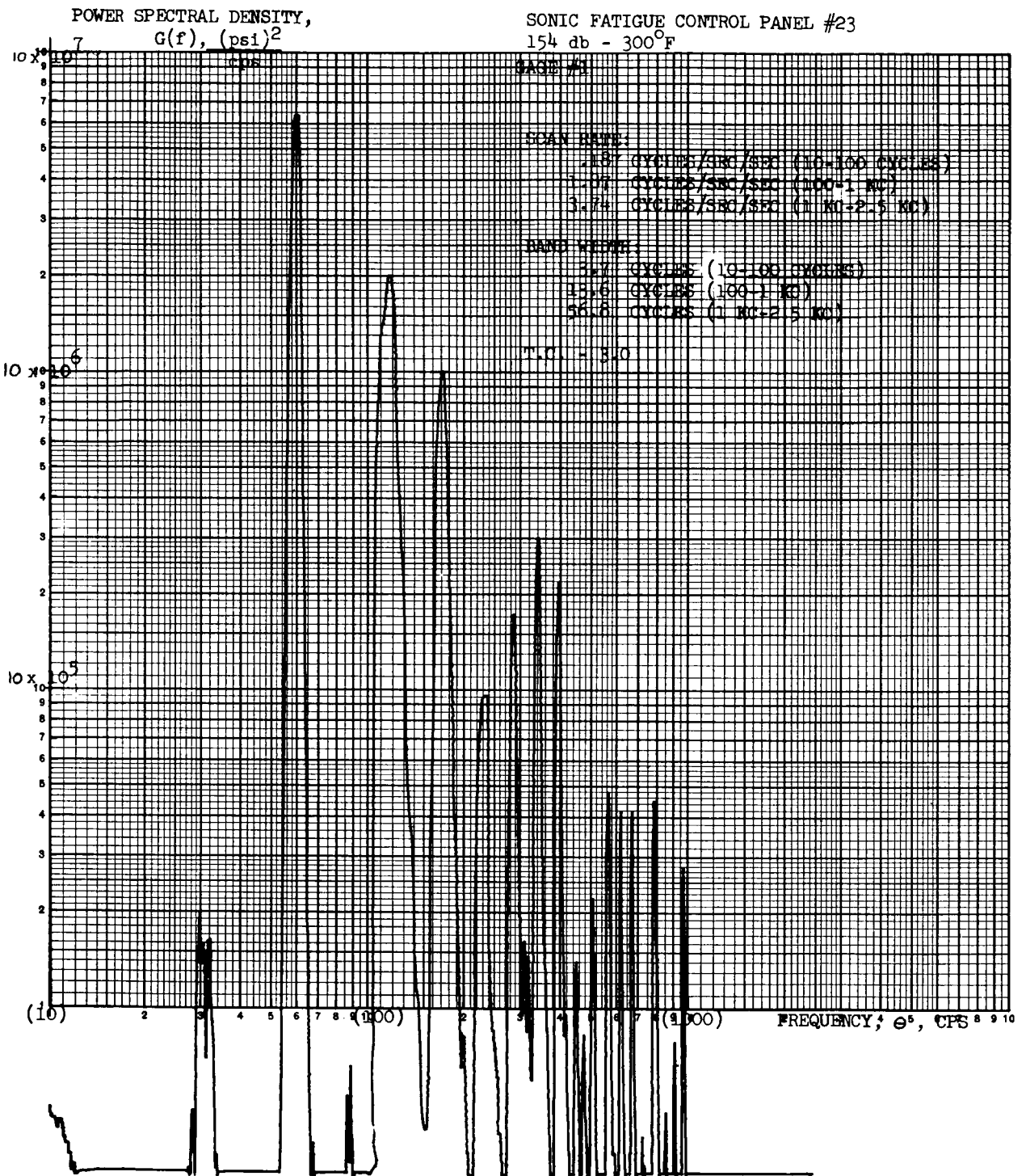


FIGURE 22 - POWER SPECTRAL DENSITY, 154 DB - 300°F, GAGE #1

POWER SPECTRAL DENSITY,  
 $G(f), \frac{(\text{psi})^2}{\text{cps}}$

SONIC FATIGUE CONTROL PANEL #23  
 154 db - 300°F  
 GAGE #2

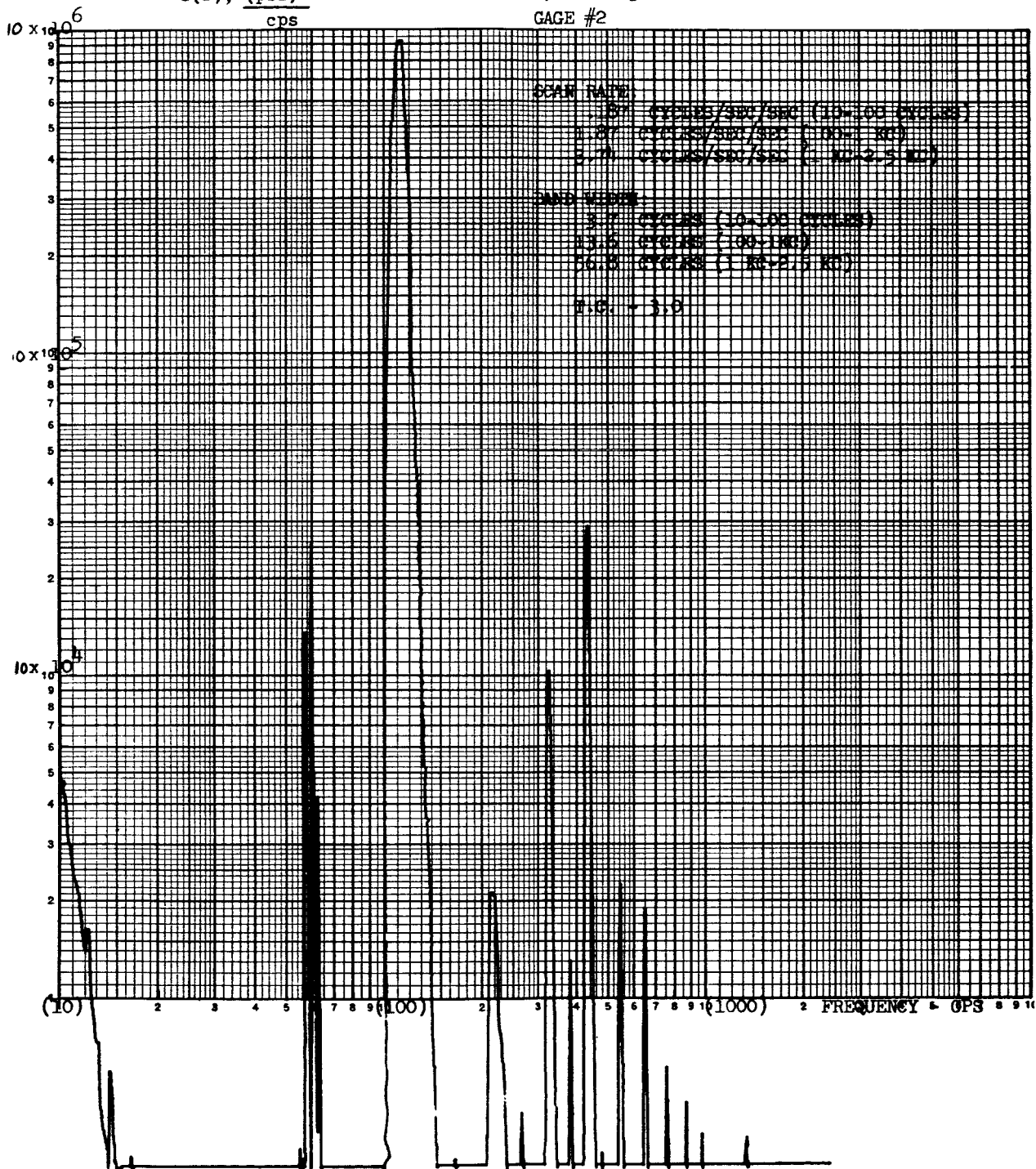


FIGURE 23 - POWER SPECTRAL DENSITY, 154 DB - 300°F, GAGE #2

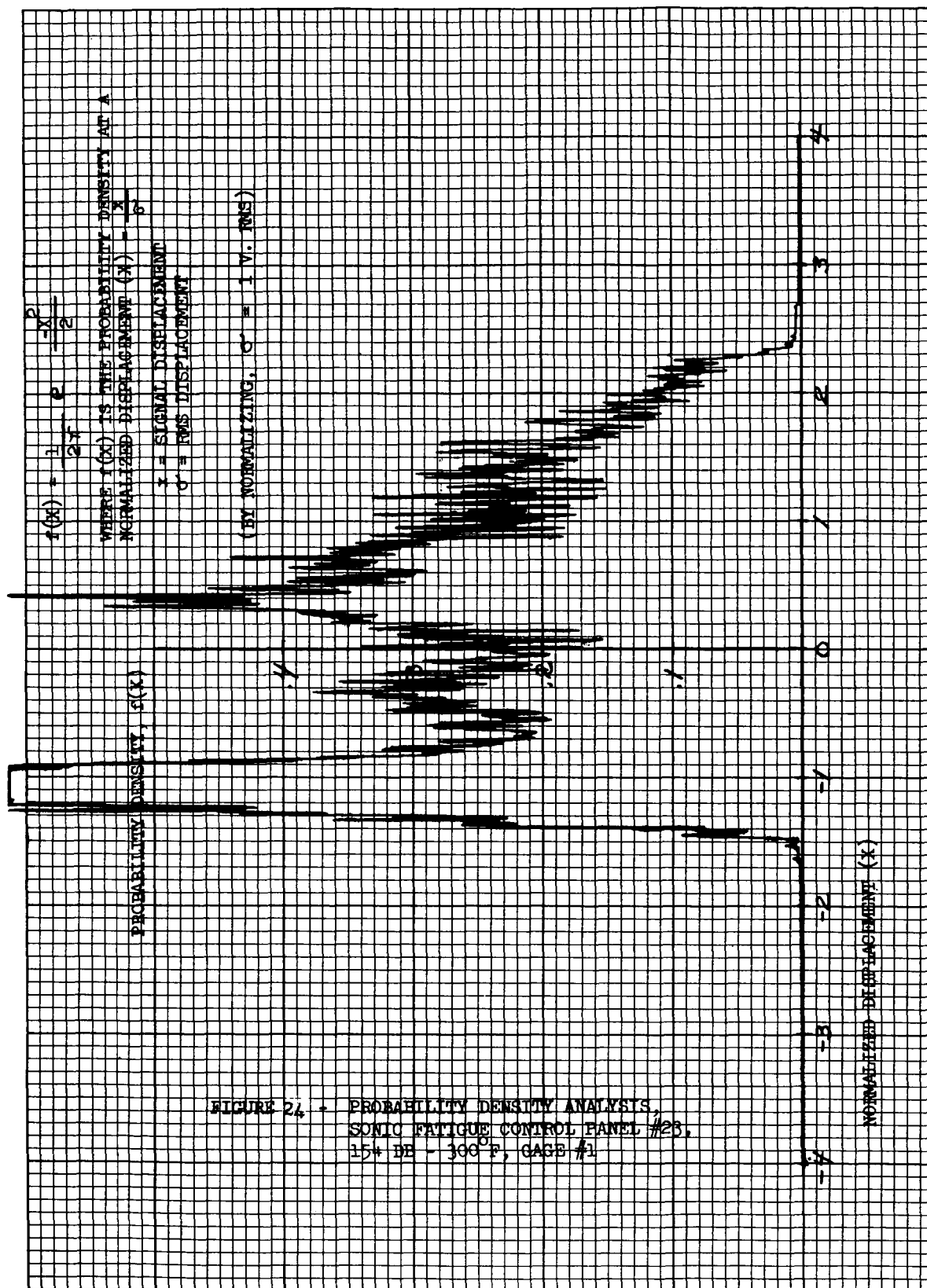
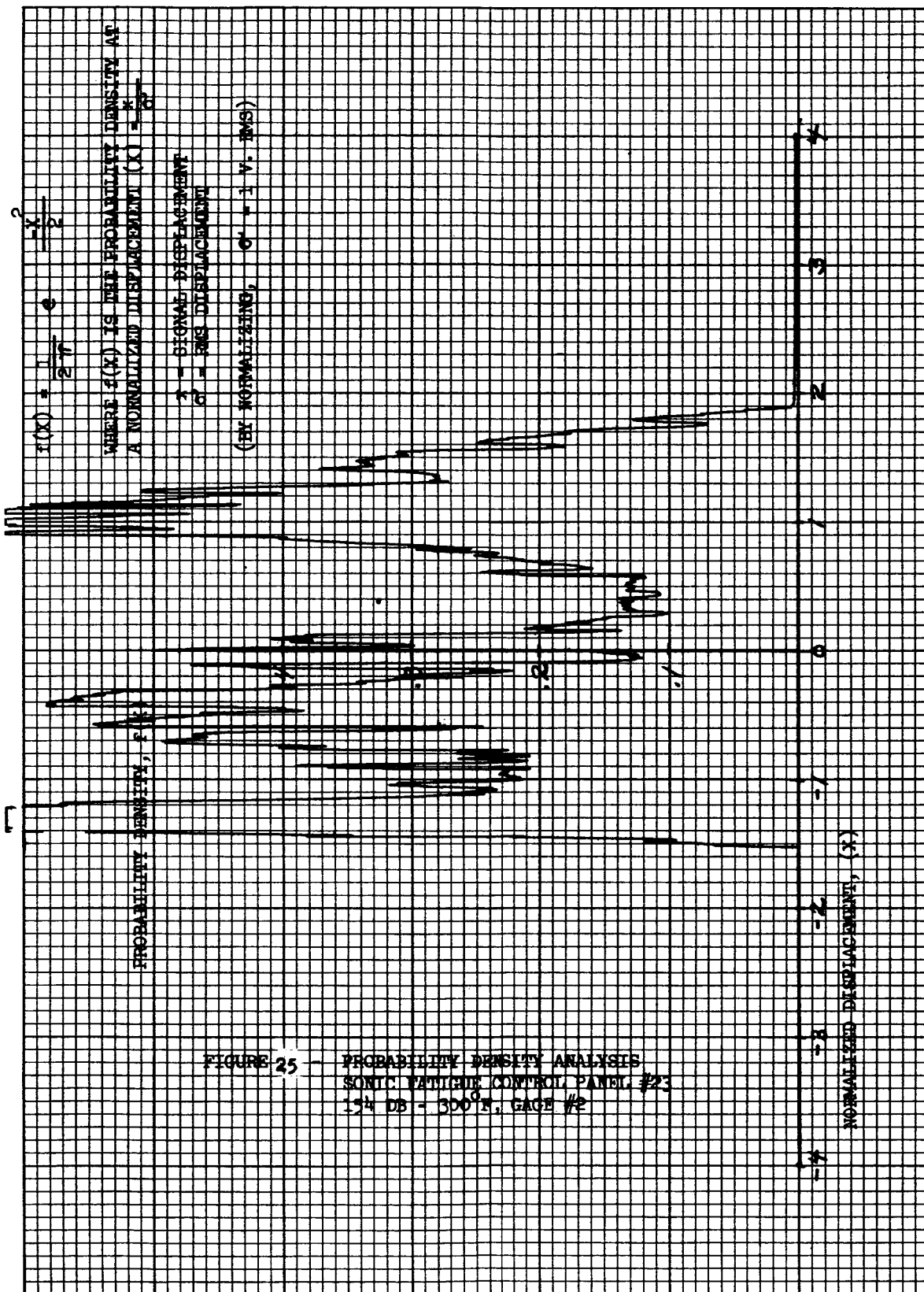


FIGURE 24 - PROBABILITY DENSITY ANALYSIS,  
 SONIC FATIGUE CONTROL PANEL #23,  
 15\* DE - 300° F, CASE #1



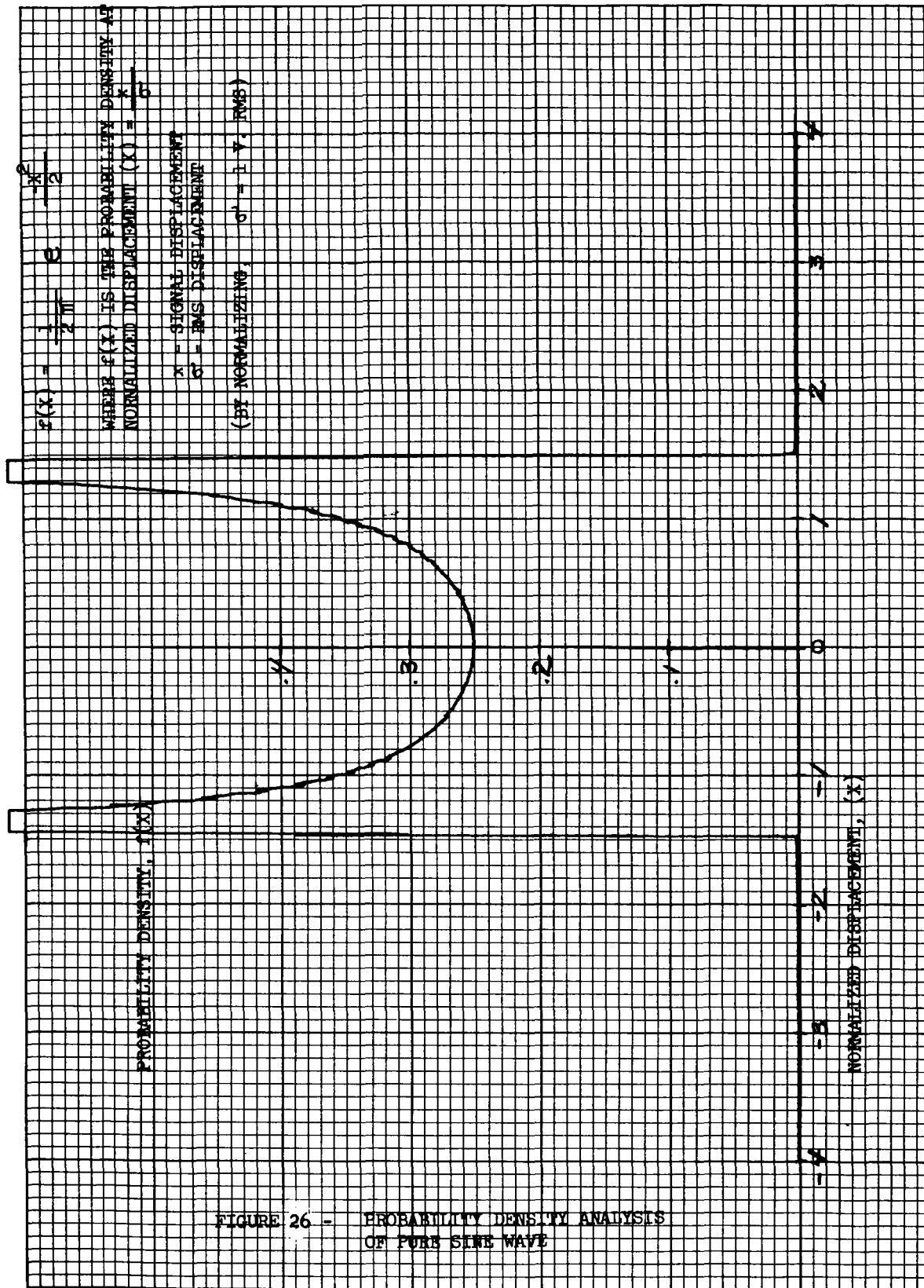
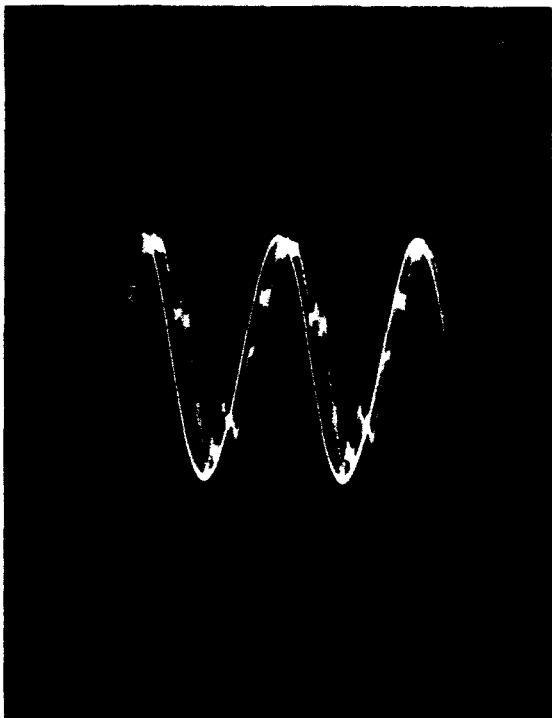
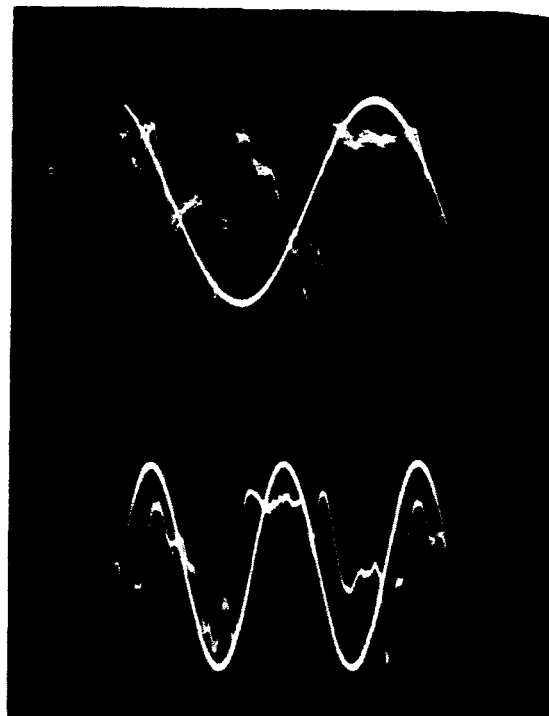


FIGURE 26 - PROBABILITY DENSITY ANALYSIS  
OF PURE SINE WAVE

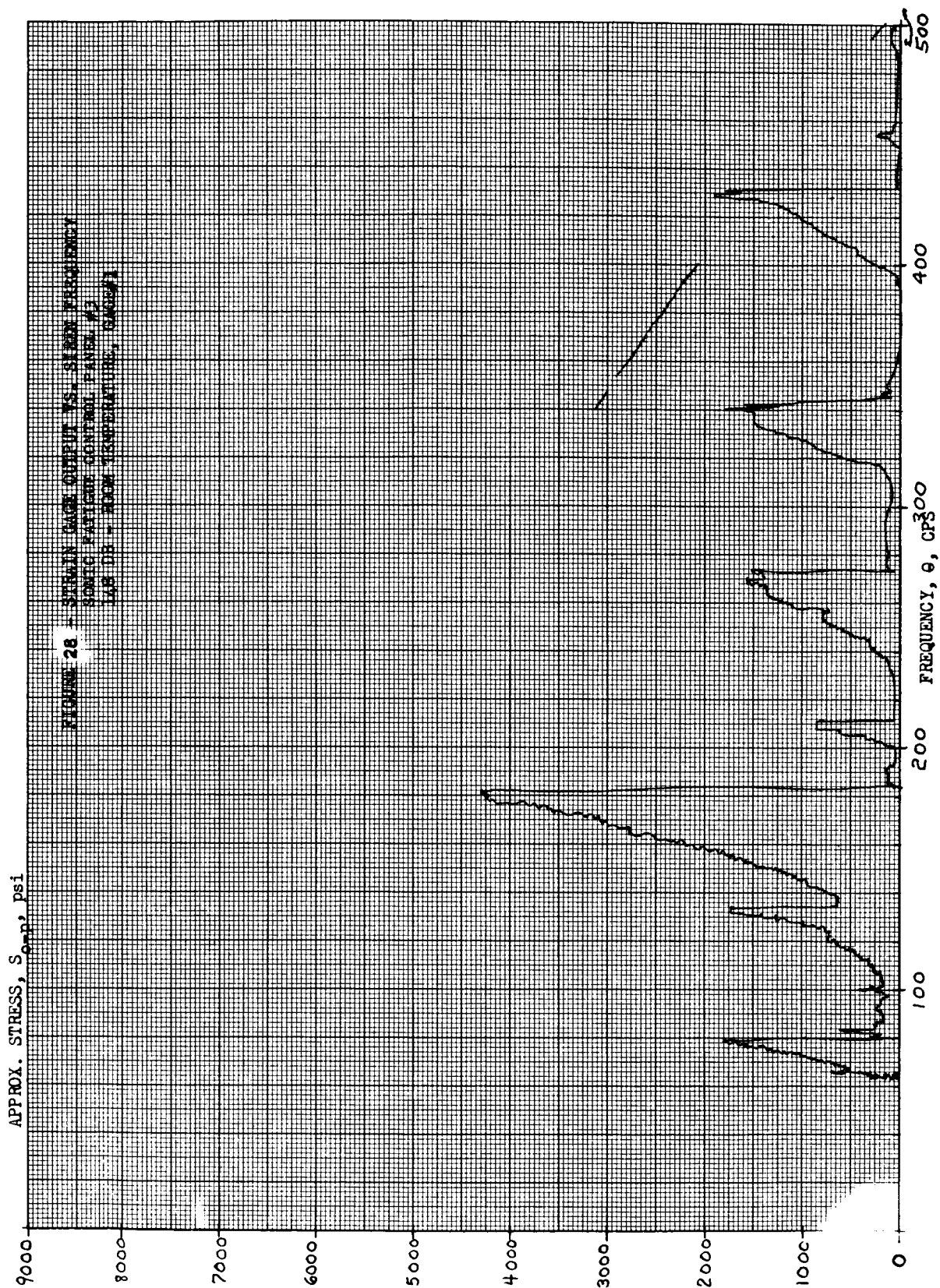


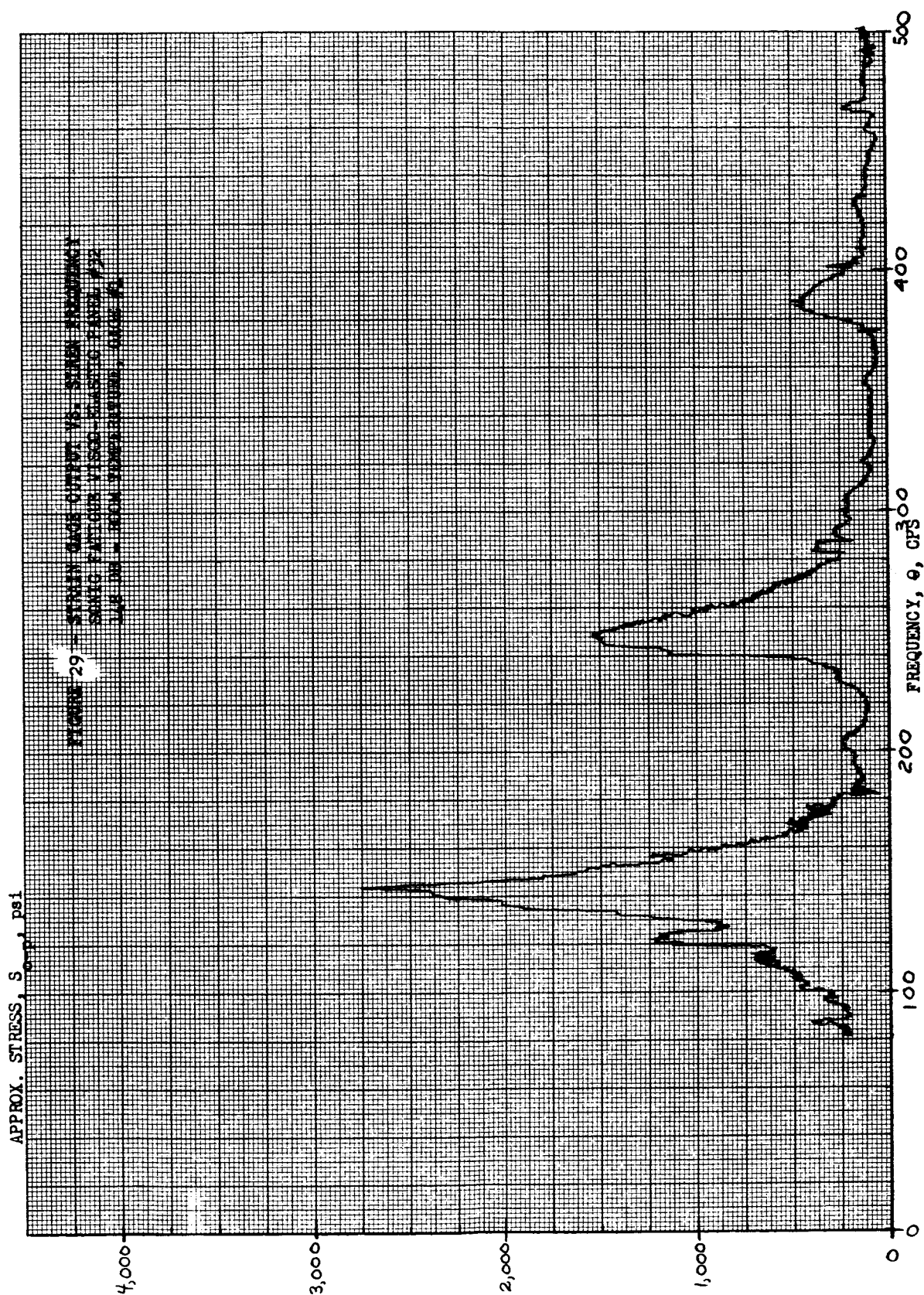
PANEL #23 - GAGE #2

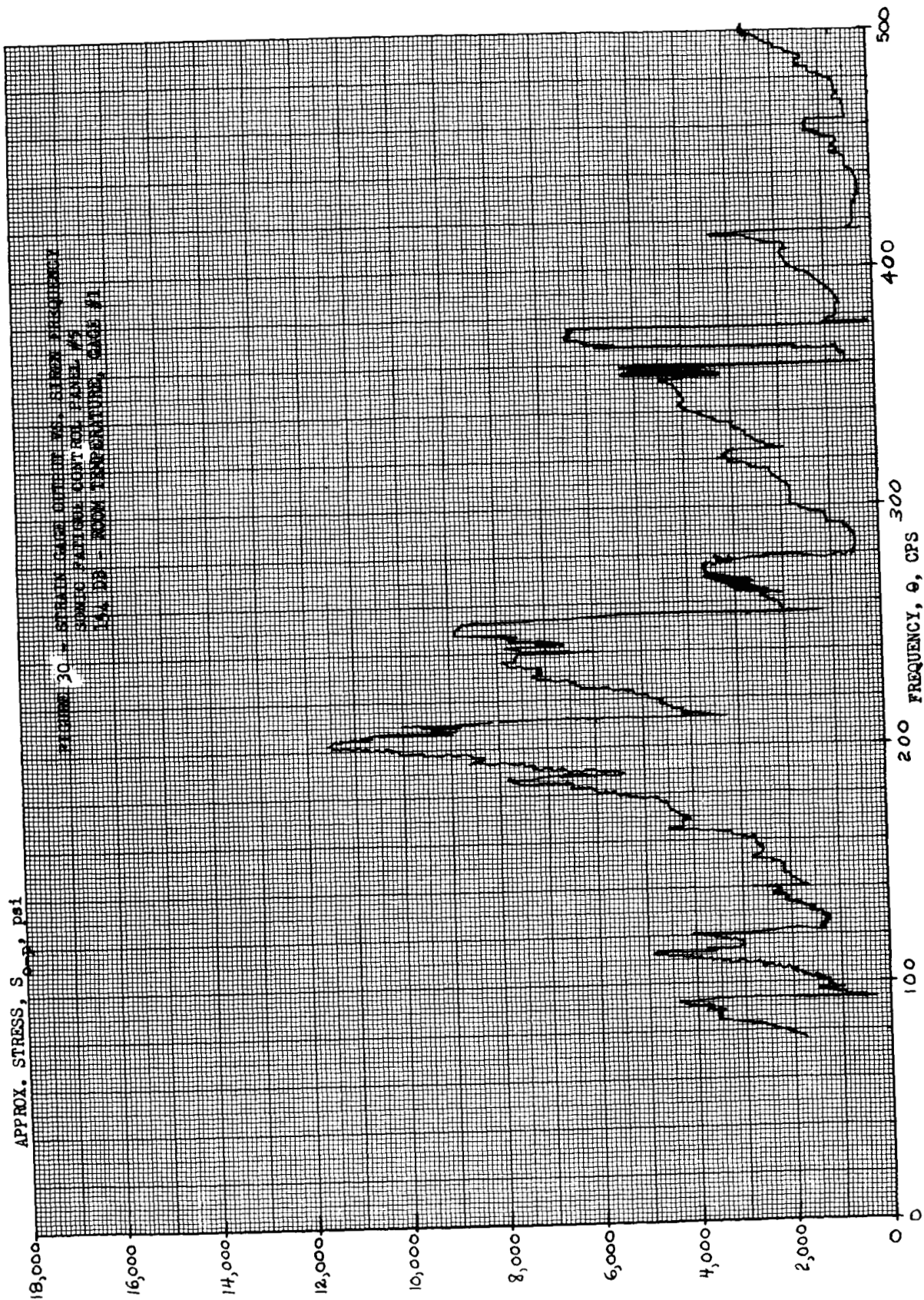


PANEL #23 - GAGE #1

FIGURE 27 - OSCILLOSCOPE DISPLAYS SHOWING PRESENCE OF HIGHER FREQUENCY MODES WITH FUNDAMENTAL MODE IN SONIC FATIGUE PANELS TESTED AT 300°F. (PURE SINE WAVE SUPERIMPOSED)

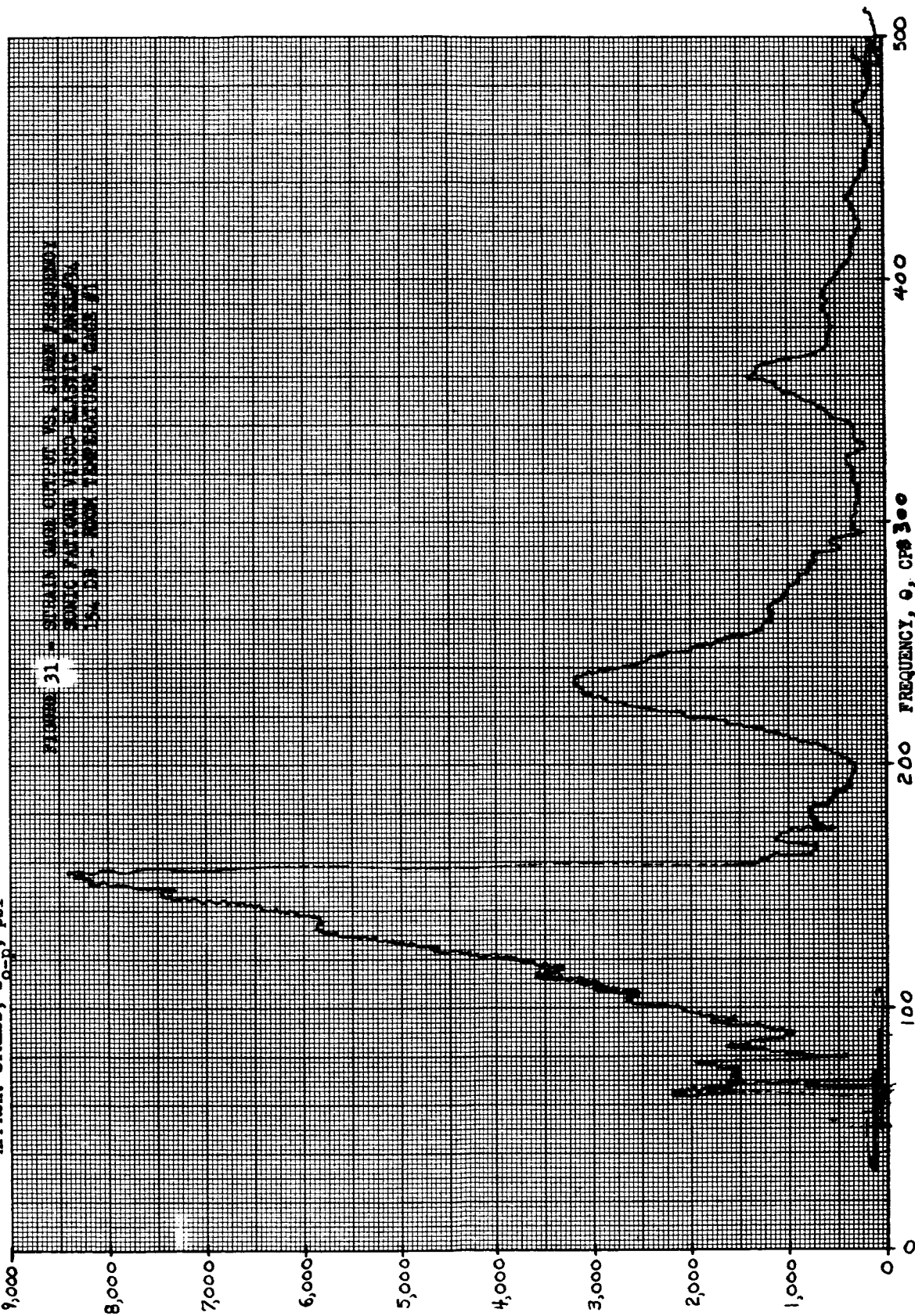




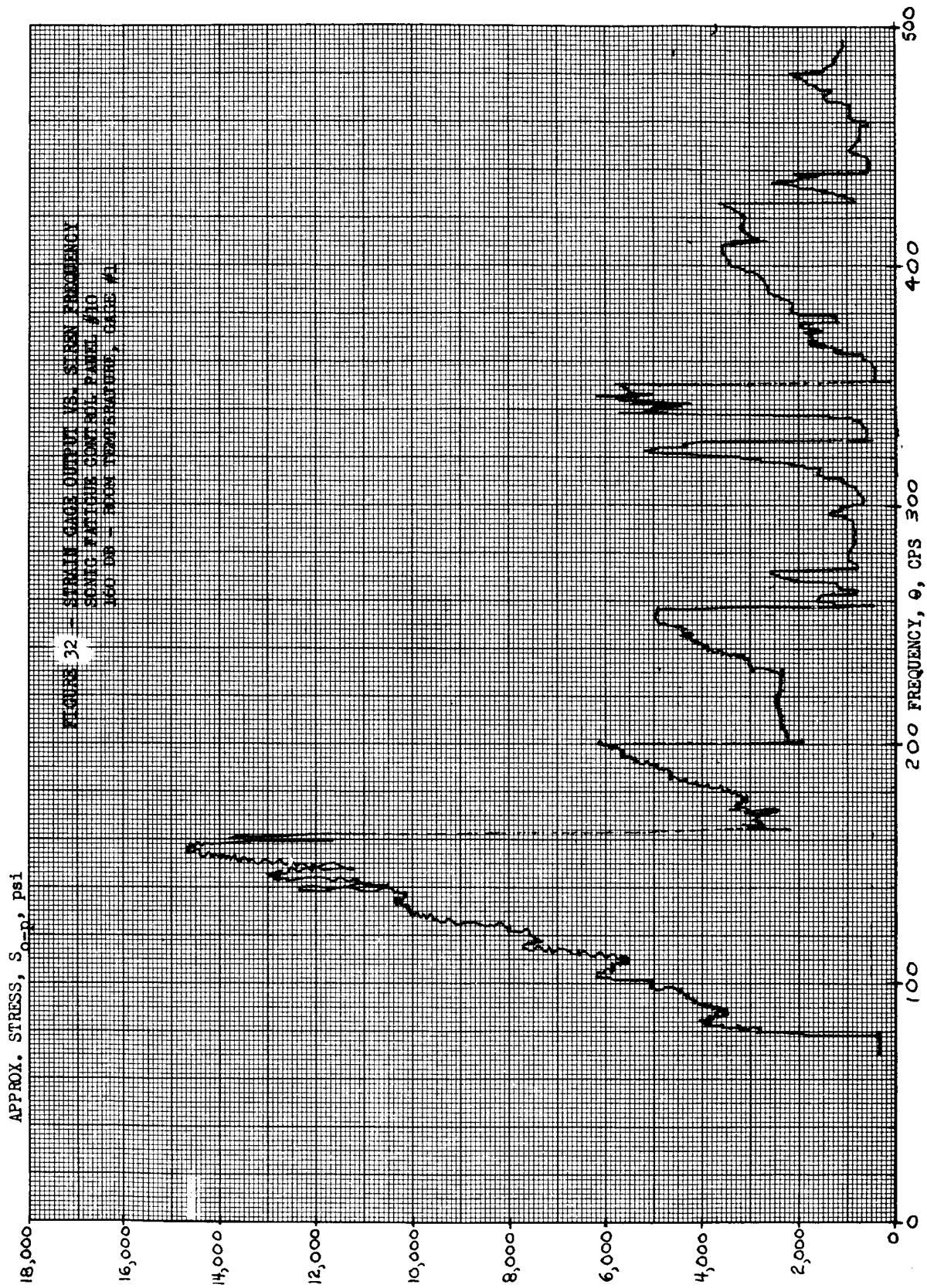


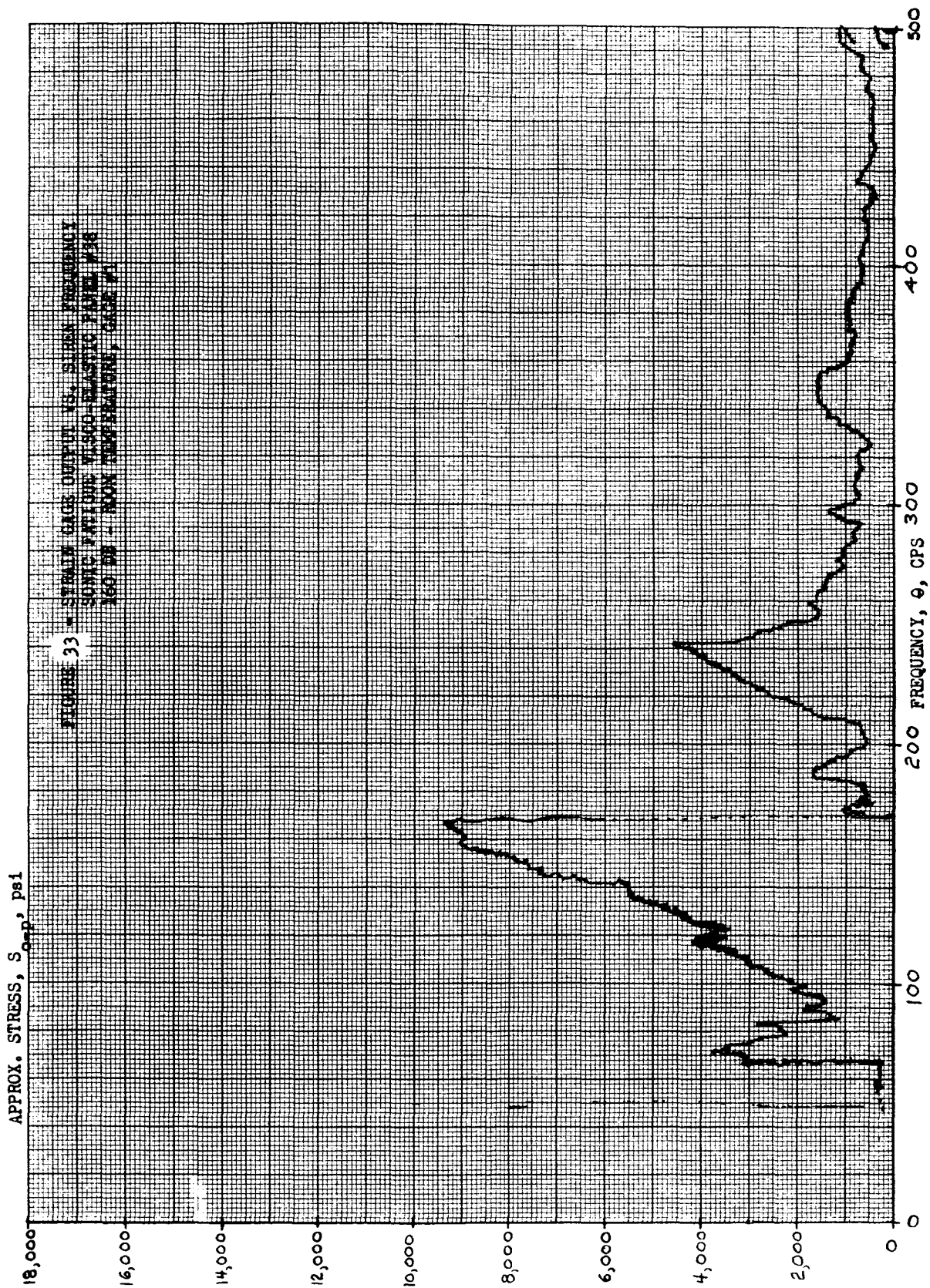
APPROX. STRESS,  $S_{o-p}$ , psi

FIGURE 31 - STRAIN RATE EFFECT VS. DYNAMIC TIME  
SINUSOIDAL VIBRO-ELASTIC MATERIAL  
(50, 50) - ROOM TEMPERATURE, CASE 1

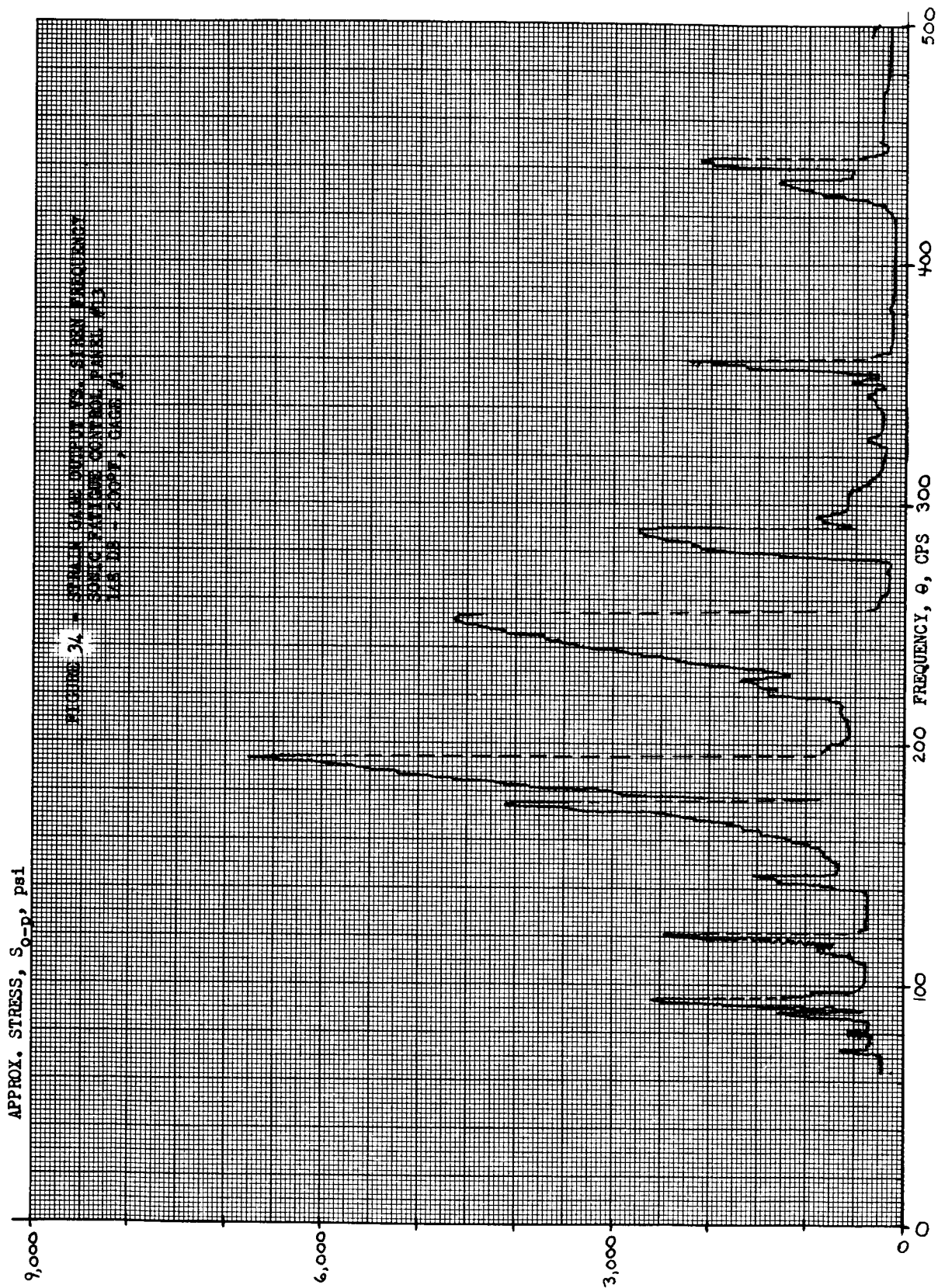


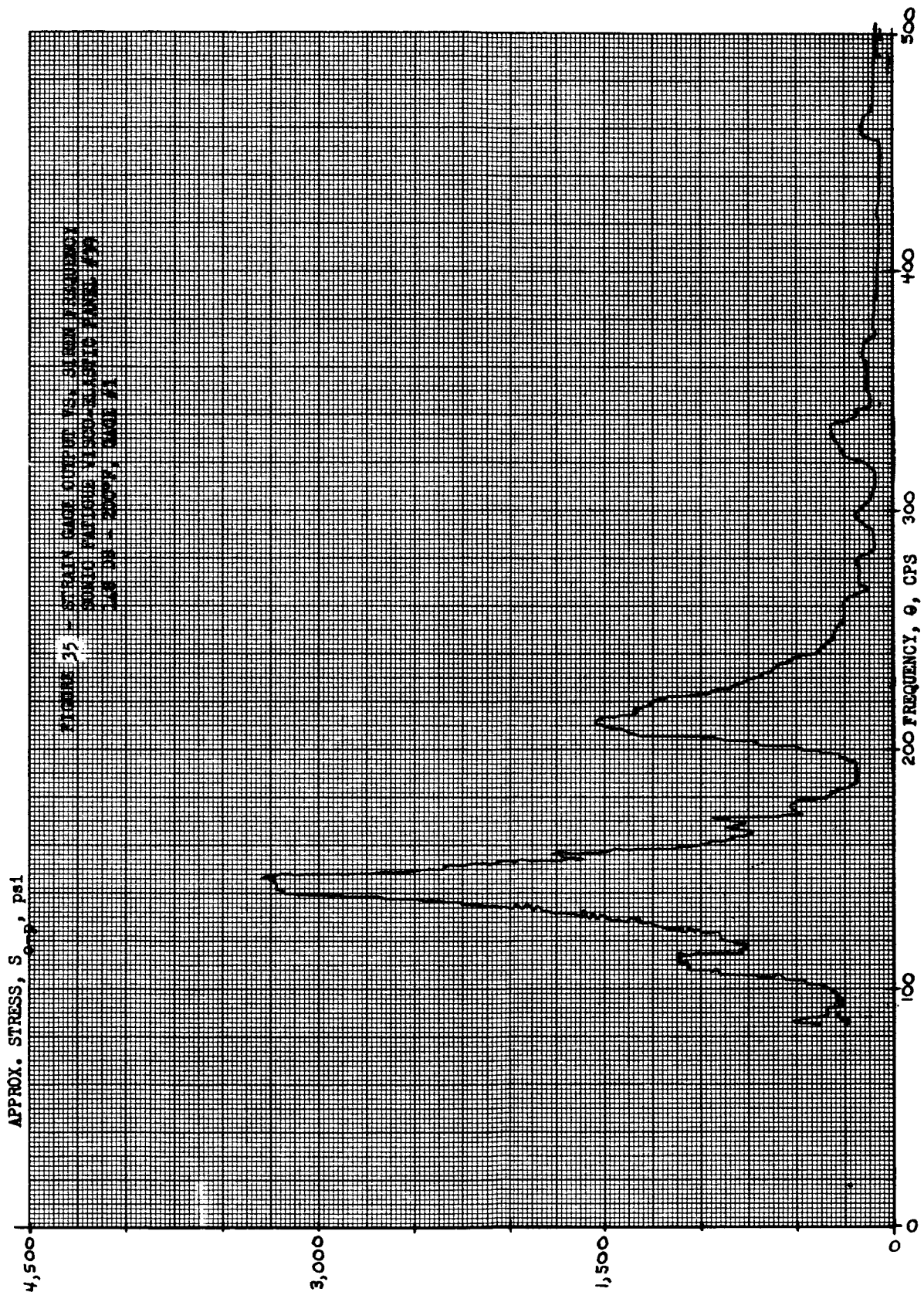
APPROX. STRESS,  $S_{o-p}$ , psi



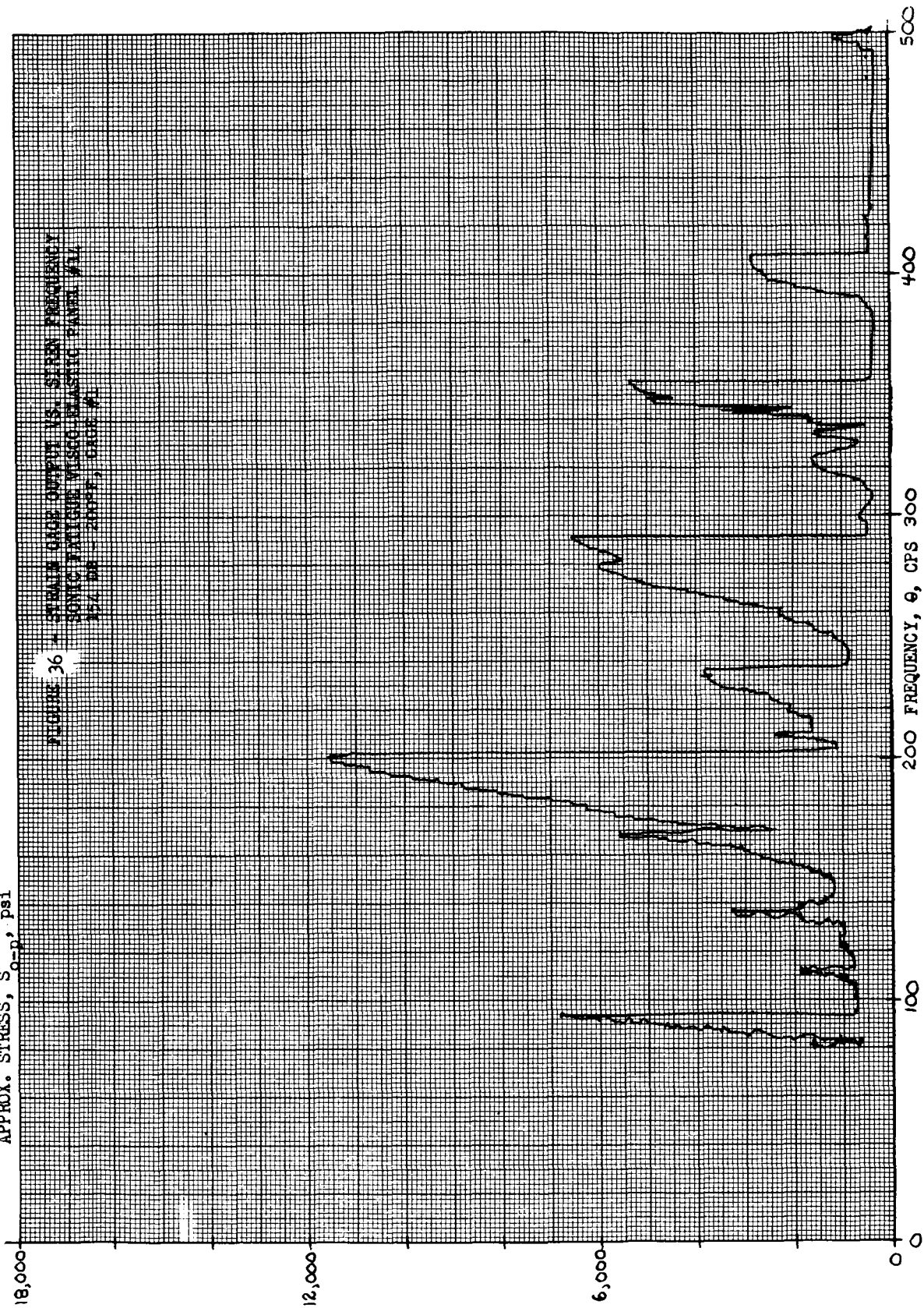


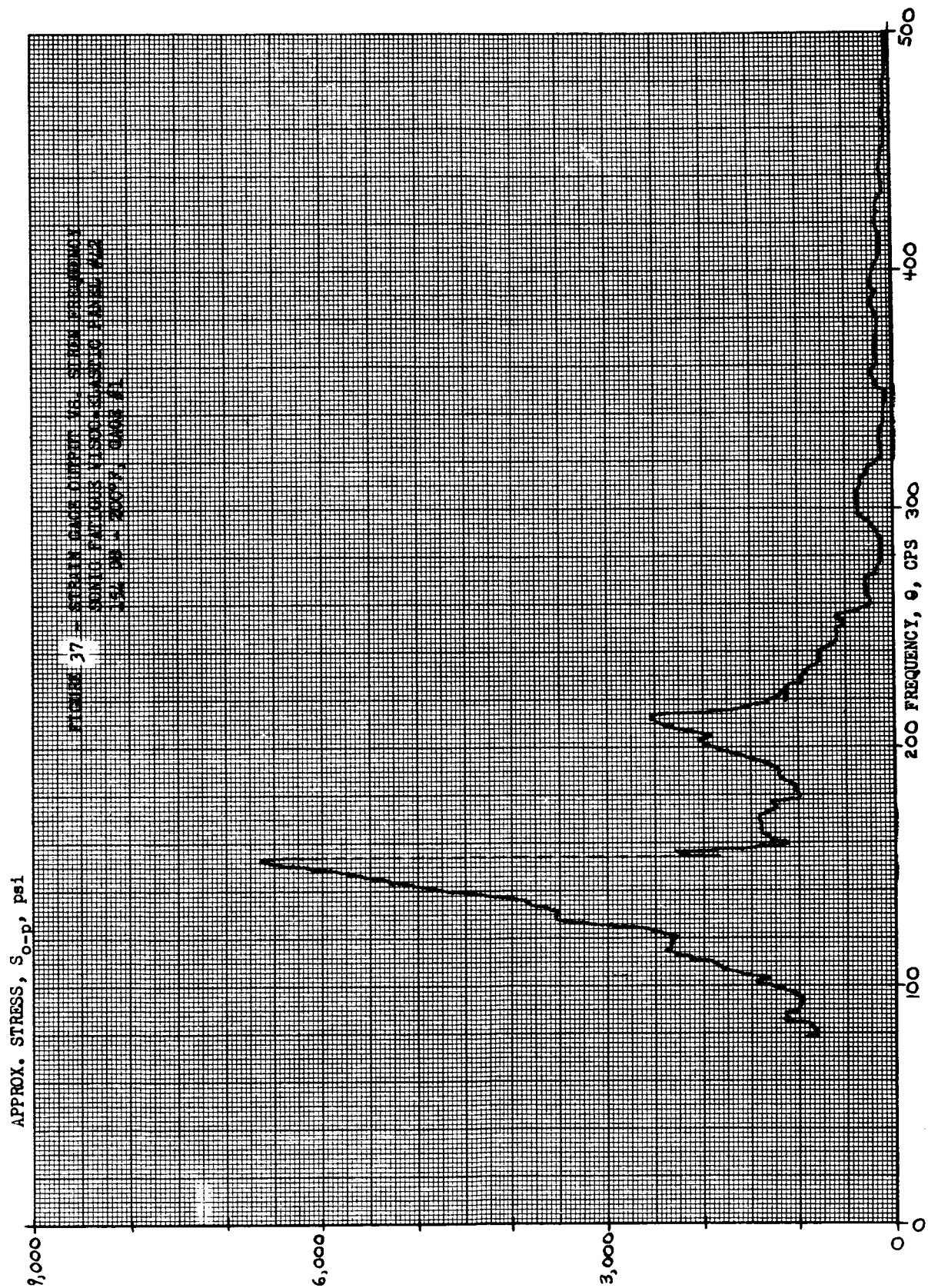
APPROX. STRESS,  $S_{o-p}$ , psi



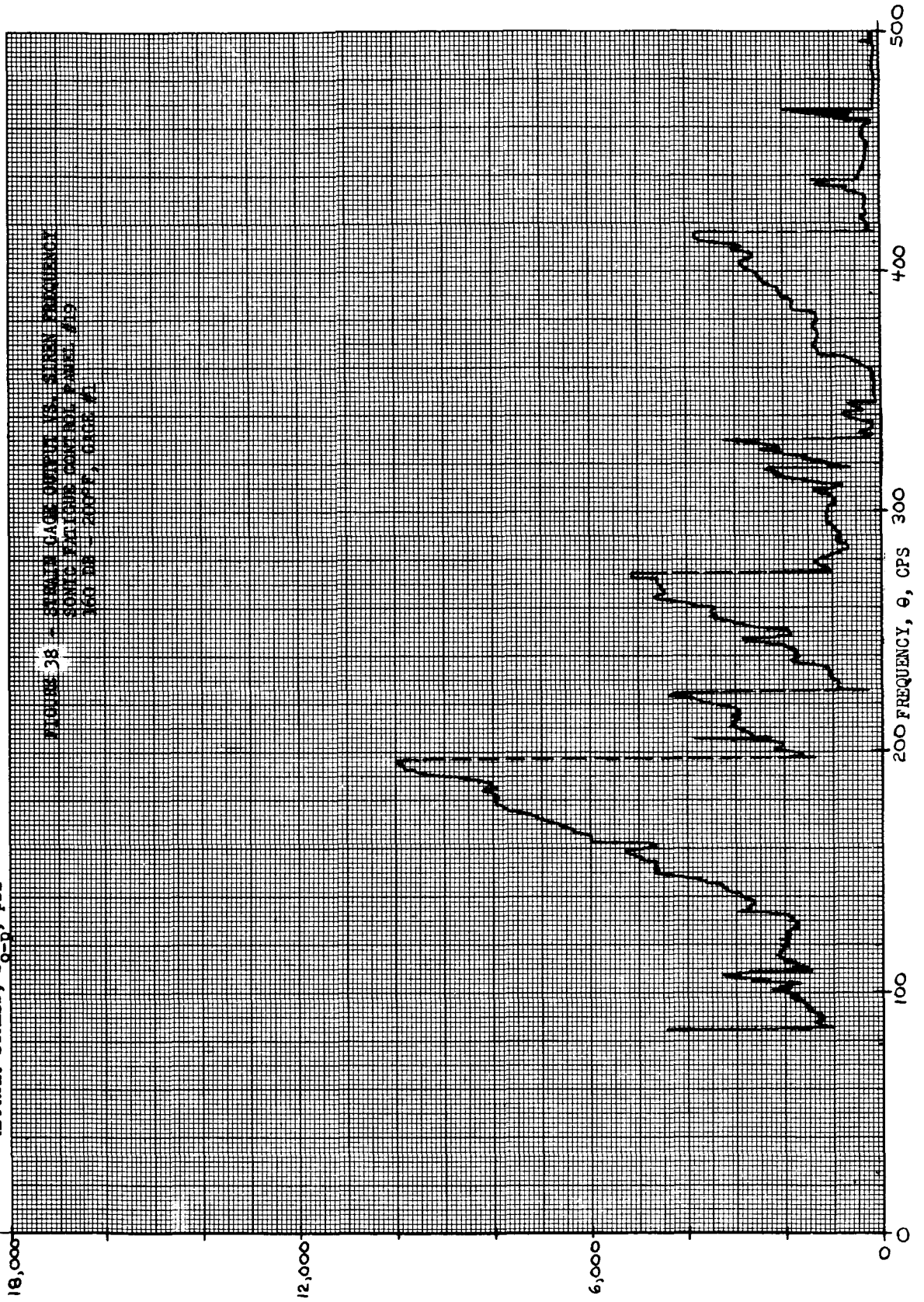


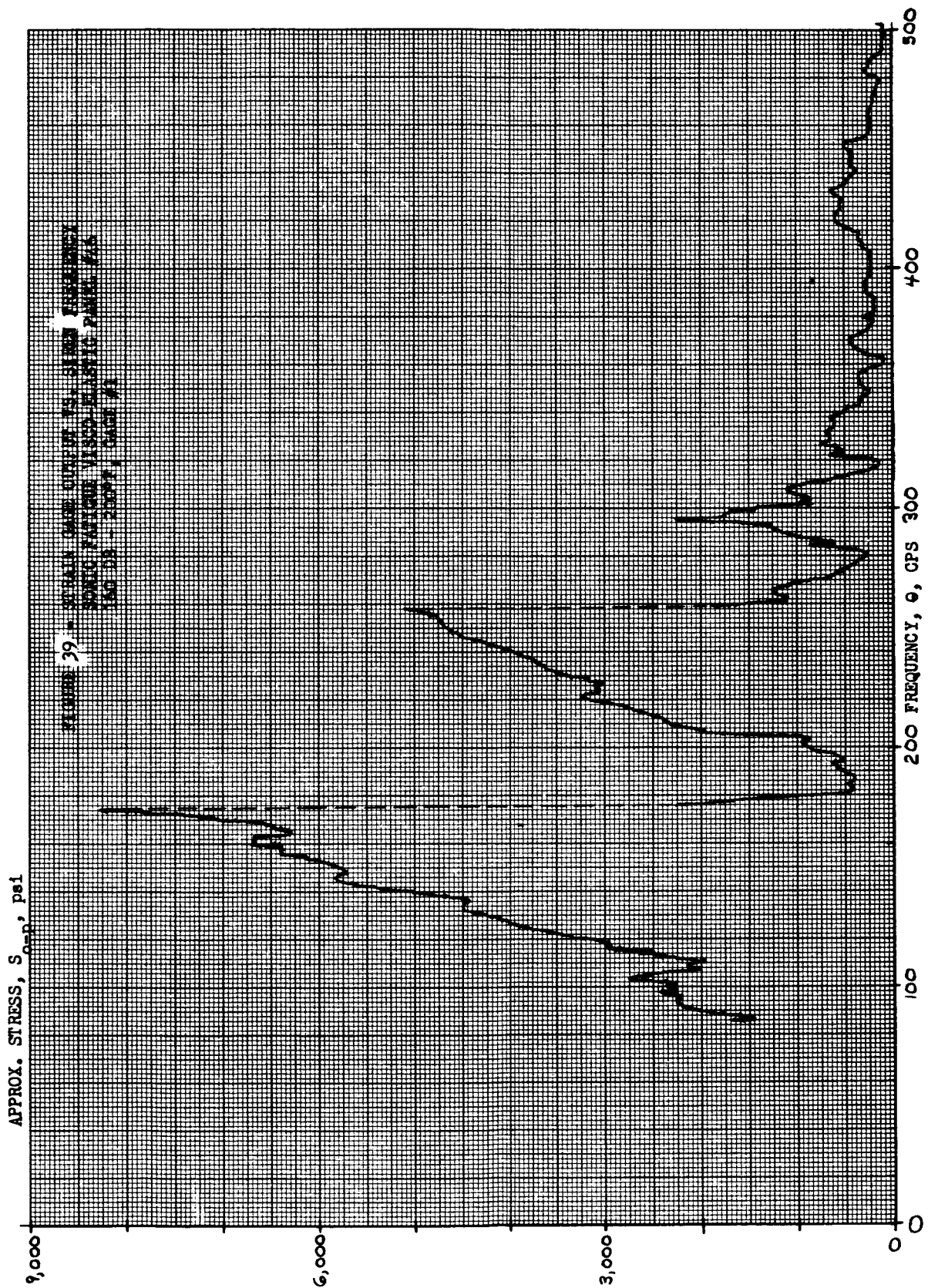
APPROX. STRESS,  $S_{o-p}$ , psi

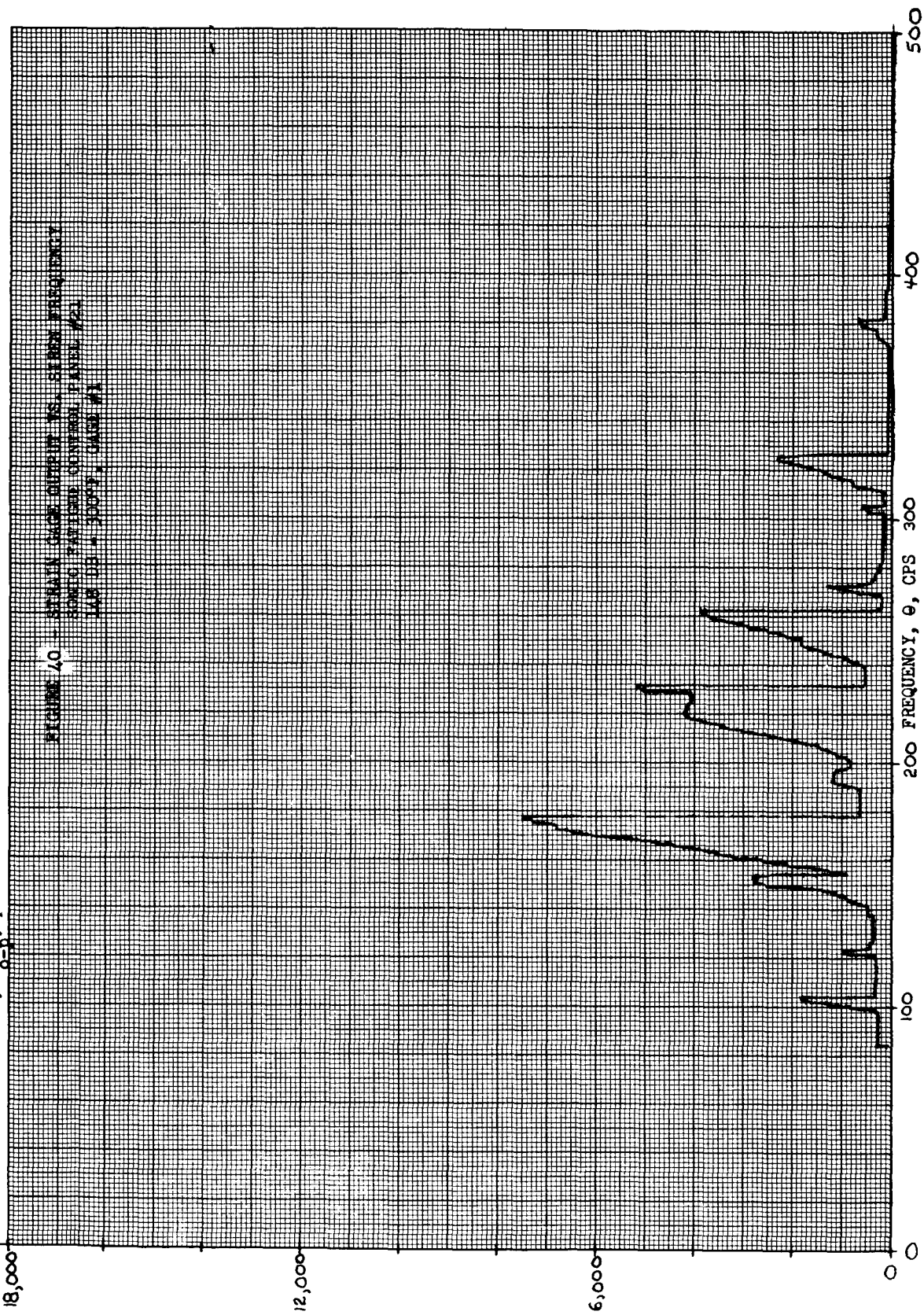


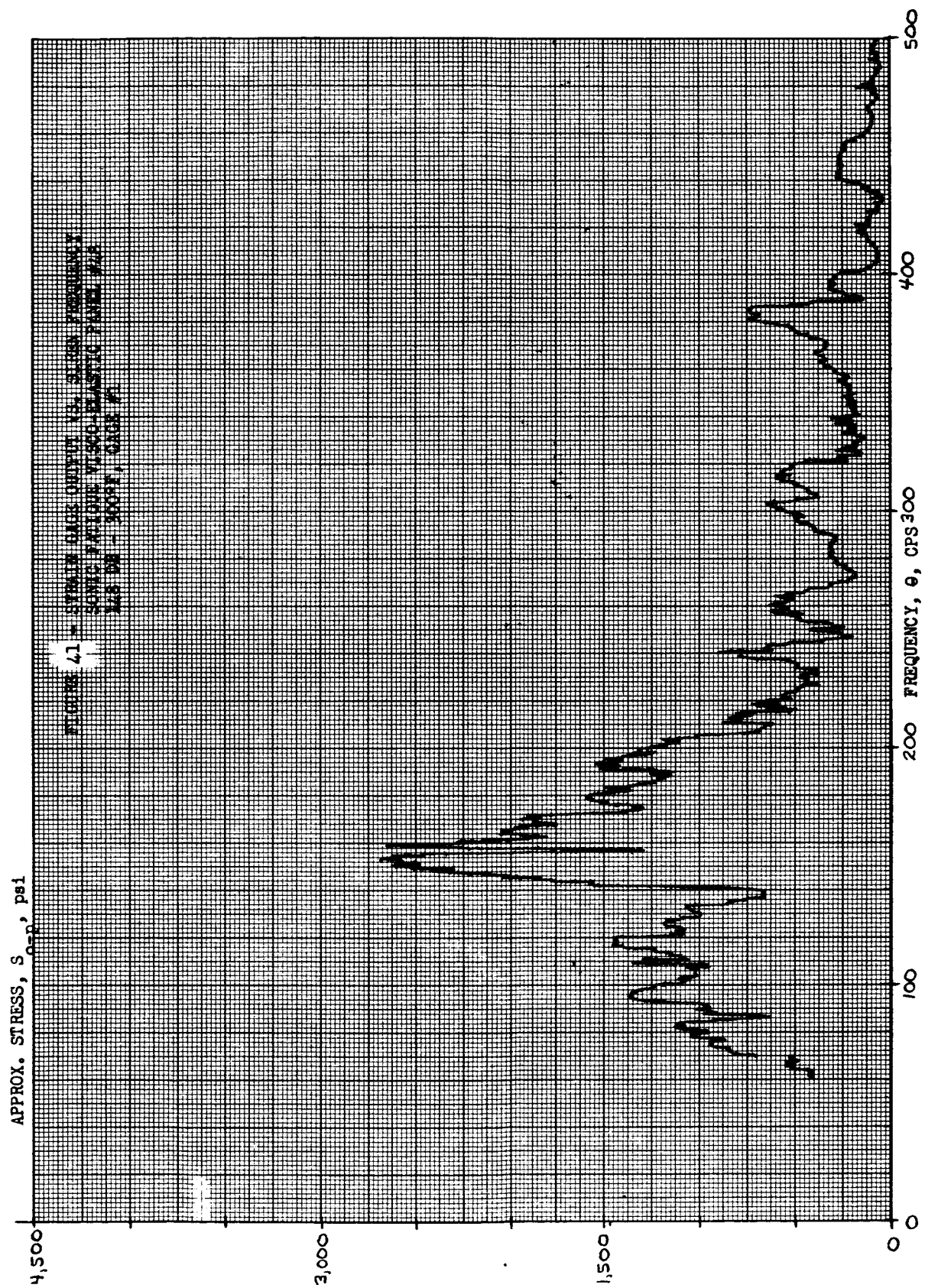


APPROX. STRESS,  $S_{o-p}$ , psi

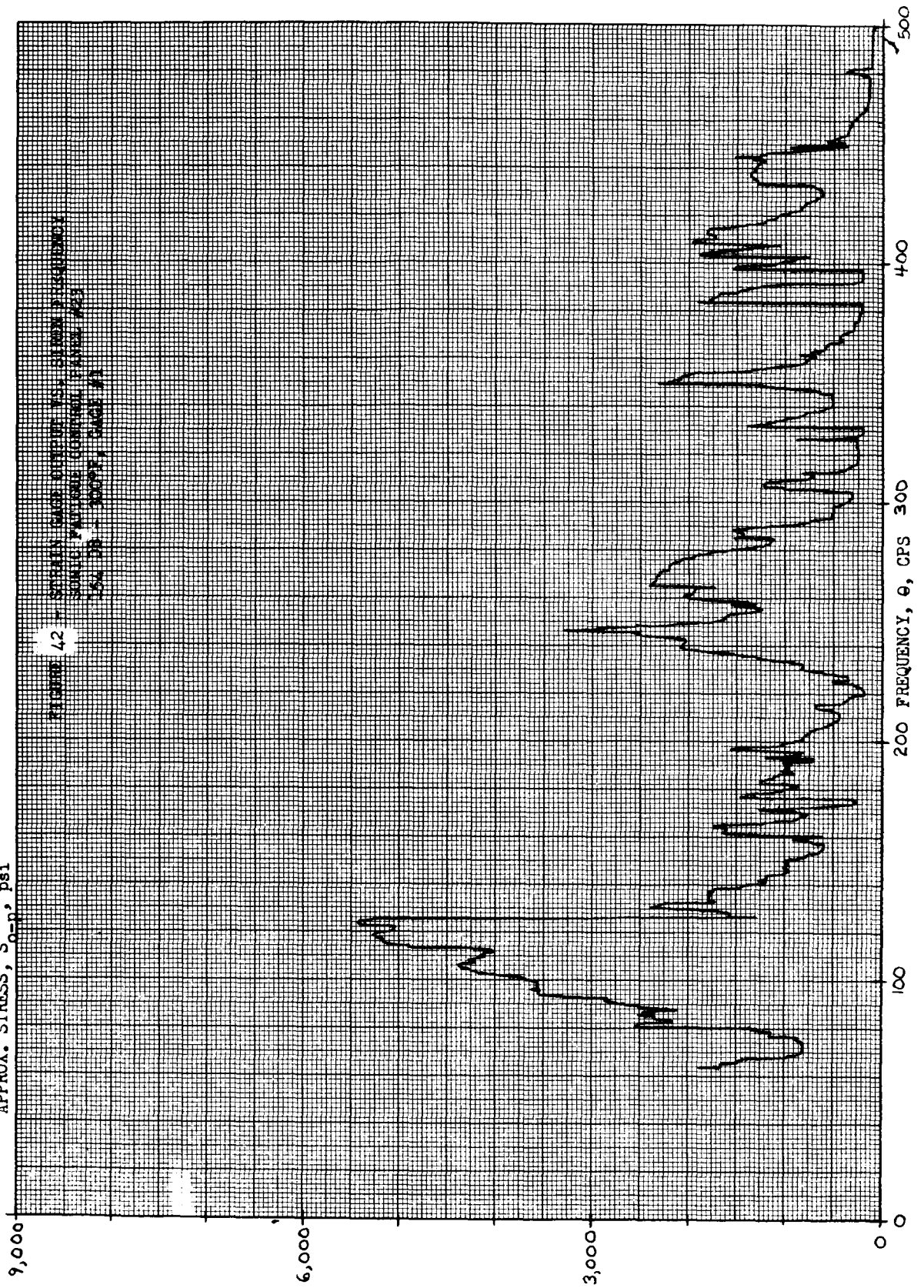


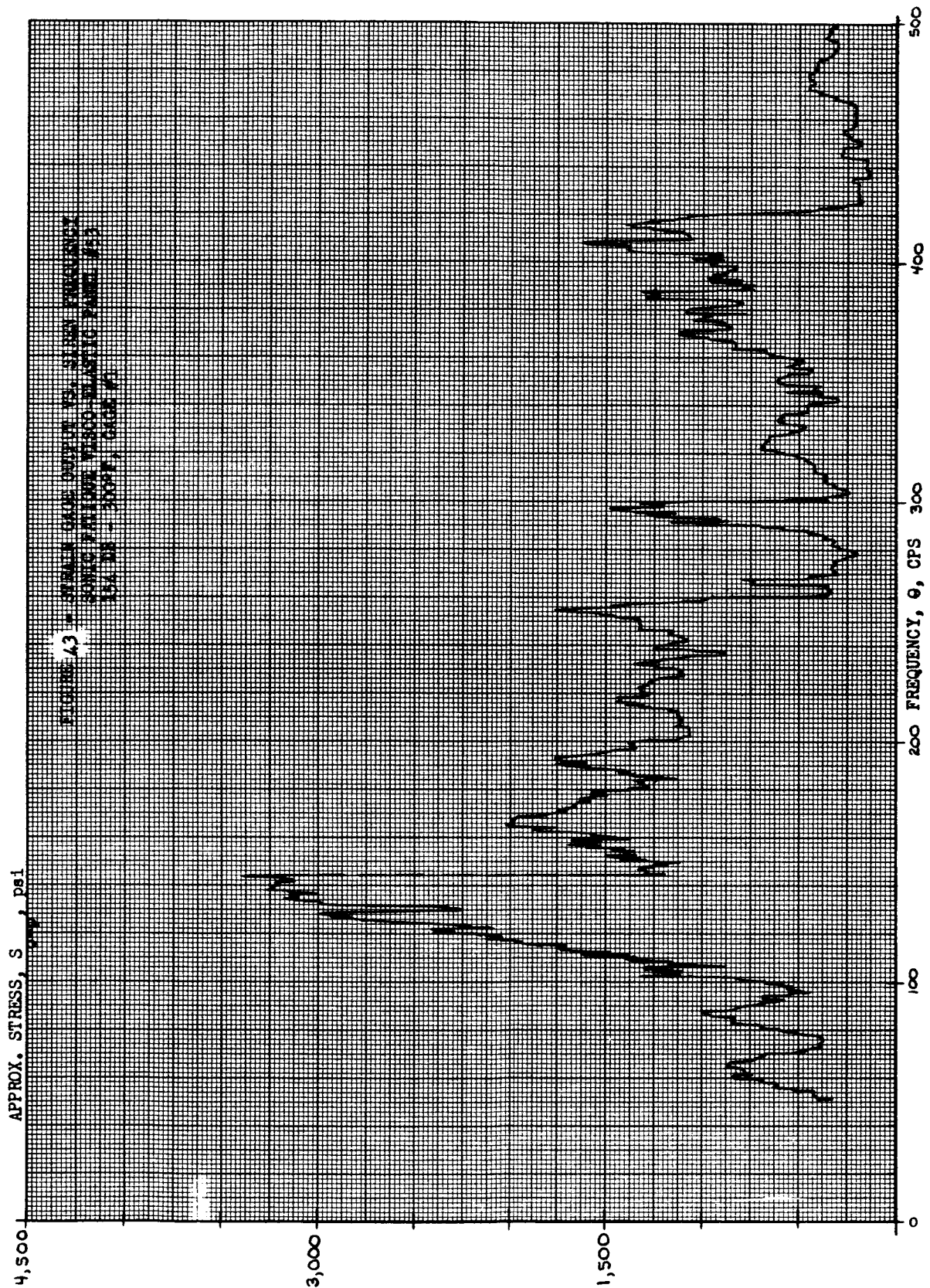


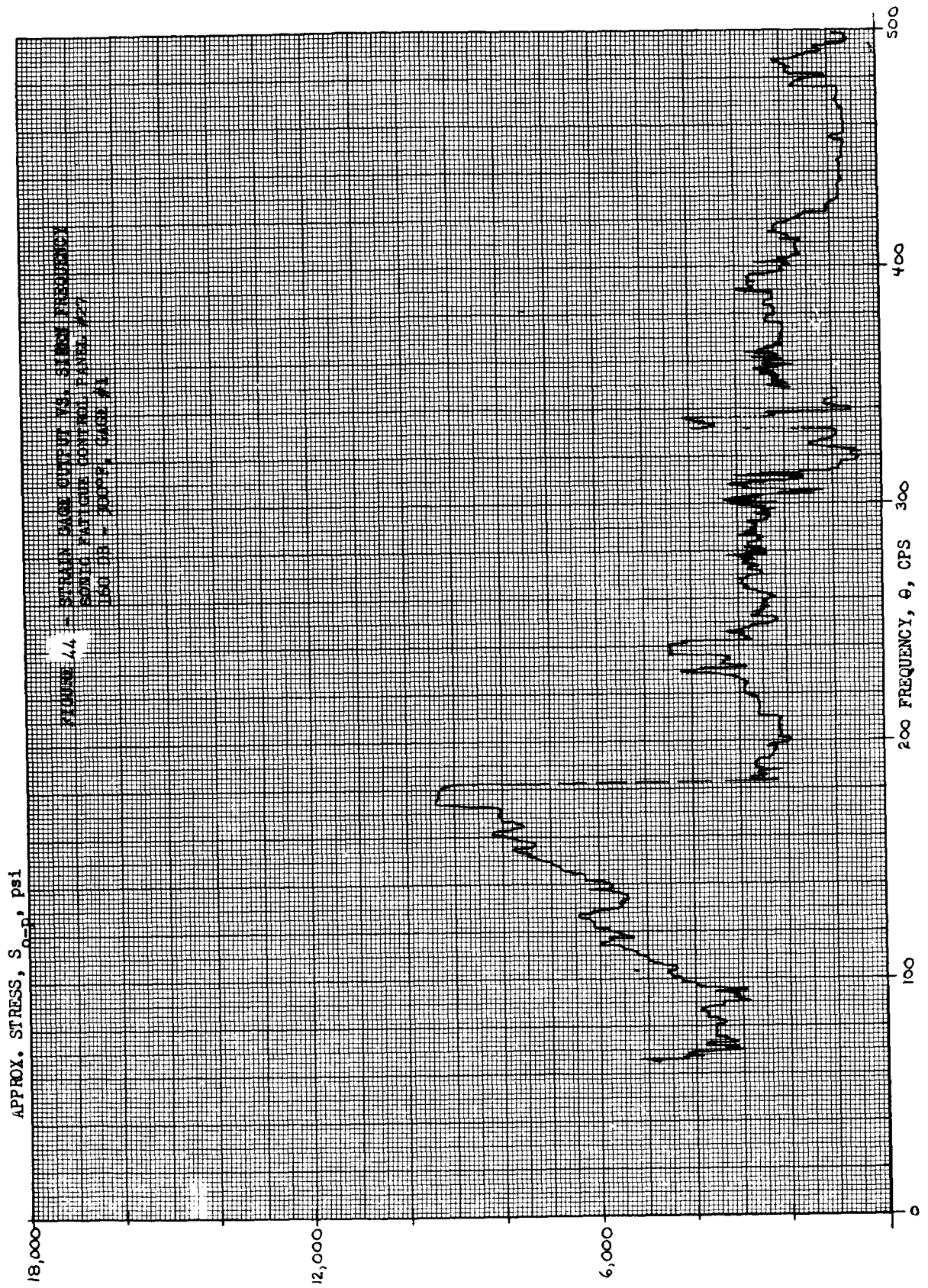
APPROX. STRESS,  $S_{o-p}$ , psi

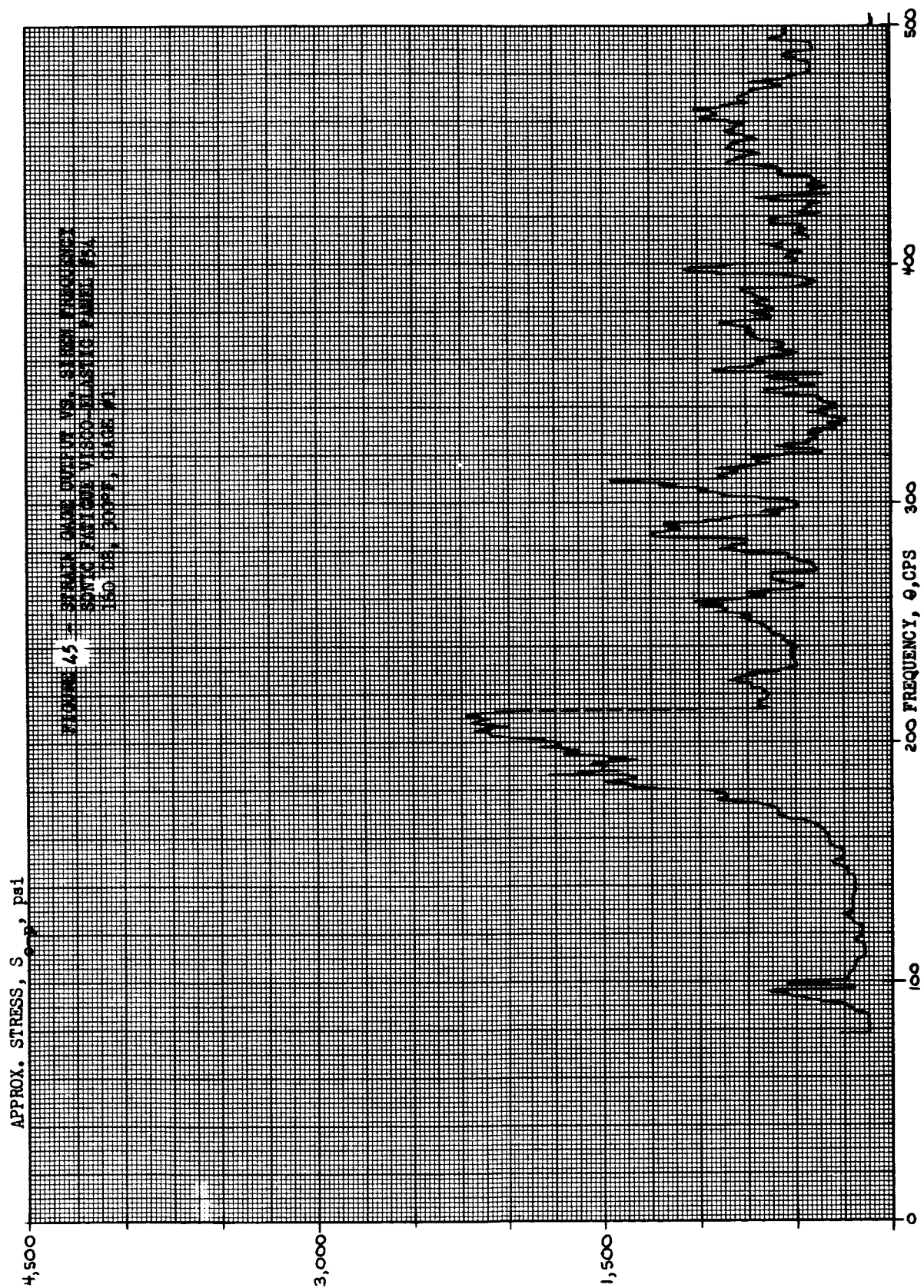


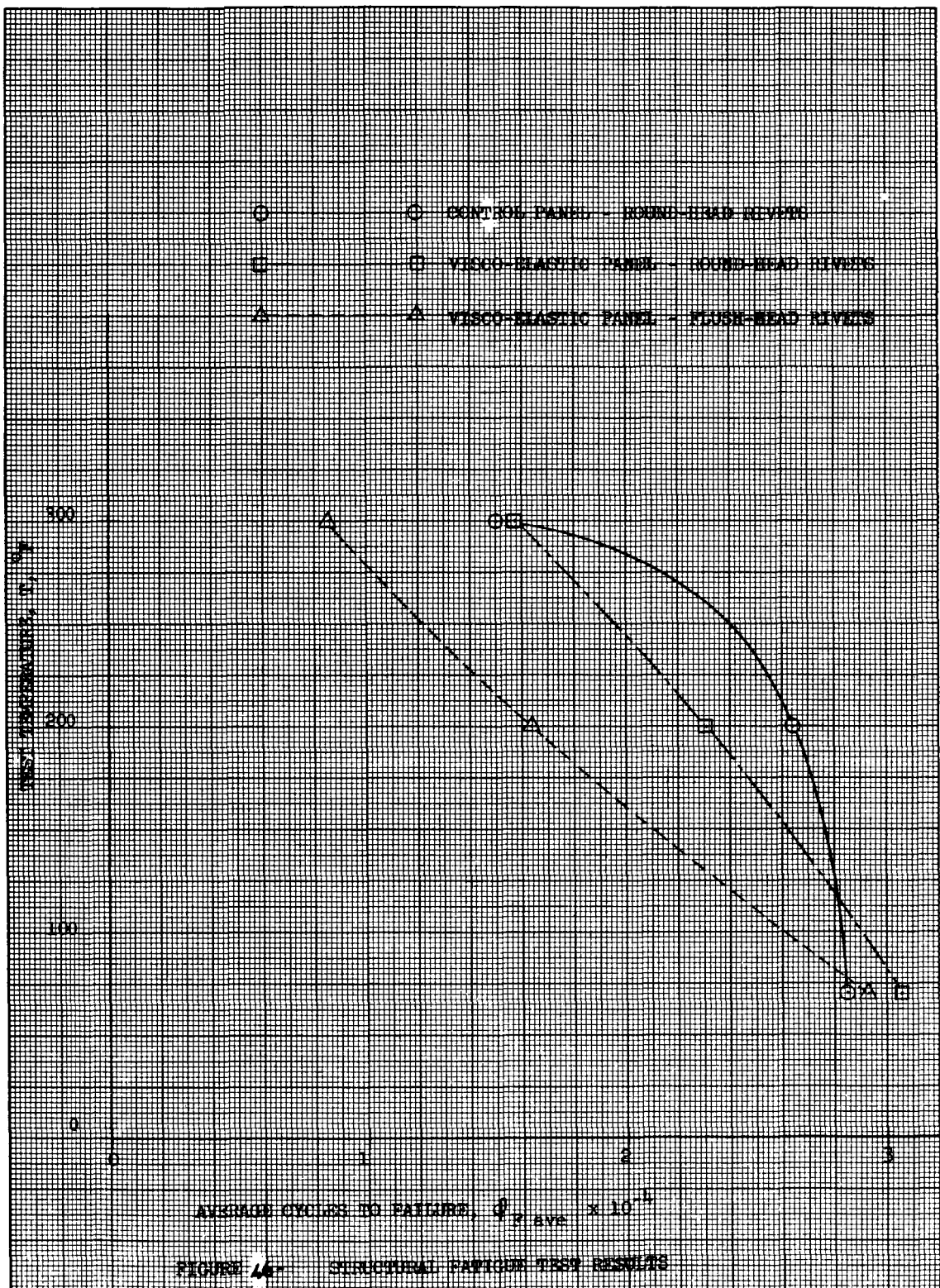
APPROX. STRESS,  $S_{0-p}$ , psi

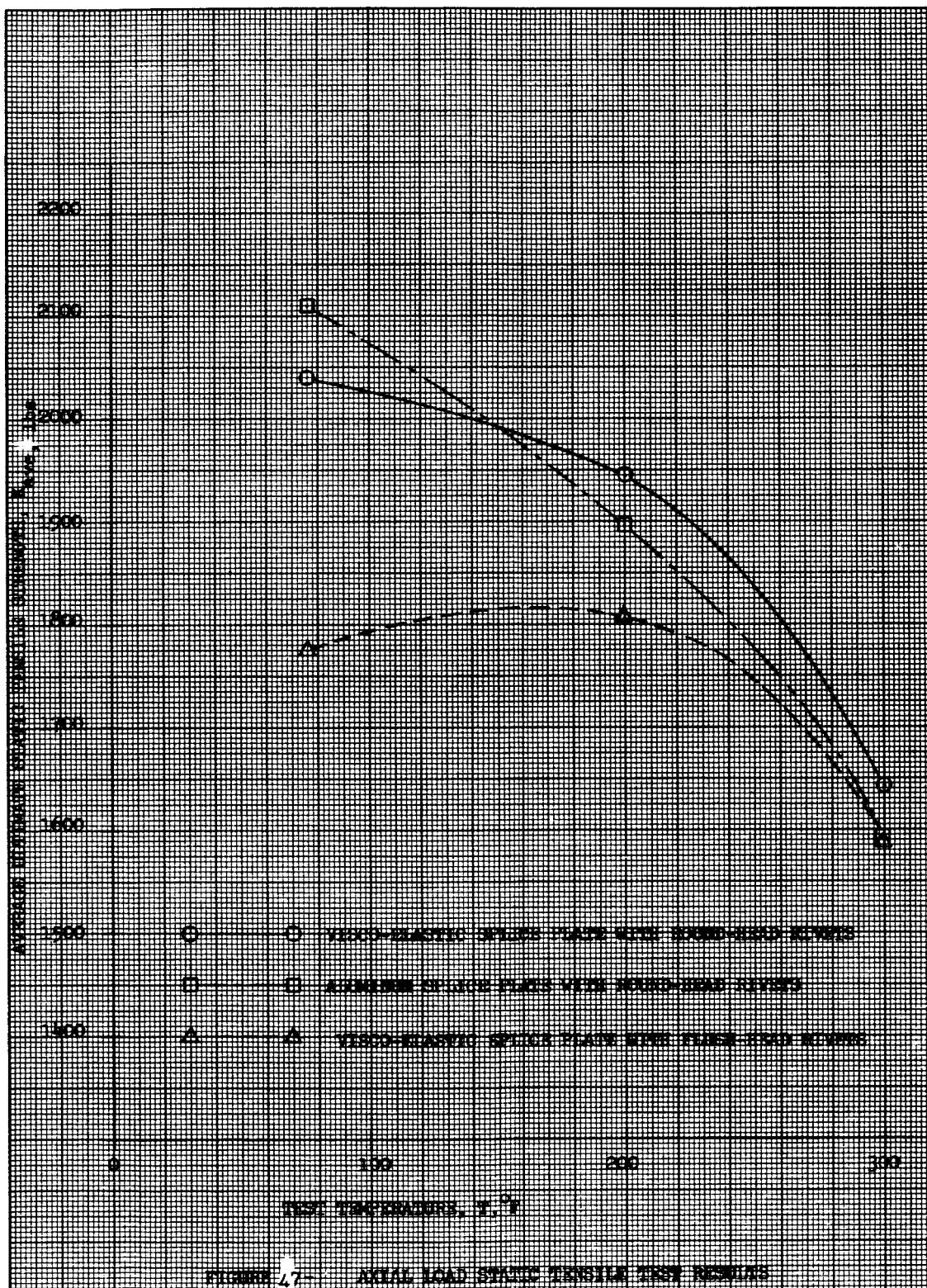












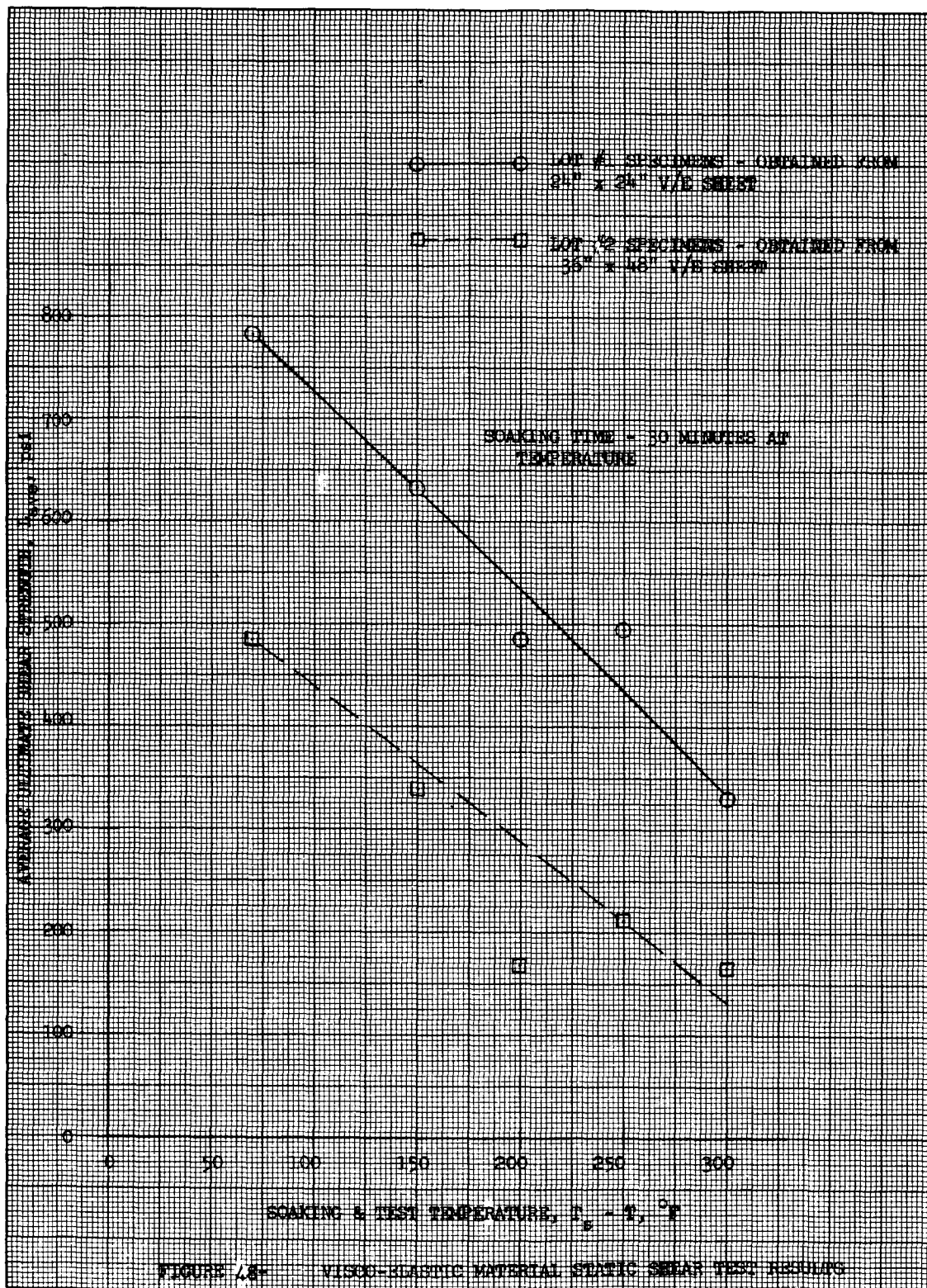
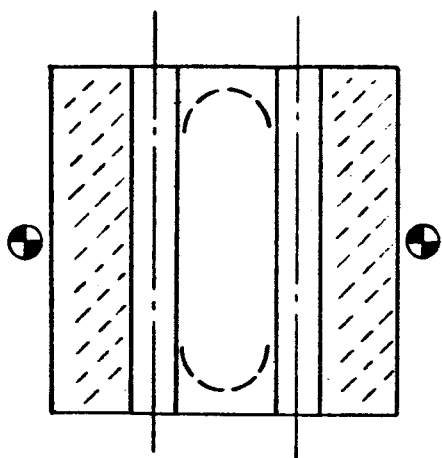
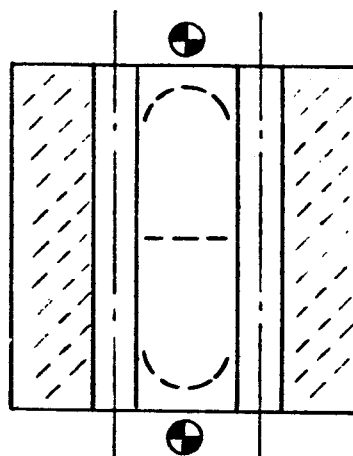


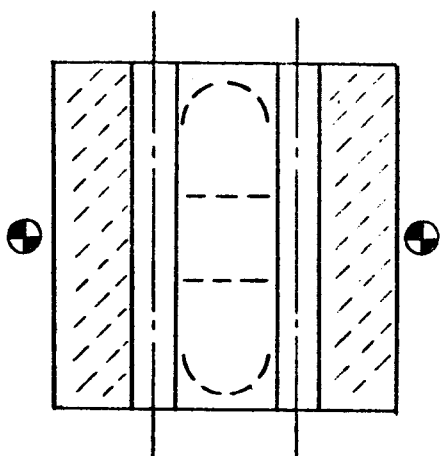
FIGURE 18- VISCO-ELASTIC MATERIAL STATIC SHEAR TEST RESULTS



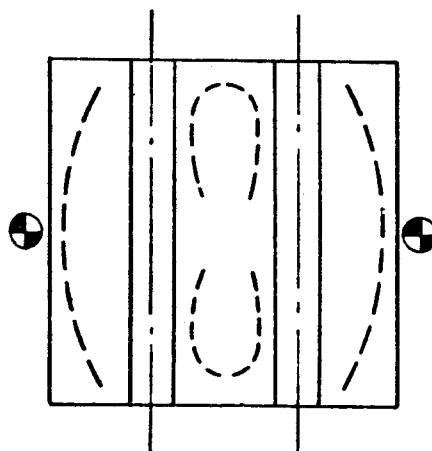
1ST MODE  $\Theta = 142 \text{ CPS}$   
 $c/c_c = .0103$



2ND MODE  $\Theta = 198 \text{ CPS}$   
 $c/c_c = .0030$



3RD MODE  $\Theta = 250 \text{ CPS}$   
 $c/c_c = .0069$



4TH MODE  $\Theta = 352 \text{ CPS}$   
 $c/c_c = .0036$

SONIC FATIGUE CONTROL PANEL #28



SHAKER LOCATIONS

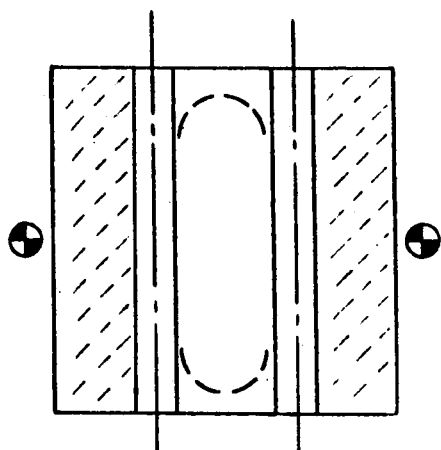


NODE LINES

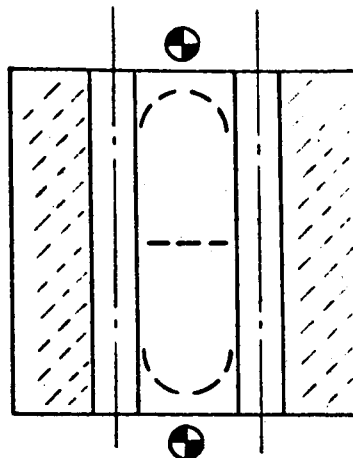


DEAD AREAS

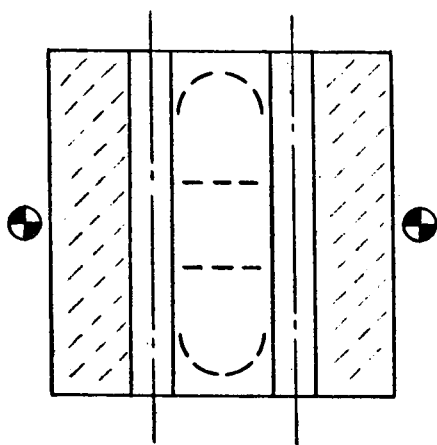
FIGURE 49 - NODE LINES OF FUNDAMENTAL MODES FROM VIBRATION TESTS ON SONIC FATIGUE CONTROL PANEL, SOFT SUSPENSION SYSTEM AT ROOM TEMPERATURE



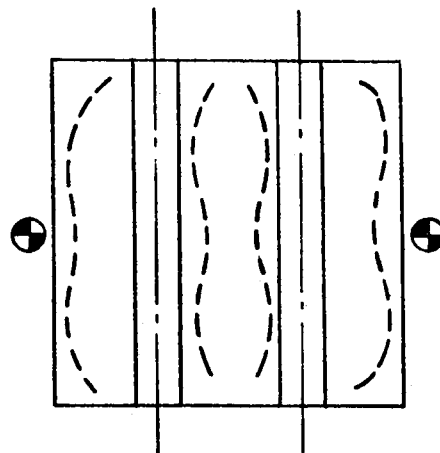
1ST MODE  $\Theta = 152$  CPS  
 $c/c_c = .0143$



2ND MODE  $\Theta = 201$  CPS  
 $c/c_c = .0106$



3RD MODE  $\Theta = 250$  CPS  
 $c/c_c = .0128$



4TH MODE  $\Theta = 351$  CPS  
 $c/c_c = .0024$

#### SONIC FATIGUE VISCO-ELASTIC PANEL #56

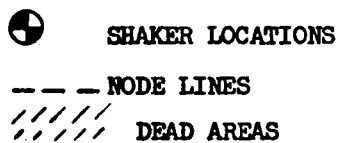
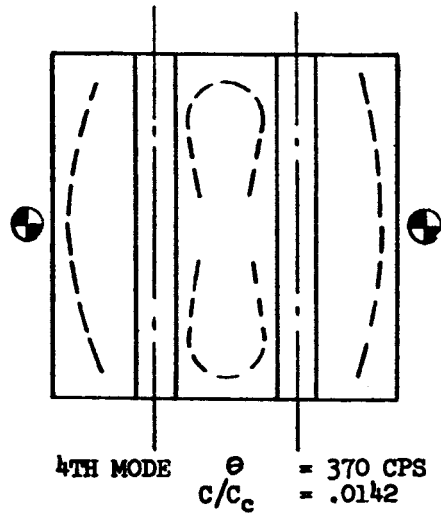
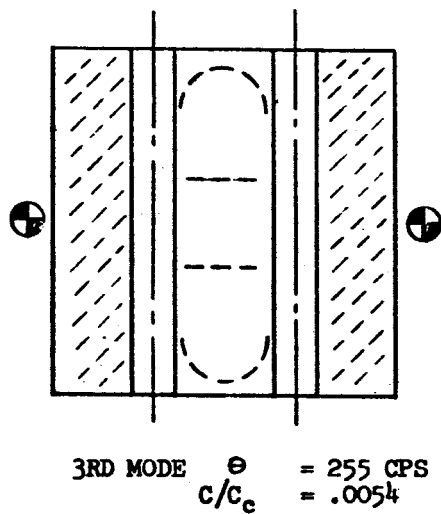
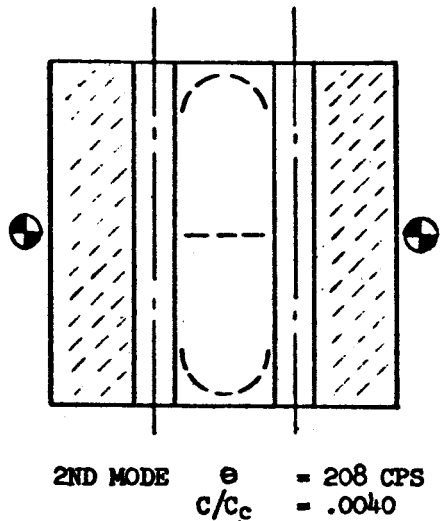
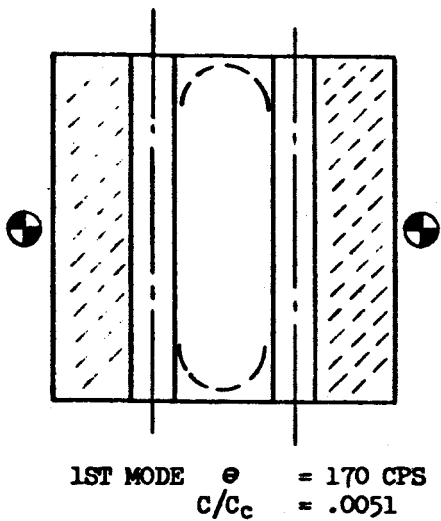


FIGURE 50 - NODE LINES OF FUNDAMENTAL MODES FROM VIBRATION TESTS ON SONIC FATIGUE VISCO-ELASTIC PANEL, SOFT SUSPENSION SYSTEM AT ROOM TEMPERATURE



# SONIC FATIGUE CONTROL PANEL #28



SHAKER LOCATIONS

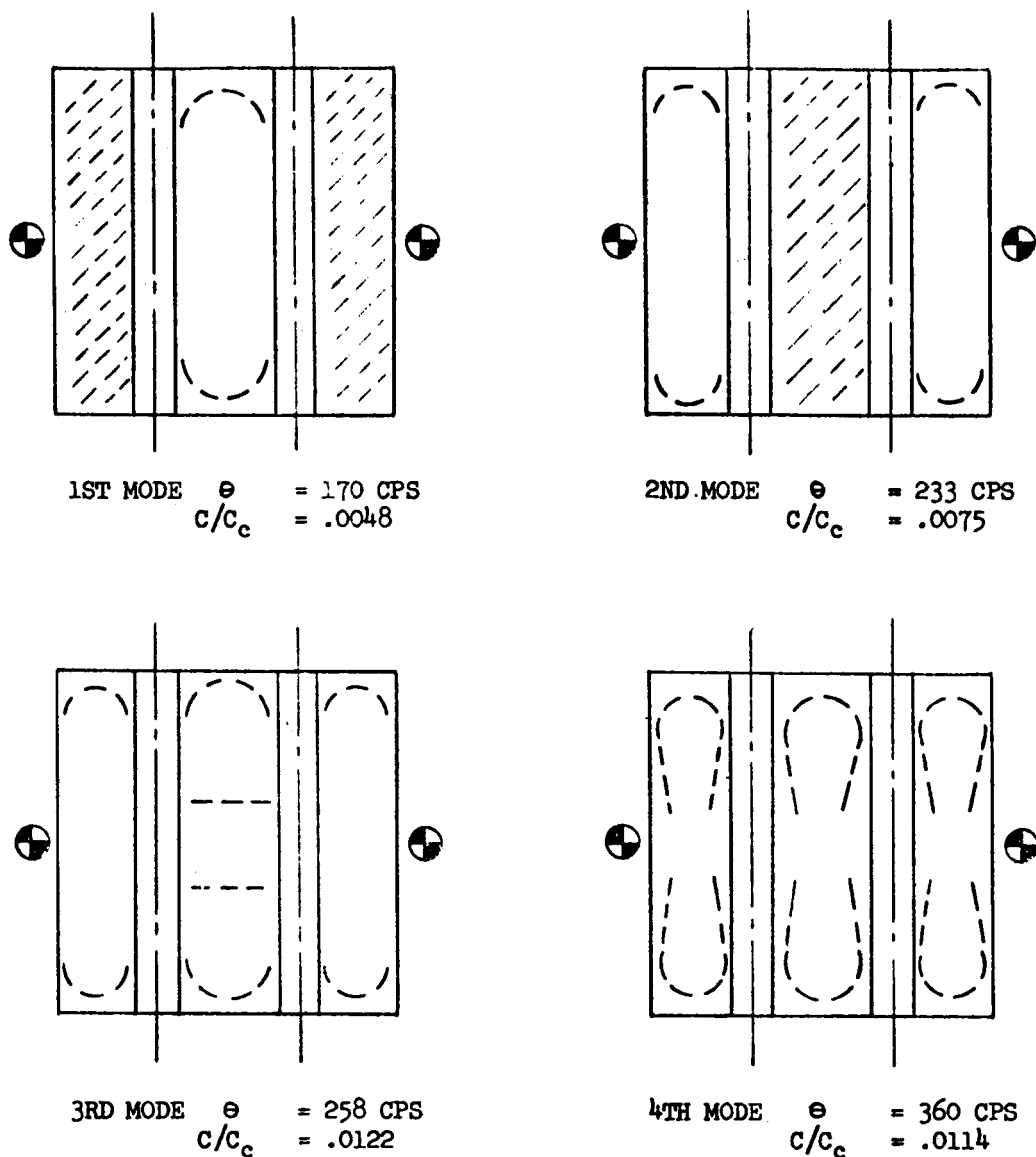


NODE LINES



DEAD AREAS

FIGURE 51 - NODE LINES OF FUNDAMENTAL MODES FROM VIBRATION TESTS ON SONIC FATIGUE CONTROL PANEL, HARD SUSPENSION SYSTEM AT ROOM TEMPERATURE



SONIC FATIGUE VISCO-ELASTIC PANEL #56


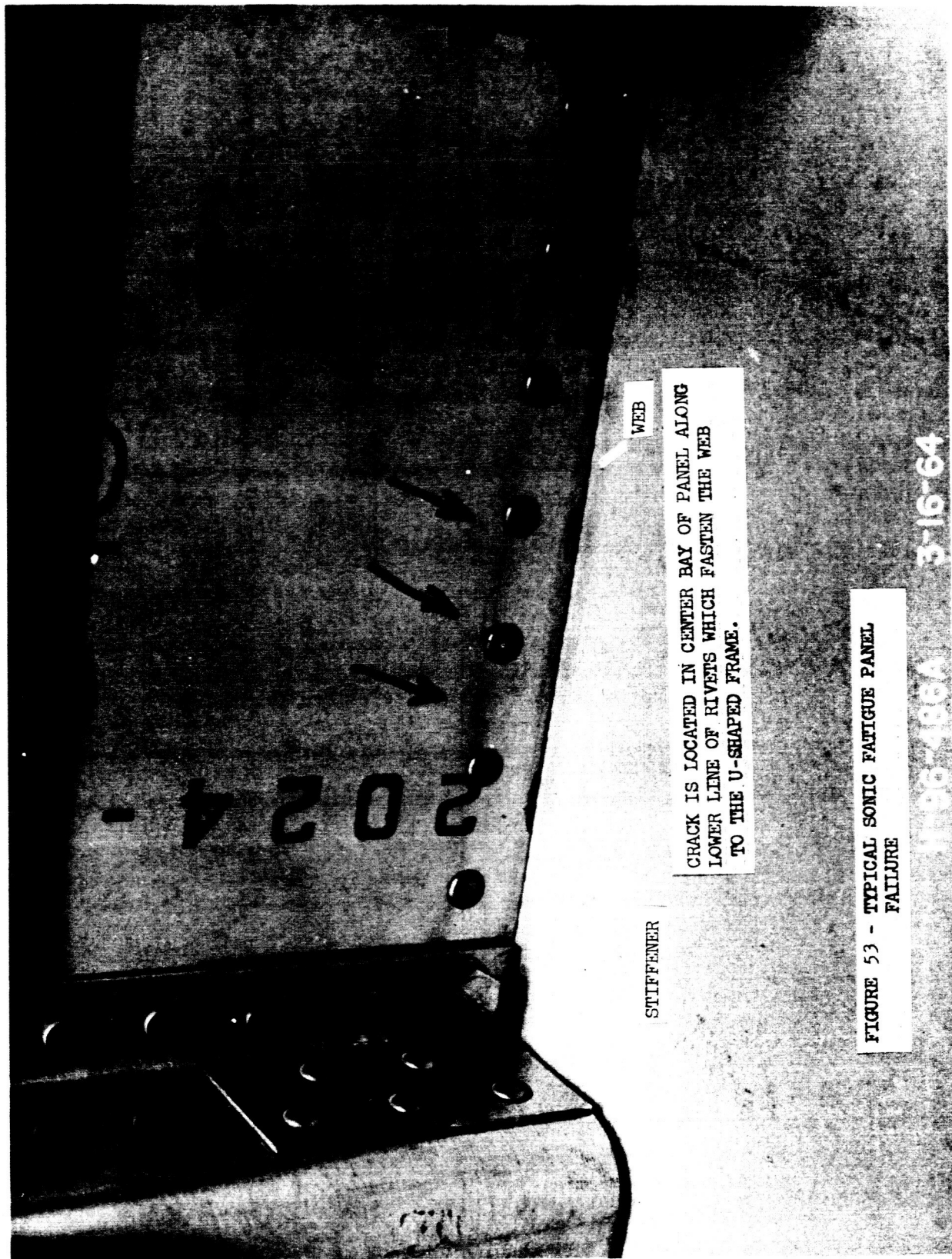
 SHAKER LOCATIONS  
 --- NODE LINES  
 ///// DEAD AREAS

FIGURE 52 - NODE LINES OF FUNDAMENTAL MODES FROM VIBRATION TESTS ON SONIC FATIGUE VISCO-ELASTIC PANEL, HARD SUSPENSION SYSTEM AT ROOM TEMPERATURE



WEB

CRACK IS LOCATED IN CENTER BAY OF PANEL ALONG LOWER LINE OF RIVETS WHICH FASTEN THE WEB TO THE U-SHAPED FRAME.

STIFFENER

FIGURE 53 - TYPICAL SONIC FATIGUE PANEL FAILURE

3-16-64

1796-486A

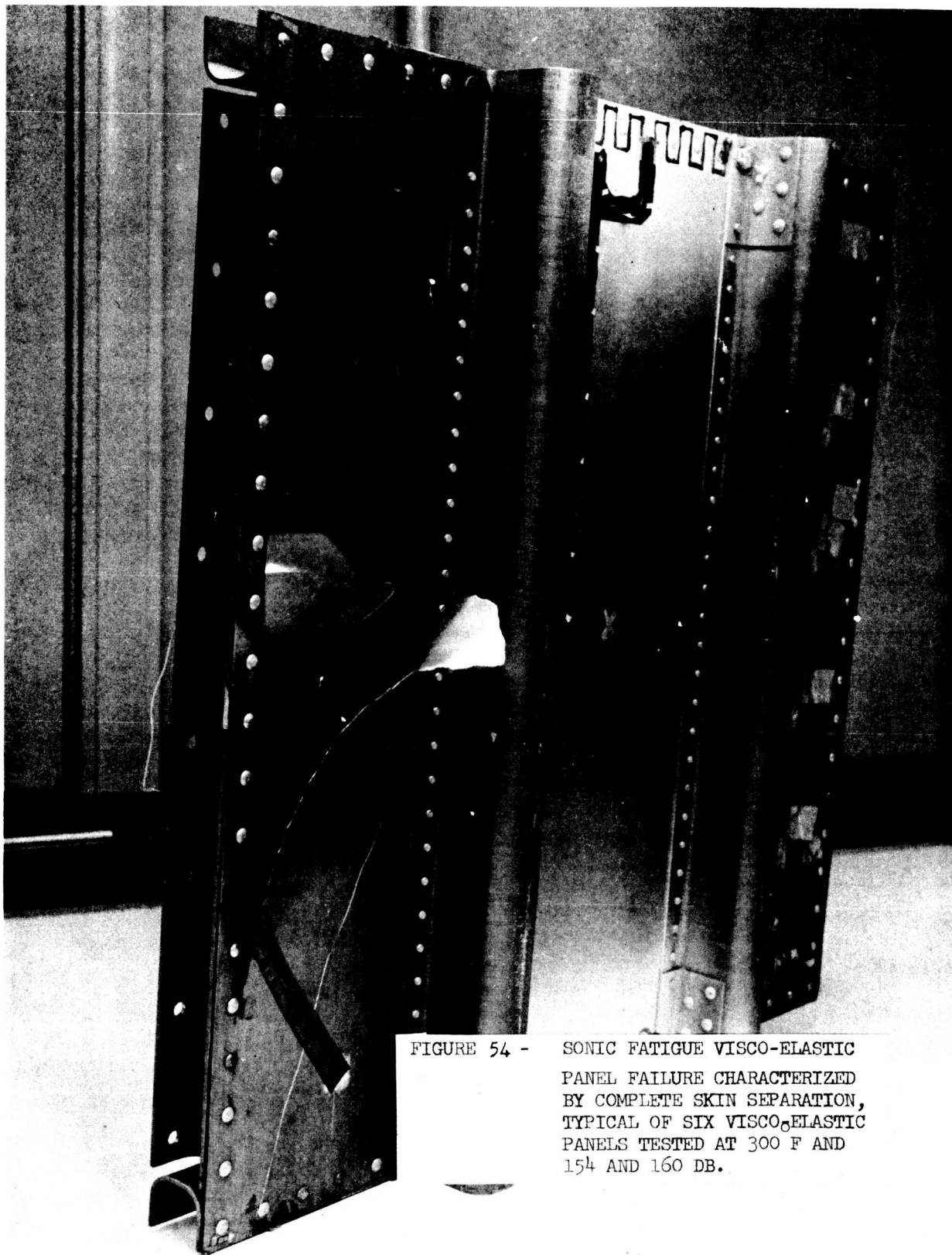


FIGURE 54 - SONIC FATIGUE VISCO-ELASTIC  
PANEL FAILURE CHARACTERIZED  
BY COMPLETE SKIN SEPARATION,  
TYPICAL OF SIX VISCO-ELASTIC  
PANELS TESTED AT 300 F AND  
154 AND 160 DB.

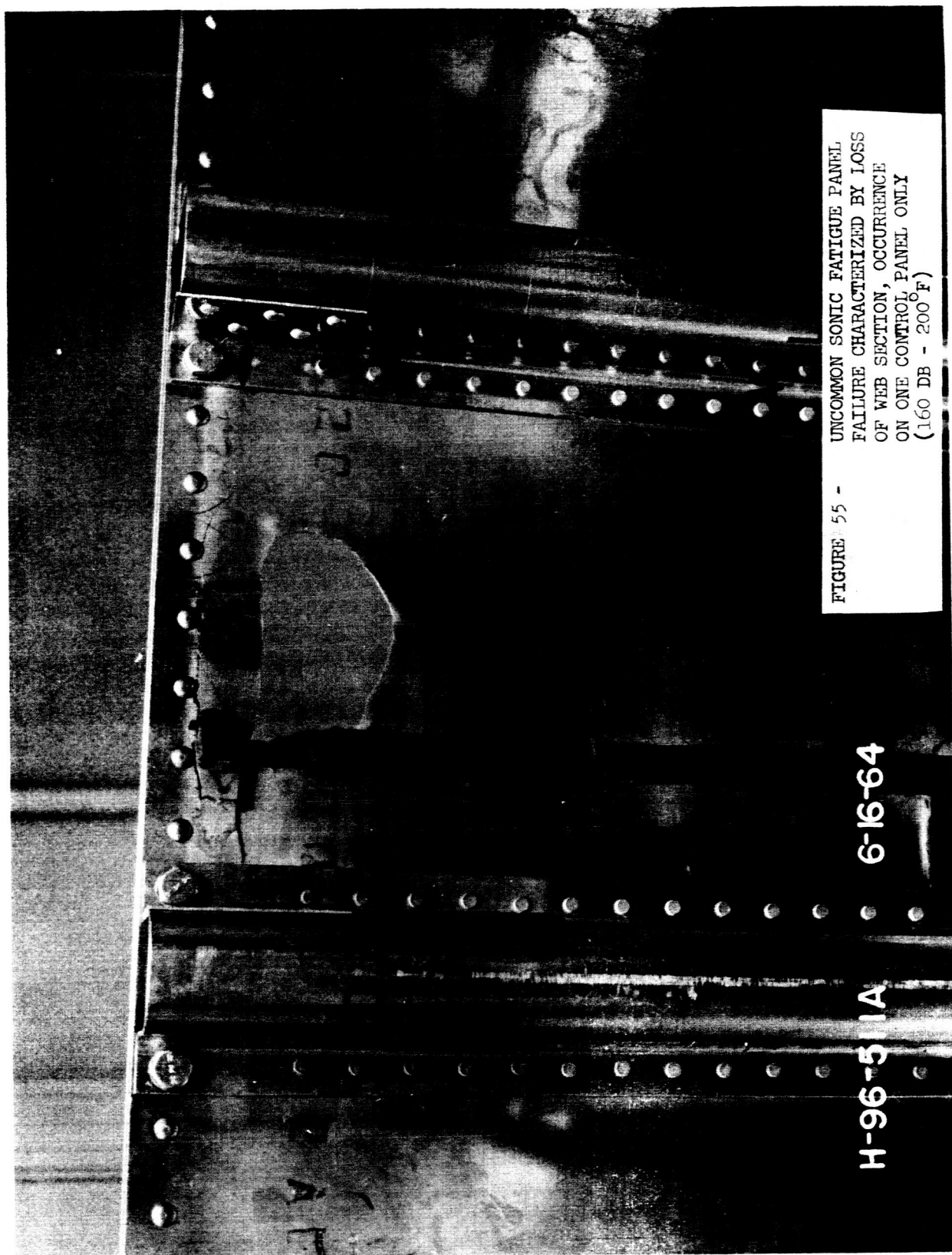


FIGURE 55 -  
UNCOMMON SONIC FATIGUE PANEL  
FAILURE CHARACTERIZED BY LOSS  
OF WEB SECTION, OCCURRENCE  
ON ONE CONTROL PANEL ONLY  
(160 DB - 200 F)

H-96-51A 6-16-64

105

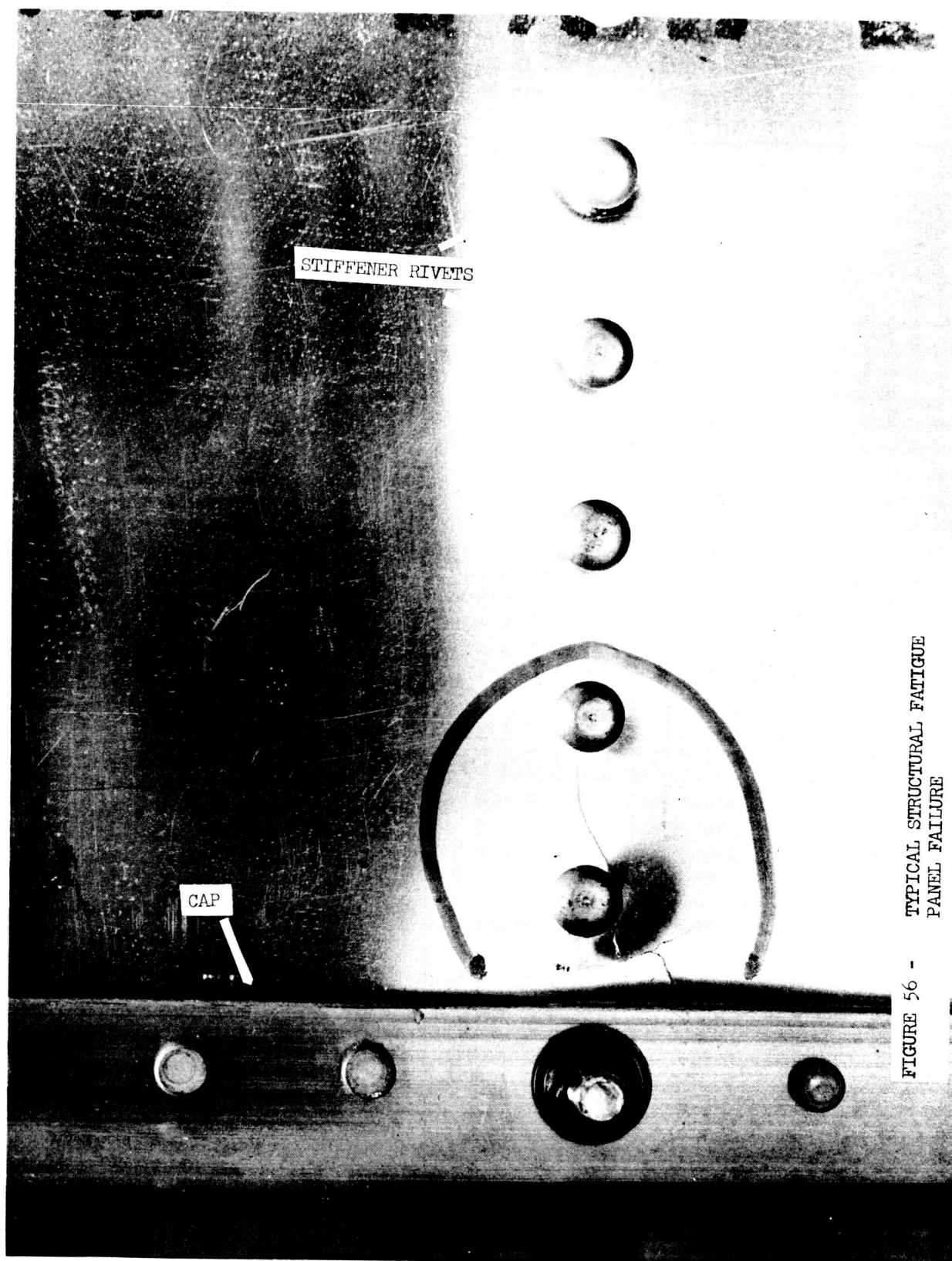


FIGURE 56 - TYPICAL STRUCTURAL FATIGUE  
PANEL FAILURE

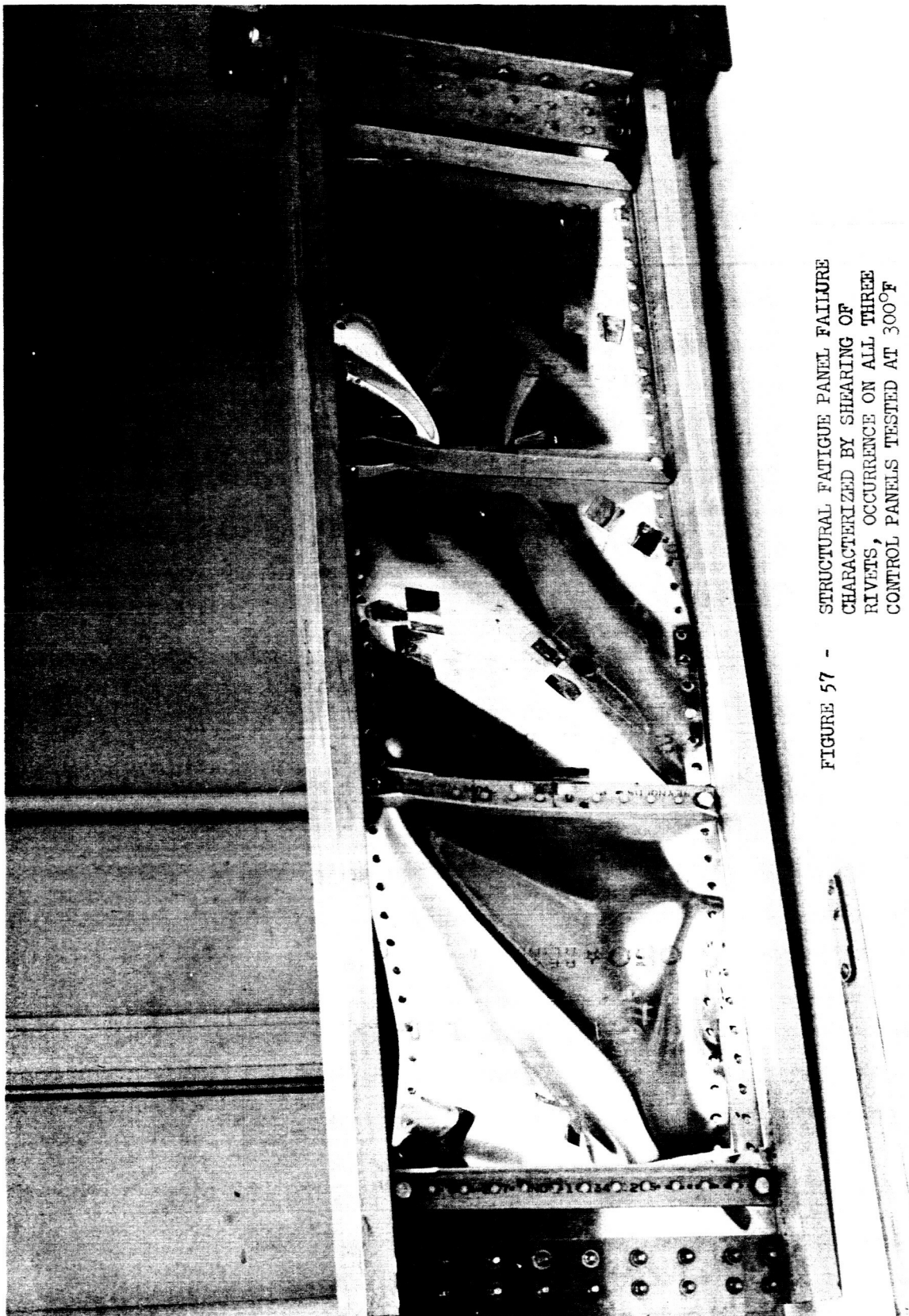
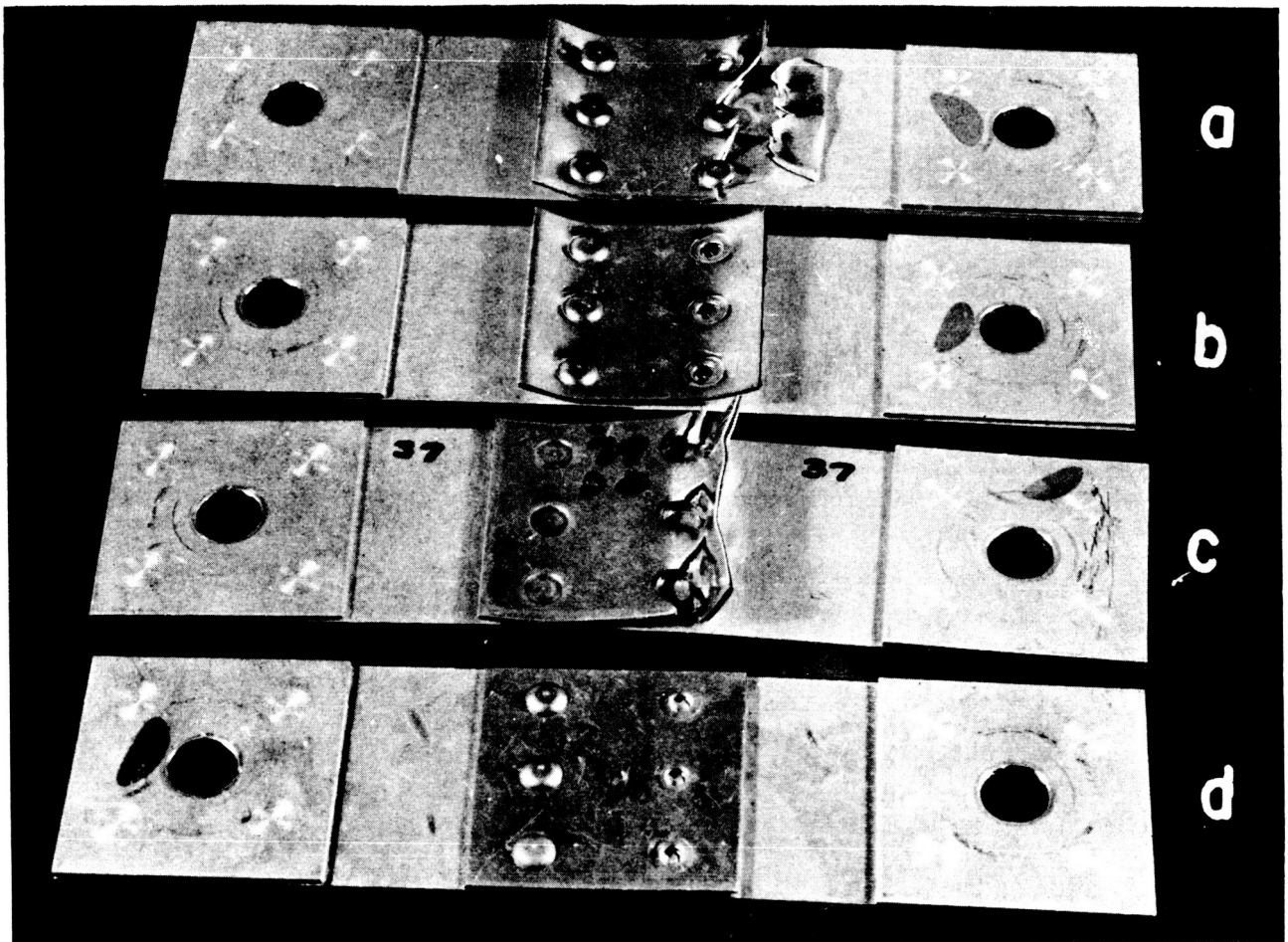


FIGURE 57 -  
STRUCTURAL FATIGUE PANEL FAILURE  
CHARACTERIZED BY SHEARING OF  
RIVETS, OCCURRENCE ON ALL THREE  
CONTROL PANELS TESTED AT 300°F

# SPLICE PLATE



- a. TYPICAL OF SPECIMENS #1-12. FAILURE PRODUCED BY COMBINATION OF TEARING OF VISCO-ELASTIC MATERIAL & RIVET FAILURE.
- b. TYPICAL OF SPECIMENS #13-36. FAILURE BY SHEARING RIVETS.
- c. TYPICAL OF SPECIMENS #37-54. FAILURE BY TEARING VISCO-ELASTIC MATERIAL AT THE RIVETS.
- d. TYPICAL OF SPECIMENS #55-72. FAILURE BY SHEARING RIVETS.

FIGURE 58 - TYPICAL FAILURE MODES OF AXIAL-LOAD  
STATIC TENSILE SPECIMENS

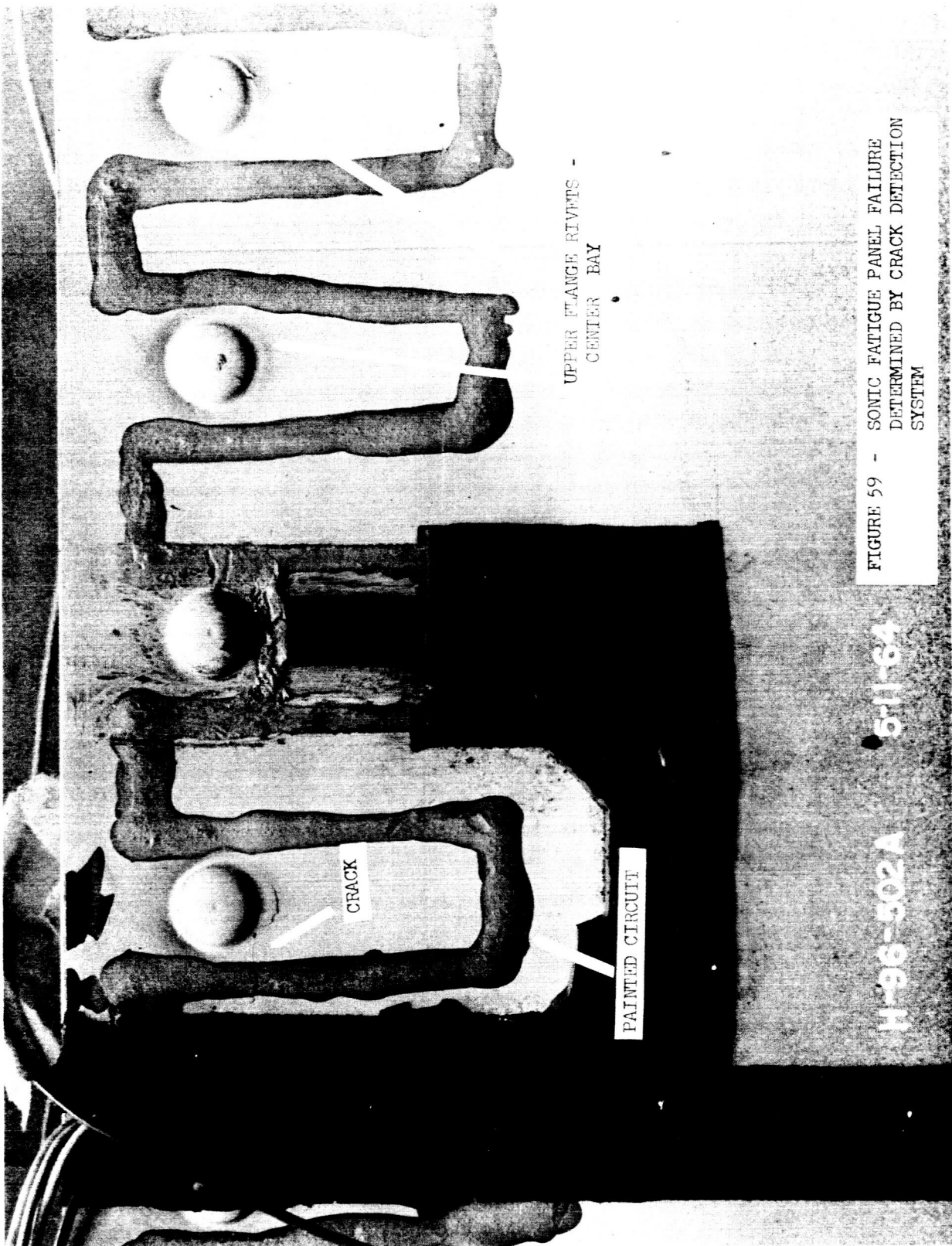


FIGURE 59 - SONIC FATIGUE PANEL FAILURE  
DETERMINED BY CRACK DETECTION  
SYSTEM